SOLAR ENERGY

THE JOURNAL OF SOLAR ENERGY SCIENCE AND ENGINEERING

VOLUME III | DECEMBER, 1959 | NUMBER 4

PUBLISHED QUARTERLY BY THE ASSOCIATION FOR APPLIED SOLAR ENERGY SUITE 222, 3424 NORTH CENTRAL AVENUE, PHOENIX, ARIZONA, U. S. A.

EXECUTIVE COMMITTEE

JAN OOSTERMEYER, *President*
Retired President, Shell Chemical Corporation
WALTER T. LUCKING, *Vice President*
President, Arizona Public Service Company
HENRY SARGENT, *Vice President*
President, American & Foreign Power Co., New York
E. LEE MCLEAN, *Executive Vice President*
WALTER BIMSON
Chairman of the Board, Valley National Bank
WELDON B. GIBSON
Vice President, Stanford Research Institute
SHERMAN HAZELTINE
Chairman of the Board, First Nat'l Bank of Arizona
G. ROBERT HERBERGER
Director, Butler Bros., Chicago
JOHN M. JACOBS
Owner, John Jacobs Farms
JOHN MILLS
Chairman of the Board, Associated Federal Hotels
FRANK SNELL
Partner, Snell & Wilmer

EDITORIAL BOARD

Editor

JEAN SMITH JENSEN

Chief Technical Editor

ALFRED B. STAFFORD
Arizona State University

Associate Editors

GEORGE C. BEAKLEY
Arizona State University
JOHN P. DECKER
U.S. Forest Service
FRANK E. EDLIN
E. I. DuPont de Nemours & Co.
JAMES W. ELMORE
Arizona State University
MERRITT KASTENS
Union Carbide International
RUSSELL L. RIESE
Arizona State University

SUBSCRIPTIONS

The Journal is sent to AFASE members as one of their membership benefits. Non-members may purchase single copies of this issue at $3 per copy, or may obtain a subscription at $10 per year. Please send all communications and inquiries to the editor, at the above address.

TABLE OF CONTENTS

Efficiency of Some Iron-Thionine Photogalvanic Cells 1
A. E. Potter, Jr. and L. H. Thaller

The Photovoltaic Effect and its Utilization 8
Paul Rappaport

Selective Radiation Coatings—Preparation and High Temperature Stability 19
Panos Kokoropoulos, Ehab Salam, and Farrington Daniels

Optimum Storage of Heat with a Solar House 24
Edward Speyer

Design of a Sea Thermal Energy Power Plant 49
Asa E. Snyder

The Derivations of Several "Plate-Efficiency Factors" Useful in the Design of Flat-Plate Solar Heat Collectors 55
Raymond W. Bliss, Jr.

A Stationary Solar Energy Concentrator 65
Paul B. Archibald

Calculation of the Concentration of Energy at Points Outside the Focal Spot of a Parabolic Condenser 67
Alfred W. Simon

Comments on Papers 70

Solar Abstracts 71

COVER PHOTO:

The world's largest solar energy converter, "Big Bertha," has been installed on the roof of the recently opened Hoffman Semiconductor Center in El Monte, Calif. Its 7,800 solar cells provide electricity for the center's solar energy exhibits.

Photo courtesy Hoffman Electronics Corporation

VOL. 3 1959

SOLAR ENERGY

THE JOURNAL OF SOLAR ENERGY SCIENCE AND ENGINEERING

VOLUME III | DECEMBER, 1959 | NUMBER 4

PUBLISHED QUARTERLY BY THE ASSOCIATION FOR APPLIED SOLAR ENERGY SUITE 222, 3424 NORTH CENTRAL AVENUE, PHOENIX, ARIZONA, U. S. A.

EXECUTIVE COMMITTEE

JAN OOSTERMEYER, *President*
Retired President, Shell Chemical Corporation
WALTER T. LUCKING, *Vice President*
President, Arizona Public Service Company
HENRY SARGENT, *Vice President*
President, American & Foreign Power Co., New York
E. LEE MCLEAN, *Executive Vice President*
WALTER BIMSON
Chairman of the Board, Valley National Bank
WELDON B. GIBSON
Vice President, Stanford Research Institute
SHERMAN HAZELTINE
Chairman of the Board, First Nat'l Bank of Arizona
G. ROBERT HERBERGER
Director, Butler Bros., Chicago
JOHN M. JACOBS
Owner, John Jacobs Farms
JOHN MILLS
Chairman of the Board, Associated Federal Hotels
FRANK SNELL
Partner, Snell & Wilmer

EDITORIAL BOARD

Editor

JEAN SMITH JENSEN

Chief Technical Editor

ALFRED B. STAFFORD
Arizona State University

Associate Editors

GEORGE C. BEAKLEY
Arizona State University
JOHN P. DECKER
U.S. Forest Service
FRANK E. EDLIN
E. I. DuPont de Nemours & Co.
JAMES W. ELMORE
Arizona State University
MERRITT KASTENS
Union Carbide International
RUSSELL L. RIESE
Arizona State University

SUBSCRIPTIONS

The Journal is sent to AFASE members as one of their membership benefits. Non-members may purchase single copies of this issue at $3 per copy, or may obtain a subscription at $10 per year. Please send all communications and inquiries to the editor, at the above address.

TABLE OF CONTENTS

Efficiency of Some Iron-Thionine Photogalvanic Cells 1
A. E. Potter, Jr. and L. H. Thaller

The Photovoltaic Effect and its Utilization 8
Paul Rappaport

Selective Radiation Coatings—Preparation and High Temperature Stability 19
Panos Kokoropoulos, Ehab Salam, and Farrington Daniels

Optimum Storage of Heat with a Solar House 24
Edward Speyer

Design of a Sea Thermal Energy Power Plant 49
Asa E. Snyder

The Derivations of Several "Plate-Efficiency Factors" Useful in the Design of Flat-Plate Solar Heat Collectors 55
Raymond W. Bliss, Jr.

A Stationary Solar Energy Concentrator 65
Paul B. Archibald

Calculation of the Concentration of Energy at Points Outside the Focal Spot of a Parabolic Condenser 67
Alfred W. Simon

Comments on Papers 70

Solar Abstracts 71

COVER PHOTO:

The world's largest solar energy converter, "Big Bertha," has been installed on the roof of the recently opened Hoffman Semiconductor Center in El Monte, Calif. Its 7,800 solar cells provide electricity for the center's solar energy exhibits.

Photo courtesy Hoffman Electronics Corporation

VOL. 3 1959

Efficiency of Some Iron-Thionine Photogalvanic Cells

By A. E. Potter, Jr., and L. H. Thaller

Lewis Research Center, National Aeronautics and Space Administration, Cleveland, Ohio

Rabinowitch has suggested that the photogalvanic effect might be used to convert sunlight into electricity. In order to explore this suggestion, some photogalvanic cells using the iron-thionine system as the photosensitive fluid were built and tested. The observed maximum power conversion efficiency was 3×10^{-4} per cent, based on light absorbed. The principal reason for the low efficiency was shown to be polarization of the polished platinum electrodes. Coating the electrodes with platinum black reduced polarization sufficiently, so that it appeared possible to achieve an efficiency of 6×10^{-2} per cent, although this value was not actually observed. In principle, it appeared possible to make further increases in efficiency by increasing electrode area and decreasing the electrolyte resistance.

Aside from electrode polarization, the major problem encountered was the rapid loss of the photochemical activity of the dye. No further progress can be made until this problem is solved.

INTRODUCTION

When certain dyes are dissolved in a solution containing a suitable reducing agent, the solution becomes photochemically active, in the sense that the dissolved dye can be reduced to a colorless form by exposure to light.[1–8] When illumination is terminated, the reaction reverses, and the dye reappears in its original form. A change in the potential of the solution accompanies the photoreduction of the dye. This latter phenomenon has been called the photogalvanic effect by Rabinowitch[2, 3] who studied the iron-thionine system. This system can be represented by the equilibrium

$$Fe^{II} + \text{thionine} \rightleftarrows Fe^{III} + \text{reduced thionine}$$

In the dark, this equilibrium lies far to the left as a result of the relatively large difference between the oxidation-reduction potentials of the iron and dye systems. Under strong illumination, the equilibrium is shifted to the right, and the solution bleaches. The basic reason for the photosensitivity of the equilibrium appears to be the formation of a long-lived electronically excited state by thionine upon absorption of light.[9] This state is very reactive and rapidly oxidizes ferrous ion. In the bleached solution, the major reduced dye species appears to be semithionine.[11] With intense illumination, the potential of the bleached solution can be as much as 0.25 v more negative than that of the unbleached solution. The relation between the amount of bleaching and the potential of the solution is very complex, and poses an unusual problem which has not yet been satisfactorily solved. This research concerns the possible use of the potential difference between illuminated and dark iron-thionine solutions for conversion of sunlight into electricity. This use has been suggested by Rabinowitch, who states that an efficiency approaching 1 per cent based on light absorbed was attained in preliminary experiments.[10] The reported efficiency was thought to be sufficiently promising to justify an attempt to uncover the factors limiting efficiency in this cell, with the hope that the efficiency could be improved. For this reason, some iron-thionine photogalvanic cells were constructed, and their efficiency measured.

EXPERIMENTAL DETAILS

The Photogalvanic Cells

Basically, a photogalvanic cell consists of a pair of inert electrodes immersed in a solution of dye and reducing agent. One electrode and the solution surrounding it is illuminated. The other electrode is not illuminated. A potential difference between the two electrodes is produced as a result of concentration differences at these electrodes, and may be used to perform electrical work. The potential of the illuminated solution is such that electrons flow through an external circuit from the illuminated electrode to the dark electrode.

Two phenomena connected with the transfer of electrons from the light to the dark solution must be considered in the design and operation of photogalvanic cells. They are: (1) concentration polarization of the bulk of the solution, and (2) competition between the electrode reaction and the solution reaction.

Let us first consider concentration polarization of the bulk of the solution. In the opinion of Rabinowitch,[3]

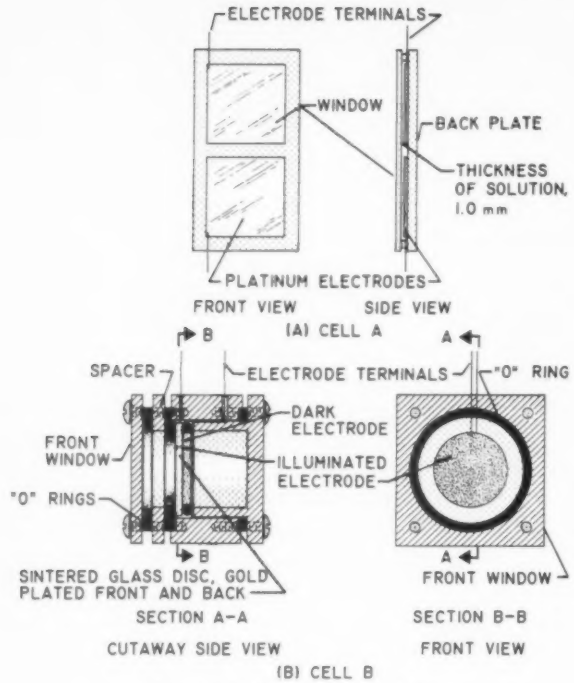

FIG. 1—Photogalvanic cells.

the principal species which delivers electrons to the illuminated electrode is some form of the reduced dye, probably semithionine, since it is the predominant dye species in the illuminated solution.[11] The ionic species which accepts electrons from the electrode in the dark solution is ferric ion. Thus, when electrons are transferred from illuminated to dark solution through an external circuit, the following electrode reactions occur:

Illuminated electrode

$$\text{semithionine} \rightarrow \text{thionine} + \text{electron}$$

Darkened electrode

$$Fe^{III} + \text{electron} \rightarrow Fe^{II}$$

In the illuminated solution, the thionine formed at the electrode will react with Fe^{II} in the presence of light to reform semithionine and to produce Fe^{III}. The net result of the electron transfer is thus an accumulation of Fe^{III} in the illuminated solution and of Fe^{II} in the dark solution. The resultant potential difference counters that produced by photoreduction of the dye. Thus, if sufficient power is withdrawn from the cell, it becomes polarized because of concentration differences between the solutions. Two approaches to a solution of this problem were made. The simplest way to describe them is to discuss the particular cells which were built. These are shown in Figs. 1(a) and (b). Cell A, shown in Fig. 1(a), consists of two polished plates of platinum cemented to a glass backing plate and covered with a thin (1-mm) layer of photogalvanic solution. One plate or electrode is illuminated, the other is not. The intended method of operation was as follows: power would be withdrawn from the cell until volume polarization reduced the output appreciably. Then, the illuminated electrode would be darkened, and the previously darkened electrode would be illuminated. Current would then flow in the opposite direction than previously. When volume polarization again reduced power output, the operation would be repeated. By see-sawing the cell in this manner, the effect of volume polarization on power production can be minimized. The second approach to the volume polarization problem is seen in cell B, shown in Fig. 1(b). This cell consists of a sintered glass disk whose front and back are covered with a thin porous layer of gold. The gold layers form the two electrodes of the cell. The disk is immersed in a photogalvanic solution. One face, or electrode, is illuminated, the other is not. When power is withdrawn from the cell and volume polarization sets in, a concentration gradient is produced across the sintered glass separating the two electrodes and the illuminated and dark parts of the solution. As a result of this gradient, interdiffusion between the two solutions will occur which will tend to counter the volume polarization.

The second and perhaps most important factor affecting cell design is the competition in the illuminated solution between the electrode reaction and the back reaction in solution. The competing reactions are as follows:

$$\underbrace{\text{reduced dye} \rightarrow \text{dye} + \text{electron}}_{\text{ELECTRODE REACTION}}$$

$$\underbrace{+ \text{oxidizing agent} \rightarrow \text{dye} + \text{reducing agent}}_{\text{SOLUTION REACTION}}$$

Unfortunately there does not seem to be any really effective means of gaining a favorable balance in this competition. This difficulty is one of the major factors which limit cell efficiency. All that can be done is to make the ratio of electrode area to solution volume as large as possible. For this reason, the depth of solution in the cell A was made as small as possible (if the depth is too small, almost no light is absorbed by the cell), and the electrode in cell B was of a rough, porous nature, thus having a large surface area.

The Photogalvanic Solution

It seemed reasonable to use a solution giving the highest possible photogalvanic potential with the light source used. The chemical variables which control the photogalvanic effect are the concentrations of Fe^{II}, Fe^{III}, H^+, and thionine. The concentrations of these species were varied in a systematic manner to

VOL. 3 1959

find the best combination. The procedure was as follows. A glass half cell was filled with a known volume of an air-free solution of a particular H^+, Fe^{II}, and Fe^{III} concentration. The anion of all the solutions studied was Cl^-. The solution was then illuminated and its potential measured with a polished platinum electrode while a concentrated thionine solution was added from a burette. The solution was constantly stirred by nitrogen bubbled through it. When addition of thionine caused no further decrease in the potential of the solution, the titration was stopped. This potential E_L of the solution and the amount of thionine added to achieve E_L were recorded. The illumination was then turned off, and after the solution returned to equilibrium the dark potential E_D was measured. The H^+, Fe^{II}, and Fe^{III} mixtures studied by this technique were all the combinations of the following concentrations (in moles/liter):

$$[Fe^{II}] = 0.5, \quad 1, \quad \text{and} \quad 2 \times 10^{-2}$$
$$[Fe^{III}] = 0.2, \quad 1, \quad \text{and} \quad 5 \times 10^{-5}$$
$$[H^+] = 1, \quad 3, \quad \text{and} \quad 6 \times 10^{-3}$$

The solution which yielded the largest photogalvanic potential of all ($E_L - E_D = 0.185$ v) had the following composition:

$$[Fe^{II}] = 1.0 \times 10^{-2}$$
$$[Fe^{III}] = 5.0 \times 10^{-5}$$
$$[H^+] = 3.0 \times 10^{-3}$$
$$[\text{Thionine}] = 1.5 \times 10^{-5}$$

The composition of this solution is almost identical with that found by Rabinowitch to give a large potential change. This solution and one having double the thionine concentration, but otherwise identical, were used in all the tests reported. It was found that the solution deteriorated rather rapidly, so that it was necessary to prepare it under nitrogen immediately before use from air-free stock solutions stored under nitrogen. The stock solutions also deteriorated rapidly, and were never more than 48 hours old. The photogalvanic potential of the solution ($E_L - E_D$) was always measured just prior to use in the photogalvanic cells.

The Light Source and Radiant Energy Measurements

The light source used in all the experiments was a 750-watt photoflood lamp. The light was filtered through 3 cm of running water and 8 cm of a saturated solution of ferrous sulfate. These filters removed the portions of the spectrum which would have been absorbed by water and the ferrous ions in the photogalvanic solution. The energy from the light was measured with a calibrated Epply thermopile in conjunction with a microvoltmeter. The light beam from the source was only approximately parallel, so that the radiant intensity varied with distance from the lamp. For this reason, when measurements of radiant energy incident on the photogalvanic cells were made, care was taken to make the measurement at the same distance from the lamp as the cell was placed.

The amount of radiant energy absorbed by the photogalvanic cell A during operation was estimated as follows: the cell was turned from its usual position normal to the incident light beam, so that it formed a slight angle from the normal to the incident beam. The beam reflected from the polished electrode could then be observed, and its intensity measured. The intensity of the reflected beam was measured with cell empty, and with the cell filled with the photogalvanic solution. Calling the energy reflected from the empty cell I_e and the energy reflected from the full cell I_f, it is evident that $I_e - I_f$ is a measure of the energy absorbed by the solution, and that $(I_e - I_f)/I_e$ is approximately the fraction of incident light absorbed by the solution. Therefore, the energy absorbed by the cell is approximately the energy of incident light times the fraction $(I_e - I_f)/I_e$. A similar procedure could not be applied to cell B, because the rough surface of the gold electrode reflected light diffusely rather than specularly. For cell B, a crude estimate of the light absorbed was made as follows: it was assumed that light absorption in the cells obeyed Lambert's law. Then an empirical absorption coefficient was calculated from the light absorbed in cell A, and used to estimate the light absorbed in cell B. The amount of absorbed radiant energy calculated by this procedure is certainly accurate to within an order of magnitude, and is probably better than that. It will be seen that the accuracy is sufficient for the purposes of this research.

For the power measurements reported here, the amount of radiant energy incident on the cells was about 3×10^{-3} watts per sq cm. Between 10 and 20 per cent of this energy was absorbed by the cells. It was found that sunlight of about ten times the intensity of the filtered lamplight was needed to produce the same cell voltage as the lamplight. Thus, the cells can effectively use only about one per cent of the energy of sunlight.

POWER AND EFFICIENCY OF THE CELLS

In order to eliminate spurious voltages arising from dirty electrodes, it was necessary to soak the cells in concentrated HCl for a day or two before use. The voltage of the cells when exposed to light from the lamp and filled with the photogalvanic solution containing 1.5×10^{-5} moles per liter thionine was only about 80 mv, less than half the expected value of 185 mv. Possibly this was because of leakage of light from

one side of the cell to the other. When a solution containing 3×10^{-5} moles per liter thionine was used in cell A, a voltage of 126 mv was observed. Possibly less light leaked to the dark side of the cell when the more concentrated dye solution was used, so that a higher voltage was obtained than before. The cell with this solution yielded a voltage of 170 mv in direct sunlight of 0.068 watt per sq cm. It was estimated that a voltage of 182 mv would have been produced in the most intense sunlight available at the earth's surface.

The power output of the cells was determined by measuring the voltage drop across a resistance connected across the cell terminals. Resistances ranging from 10^2 to 10^7 ohms were used. Current was withdrawn only for very short periods of time to minimize concentration polarization in the bulk of the solution.

It was found that the cell would never return to its initial voltage after power had been withdrawn from it. This was the result of irreversible changes in the dye. Thus, in one case, the initial cell voltage was 126 mv. After about three minutes of operation at maximum current, the cell voltage dropped to 105 mv, and could not be increased to the original value in spite of the fact that concentration polarization was eliminated by back-electrolysis of the cell solution. Paper chromatographs of the solution from the cell showed that a new, nearly colorless compound had appeared in the solution. Thus, side reactions occurred which converted the dye into a substance having no photochemical activity. Because of this discouraging result, it was not thought worthwhile to operate the cells for the half-hour or so required to produce sufficient concentration polarization in the bulk of the solution to test the means for combating it.

The efficiency of the cells was calculated by dividing the power output by the radiant energy absorbed by the cell. Since so little power could be withdrawn from the cells, it seemed reasonable to assume that the withdrawal of power did not appreciably affect the absorption of radiant energy. This considerably simplified the measurements, since the radiant energy absorbed by the cells could be assumed constant and equal to that absorbed when no power was withdrawn. This assumption also has the result that maximum efficiency is observed when maximum power is developed by the cell. This is in contrast to the common galvanic cell where maximum efficiency is achieved as the power approaches zero. The cell efficiencies are shown in Fig. 2. Cell A was tested with photogalvanic solutions containing 1.5 and 3.0×10^{-5} moles per liter of thionine. Cell B was tested with only the solution containing 1.5×10^{-5} moles per liter. The highest efficiency is observed for cell A with the high concentration of thionine. Even for this case, the maximum efficiency is very low, hardly reaching 3×10^{-4} per cent.

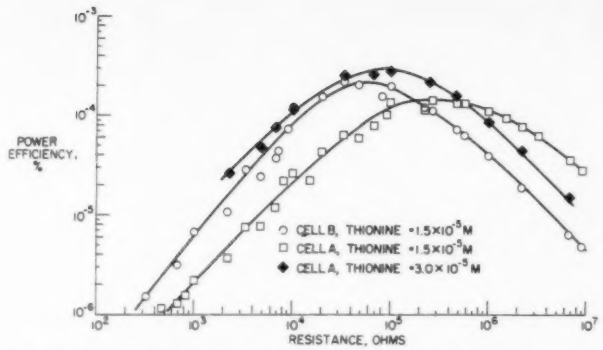

FIG. 2—Power efficiency as a function of load resistance for two photogalvanic cells.

It can be seen in Fig. 2 that the load resistance at which the cells reach maximum power and efficiency is in the range of 10^4 to 10^5 ohms. It can be shown that the power delivered to a load resistance by a simple battery is a maximum when the load resistance equals the internal resistance of the battery. Consequently, the apparent internal resistance of the cells is 10^4 to 10^5 ohms. However, the resistance of the electrolyte in the cells is calculated (from cell dimensions and the conductance of the solution) to be of the order of 10^2 ohms. Thus, some factor other than just the resistance of the electrolyte limits the power output of the cells. This factor will be shown later to be chemical polarization of the electrodes.

The experimental results pose two questions: (1) Why is the cell efficiency so small? (2) What measures are required to increase the cell efficiency?

In order to discuss these questions, it is helpful to have some idea of the maximum efficiency that could in theory be attained by a photogalvanic cell. It can be shown that the maximum power that can be developed in a circuit consisting of a battery, the internal resistance of the battery, and an external load resistance is $E_c^0 I_c$, where E_c^0 is the zero-current voltage, and I_c is the short-circuit current yielded by the battery. At most, one-half of this power can be developed in the external load resistance. The other half of the power is lost in the internal resistance of the battery. The maximum power output is thus $\frac{1}{2} E_c^0 I_c$. The power efficiency η is defined as the ratio of power input to power output. Since we have assumed a constant power input, the maximum power efficiency for the photogalvanic cell is

$$\eta = \frac{1}{2} \frac{E_c^0 I_c}{\epsilon N} \qquad [1]$$

where ϵ is the energy per absorbed photon, and N is the number of photons absorbed per second. As

VOL. 3 1959

written, the equation is strictly correct only for monochromatic light. This is a convenient approximation for the iron-thionine system, since most of the light is absorbed near 5900 Å. Equation [1] shows that even if the conversion of light into electric current is perfectly efficient, so that $E_c^0 I_c = \epsilon N$, the power efficiency of the cell is 50 per cent. This is because the cell cannot deliver more than half the absorbed power to an external load.

Equation [1] can also be used to estimate the maximum efficiency that is possible for the cells used in this research. For this purpose, it is convenient to consider the power efficiency as the product of two other efficiencies, one I_c/N, the other E_c^0/ϵ. The ratio I_c/N can be considered as a photon efficiency; the number of electrons produced in the circuit per photon absorbed. If one assumes that each molecule of reduced dye formed by the photochemical reaction yields one electron at the electrode, the maximum value of the photon efficiency must be the quantum yield of the photoreduction. The data of Hardwick[11] may be used to calculate the quantum yield for the solution used in the cells. The value obtained is 0.7, corresponding to a maximum photon efficiency of 70 per cent. The ratio E_c^0/ϵ may be regarded as a voltage efficiency. Its value may be calculated, since E_c^0 was measured, and the energy per photon absorbed by thionine is about 2.1 ev. As mentioned previously, cell A in maximum sunlight will yield an open-circuit voltage E_c^0 of 0.182 v, which gives a maximum voltage efficiency of 8.7 per cent. When these maximum theoretical values of the photon and voltage efficiency are used in Equation [1], it is found that the maximum power efficiency is 3 per cent. The voltage efficiency is the major factor making the theoretical power efficiency so small. The voltage of the cell is small because the back reaction between reduced dye and oxidizing agent keeps the concentration of reduced dye low. It does not seem reasonable to expect voltages much larger than about 0.5 v in sunlight, corresponding to a possible power efficiency of about 12 per cent, assuming a quantum yield of unity.

Returning to the original question, why is the observed efficiency a factor of about 10^4 less than the theoretical maximum? For the answer, compare the observed photon efficiency with the theoretical maximum of 70 per cent. The largest observed photon efficiencies are of the order of 10^{-4} per cent. Therefore, the poor efficiency of the cells is primarily the result of a very small photon efficiency, which is to say, a very small current from the cell.

A possible cause of the smallness of the current from the cell is electrode polarization. Electrode polarization will cause the cell potential to decrease as the current withdrawn from the cell increases, and thereby will limit the maximum current that can be withdrawn. In order to measure this effect, the potential of a small platinum electrode immersed in the photogalvanic solution was measured as a function of current density. The experimental arrangement was similar to that described on page 436 of Ref. 12. The overvoltage, the difference between the reversible electrode potential and the observed electrode potential, is plotted against current density in Fig. 3. Results are given for both anodic and cathodic polarization. In the photogalvanic cell, the electrode in the dark solution is the anode, and the electrode in the illuminated solution is the cathode. Accurate measurements of the cathodic polarization in illuminated solutions could not be obtained because the passage of current slowly destroyed the photochemical activity of the dye, so that the reversible electrode potential changed as current flowed. However inaccurate they may be, the results that were obtained for cathodic polarization in the illuminated solution are seen in Fig. 3 to be very similar to those obtained for cathodic polarization in the dark solution. This is a somewhat surprising result, since the cathode reaction should be different in the dark and illuminated solutions. Both anodic and cathodic overvoltages are directly proportional to the current density at low current densities. At higher current densities, the overvoltages become proportional to the logarithm of the current density. This behavior is typical of the iron group metals and is displayed when a reaction at the electrode is the rate-determining step in the discharge of an ion at the electrode (Ref. 12, p. 462).

The experimental results shown in Fig. 3 may be used to calculate the variation of voltage of the iron-thionine photogalvanic cell with current density. At low current densities (0.2 μa per sq cm or less), the result is

$$E_c = E_c^0 - 10^6 I_d \qquad [2]$$

where E_c is the cell voltage, I_d is the current density

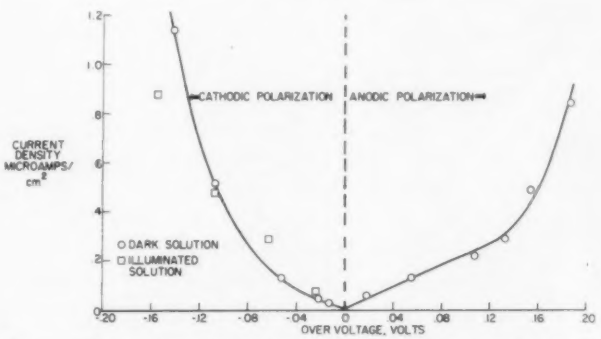

FIG. 3—Electrode polarization in the iron-thionine photogalvanic solution.

in amperes per square centimeter, and E_c^0 is the cell voltage when no current is withdrawn. This result may be used to show both why the current from the cell is so small and why the load resistance at maximum efficiency does not equal the internal resistance of the cell as mentioned previously. Equation [2], which applies to the iron-thionine photogalvanic solution used here, can be written as

$$E_c = E_c^0 - \frac{b}{A} I \qquad [3]$$

where I is the current from the cell, A is the electrode area, and b is the proportionality factor between the current density and extent of electrode polarization (equal to 10^6 ohm per sq cm for the case at hand). The power developed by the cell in an external resistance R_e is

$$P = I^2 R_e \qquad [4]$$

The current in the circuit is

$$I = \frac{E_c}{R_e + R_i} \qquad [5]$$

where R_i is the internal resistance of the cell. Combining Equations [3], [4], and [5], we find that

$$P = \frac{E_c^{0^2} R_e}{\left(R_e + R_i + \frac{b}{A}\right)^2} \qquad [6]$$

This equation may be used to show that the maximum power is developed by the cell in the external resistance when

$$R_e = R_i + (b/A) \qquad [7]$$

The current when maximum power is being transferred is therefore

$$I = \frac{E_c^0}{2[R_i + (b/A)]} \qquad [8]$$

Then it follows from Equation [4] that the maximum power developed by the cell in an external resistance is

$$P_{\max} = \frac{1}{4} \frac{E_c^0}{[R_i + (b/A)]} \qquad [9]$$

The value of b as found from the electrode polarization measurements is 10^6 ohm per sq cm. The exposed area of each electrode of cell A was 6.25 sq cm. The value of b/A is therefore 1.6×10^5 ohms. Since the internal resistance of the cell was very much smaller than this, of the order of 10^2 ohms, Equation [7] indicates that the power, and hence the efficiency for constant power input, of cell A should be a maximum at a load resistance of 1.6×10^5 ohms. Examination of Fig. 2 shows this to be approximately true. Cell A with the thionine concentration at 1.5×10^{-5} molar displays a maximum efficiency at 2.5×10^5 ohms, and with the thionine concentration at 3.0×10^{-5} molar, the efficiency maximizes at about 1×10^5 ohms. The reason for the difference between the two is not clear. The reason why cell B has maximum efficiency at a lower load resistance, 5×10^4 ohms, is probably because of the greater electrode area of cell B, which makes b/A smaller. (The electrode area of B is large because the electrode surface is very rough. The actual frontal area of cells A and B is almost the same.)

Examination of Equation [8] shows that the current at maximum cell power is limited by b/A for a fixed value of E_c^0 and for negligible internal resistance of the cell. Thus, the current and therefore the photon efficiency is very low for the cell because the electrodes are so easily polarized, that is, b is very large. The major factor which limits efficiency of the iron-thionine photogalvanic cell is seen to be the easily polarized electrodes.

It is standard physical chemical laboratory practice to reduce or eliminate the polarization of platinum electrodes by coating them with platinum black. This was done for cell A, and attempts were made to repeat the efficiency experiments with the following curious results: the cell voltage did not increase quickly to a steady value upon illumination as before. Rather, it increased very slowly. With the usual photogalvanic solution, it increased from zero to 30 or 40 mv over a period of an hour. When citric acid was used instead of hydrochloric acid to acidify the solution, the cell voltage rose to 245 mv in 45 minutes under illumination of the 750-watt lamp. Obviously, efficiency measurements on such sluggish cells has little value unless one operates the cell at each load long enough to achieve equilibrium, about an hour in this case. This is not practical, since the dye deteriorates. Thus, a rapid series of power measurements were made to determine the effect of blacking the electrodes on cell polarization by measuring the load resistance at maximum power output. This resistance is equal to the internal resistance of the cell plus the apparent internal resistance caused by electrode polarization. The result was 5×10^3 ohms. The previous result for cell A with polished platinum electrodes was 1×10^5 ohms. Thus, coating with platinum black reduces the electrode polarization a great deal, by a factor of 200 in this case. As a result, the efficiency could, in principle, be increased by a factor of 200, assuming the low voltages and peculiarly sluggish behavior of the cell observed with platinum black electrodes does not signal some new undesirable phenomenon. Unfortunately, a factor of 200 brings the efficiency up to only 6×10^{-2} per cent. This is still not satisfactory, and further measures are required to increase the photon efficiency by increasing the current.

Equation [8] shows that the cell current is inversely

VOL. 3 1959

proportional to $(R_i + b/A)$, where R_i is the resistance of the electrolyte in the cell, b is the polarization constant, and A is the electrode area. The polarization constant b has been reduced to a minimum by blacking the electrodes. Any further increase in current must be the result of decreasing the electrolyte resistance R_i and increasing the electrode area A. The former could be done by adding an inert electrolyte such as KCl to the solution. The latter could be done in several ways, such as making the electrode porous and pumping the solution through it, or by making the electrode from a number of slightly separated thin plates placed parallel to the light. In order to increase the current to a value such that the 3 per cent theoretical efficiency could be achieved, the electrolyte resistance must be decreased by a factor of about 50, and the electrode area must be increased by a factor of about 250. In principle, such changes are possible, so that it should prove possible to increase the current enough to approach the theoretical efficiency.

It should be pointed out that the dye used in this work absorbs only a small fraction of the solar spectrum. For a practical cell, other photochemically active dyes which absorb in different spectral regions would have to be found, so that a mixture of such dyes could be used to absorb a large fraction of the solar spectrum. This is a smaller problem than that of the stability of the dye, since many dyes of different colors are known to be photochemically active.

CONCLUSIONS

A photogalvanic cell was constructed which would yield a voltage of 0.182 v in the brightest sunlight available at the surface of the earth. The theoretical maximum efficiency of the cell in sunlight was calculated to be 3 per cent, based on light absorbed. The observed maximum efficiency was 3×10^{-4} per cent, based on light absorbed. The reason for the low observed efficiency was shown to be the ease of polarization of the electrodes. Partial elimination of electrode polarization was achieved by coating the electrodes with platinum black. However, the reduction of polarization was insufficient to make the possible efficiency larger than 6×10^{-2} per cent. Further increases in efficiency appeared to be possible by increasing the electrode area and decreasing the electrolyte resistance, so that an efficiency of 1 per cent is not inconceivable. However, a major problem remains, that of chemical instability of the dye. No further progress is possible until this problem is solved.

ACKNOWLEDGEMENT

The assistance of Mr. Thomas P. Clark in the early phases of this work is gratefully acknowledged.

REFERENCES

1. M. Mudrovcic. *Z. Wiss. Photo.* **26:** 171, 1928.
2. E. Rabinowitch. *J. Chem. Phys.* **8:** 551, 1940.
3. E. Rabinowitch. *J. Chem. Phys.* **8:** 560, 1940.
4. Hendrich, Waclaw. *Roczn. Chem.* **31** (3): 937, 1957.
5. G. Oster; A. H. Adelman. *J. Am. Chem. Soc.* **78:** 913, 1956.
6. A. H. Adelman; G. Oster. *J. Am. Chem. Soc.* **78:** 3977, 1956.
7. G. Oster; J. S. Bellin. *J. Am. Chem. Soc.* **79:** 294, 1957.
8. J. S. Bellin; G. Oster. *J. Am. Chem. Soc.* **79:** 2461, 1957.
9. C. A. Parker; K. Bridge; G. Porter. *Nature* **182:** 130, 1958.
10. Eugene Rabinowitch. (In: *Solar Energy Research;* edited by F. Daniels and J. A. Duffie. Univ. of Wis. Press, 1955, pp. 193–202.)
11. R. Hardwick. *J. Am. Chem. Soc.* **80:** 5667, 1958.
12. S. Glasstone. *Introduction to Electrochemistry.* D. Van Nostrand Co., Inc., New York, 1942.

The Photovoltaic Effect and its Utilization*

By Paul Rappaport

RCA Laboratories, Princeton, N. J.

The growth of the photovoltaic effect from an interesting scientific phenomenon into one of the most efficient methods yet devised for converting solar energy directly into electrical energy is described. Attention is given to considerations of the optimum semiconductor material for solar energy conversion and how it changes with operating temperature. Experimental results are presented showing operating characteristics and conversion efficiencies of such materials as silicon, gallium arsenide, indium phosphide, cadmium sulfide, and others. The high voltage (~100-v) photovoltaic effect from evaporated CdTe films is described. Included is a discussion of the major problems yet to be solved.

INTRODUCTION

It is the purpose of this paper to present a current review of the photovoltaic effect with special emphasis on the problem of solar energy conversion. A testimonial to the importance of this field today is the Vanguard Earth Satellite that has been sending solar-powered signals back to Earth for a year and a half now as a direct result of the photovoltaic cells on the Vanguard's surface. In the future as power needs become greater and conventional energy sources (fossil fuel and fissionable materials) are used up, the direct conversion of solar energy striking the waste lands of the world could conceivably become an important source of power.

A major step towards the solution of this difficult problem has been achieved by the solar converter or photovoltaic cell. This device is sometimes called a solar battery; however, strictly speaking, it is incorrect to use the term battery, since the primary energy source is not self contained. Such cells have already been made that can convert the sun's radiated energy directly into electrical energy with an efficiency of up to 14 per cent, the best experimental over-all efficiency reported to date[1] for any artificial conversion method.

* Much of the work discussed in this paper was supported by the United States Army Signal Research and Development Laboratories. Also published in the *RCA Review*, September, 1959.

BRIEF HISTORY

It has been over 100 years since Becquerel in 1839 first discovered that a photovoltage was developed when light was directed onto one of the electrodes in an electrolyte solution.[2] Adams and Day[3] were the first to observe the effect in a solid, selenium, about forty years later. A number of other early solid state workers including Lange,[4] Grondahl,[5] and Schottky[6] did pioneering work on selenium and cuprous-oxide photovoltaic cells. This work eventually resulted in the photoelectric exposure meter that has become so important in photography. However, it was not until 1954 that workers became interested in energy sources utilizing the photovoltaic effect. First there was the work of the RCA group[7] who demonstrated practical efficiencies in converting radioactive radiation into electrical energy using a silicon *p-n* junction photovoltaic cell. Then using a similar method Chapin, Fuller, and Pearson[8] reported a solar conversion efficiency of about 6 per cent. A third paper appeared in 1954 by Reynolds, Leis, Antes, and Marburger[9] who reported about 6 per cent solar conversion efficiency in cadmium sulfide *p-n* junctions. Since 1954 the silicon and CdS work has been pursued with vigor. Other materials and techniques were also developed as will become evident later in the discussion.

DESCRIPTION OF PHOTOVOLTAIC EFFECT

The photovoltaic effect can be defined as the generation of a potential when radiation ionizes the region in or near the built-in potential barrier of a semiconductor. It is characterized by a self-generated emf and current that can deliver power to a load; the primary power coming from the ionizing radiation. A potential barrier can be formed in a semiconductor by several means. The two techniques of most interest to photovoltaic cells are (1) the metal-semiconductor barrier formed by the deposition of a suitable transparent metallic film by evaporation or sputtering onto a semiconductor as in the selenium cell, or (2) the *p-n* junction formed by the introduction of a suitable type impurity into the opposite impurity type semiconductor.

We will now attempt to show how the photovoltaic

VOL. 3 1959

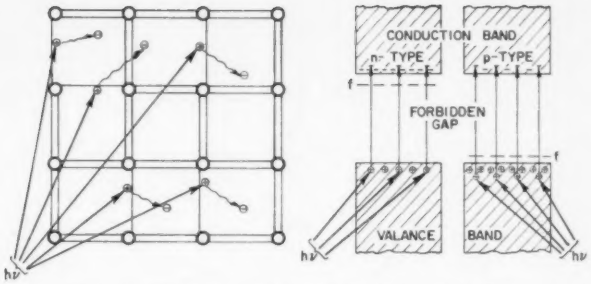

FIG. 1—Electron-hole production by photons.

effect comes about when light strikes a semiconductor *p-n* junction. The left side of Fig. 1 shows how carriers are generated when light photons enter the semiconductor crystal. The circles are the atoms in this two-dimensional crystal lattice, and the double lines represent the two electrons in the covalent bonds as in the case for silicon. Photons with energy above that required to break these bonds, i.e., 1.1 ev for silicon, will create electron-hole pairs on a unit quantum efficiency basis as shown on the diagram. The right side of the figure shows the same process using the energy band model for a semiconductor. Here are seen both an *n*- and *p*-type semiconductor. In one case, a column V element contributes extra electrons, and in the other case a column III element does not contribute enough electrons and so contributes holes.

The *n*-type material has its Fermi level (denoted by *f* in Fig. 1) near the top of the forbidden gap with many electrons, *n*, in the conduction band and few holes, *p*, in the valence band. The opposite is true in the *p*-type material. At a given temperature the product *np* is a constant ($np \sim 10^{21}$ for silicon at room temperature). For *n*-type highly conducting Si, *n* can be 10^{17} per cu cm and *p* would therefore be 10^4 per cu cm. We therefore develop the concept of the majority and minority carriers, the electrons and holes respectively in the cited case. When sunlight strikes this semiconductor, those photons with energy greater than the forbidden gap energy produce both type carriers in equal numbers. The net effect is that an intense light source can increase the minority carrier density by many orders of magnitude while the majority carrier density is barely affected. These photo-induced carriers are in excess of the thermal equilibrium number and they will diffuse randomly about the semiconductor and recombine in times of the order of tenths of microseconds.

If the *n* and *p*-type semiconductors are brought together, a *p-n* junction with a potential barrier is formed since thermodynamics requires that the average energy of the carriers (the Fermi level) be the same in the two materials. Now, excess carriers that are within a diffusion length (the average distance minority carriers diffuse before they recombine) of the potential barrier will be "trapped" by the barrier and caused to flow across it in an attempt to reduce their energy. This is shown in Fig. 2 at the bottom where the energy level diagram of a *p-n* junction is illustrated. The excess electrons will flow to the right and excess holes to the left. These constitute an electrical current, and when suitable electrical connections are made such a device will convert radiation into electricity. The current produced will be proportional to the number of photons absorbed, and the voltage will depend on the height of the barrier, which is always less than the width of the energy gap in the semiconductor depending on how heavily doped the *p* and *n* regions are.

At the top of Fig. 2 is seen a typical commercially available silicon solar cell. Boron is diffused into an originally *n*-type wafer at about 1100°C for 20 minutes, causing a *p*-type skin a few microns thick to form on all exposed surfaces. All surfaces are etched or lapped down to the *n* region except the top face. Ohmic contact is made to the top and bottom by first nickel plating and then soldering. Leads are connected to the load from the ohmic contacts, and light striking the top face will deliver a current to the load.

In order to achieve high efficiency of conversion it is desirable to produce an electron-hole pair within a diffusion length of the junction for each photon absorbed. For short diffusion length material (which is the usual result after the high temperature firing required to form the *p-n* junction) it is therefore desirable to absorb most of the photons in the region

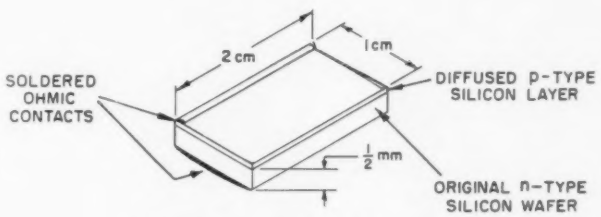

(a) SILICON SOLAR CELL

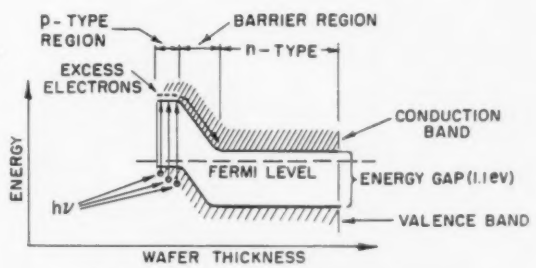

(b) ENERGY LEVEL DIAGRAM OF CELL

FIG. 2—(a) Silicon solar cell. (b) Energy level diagram of cell.

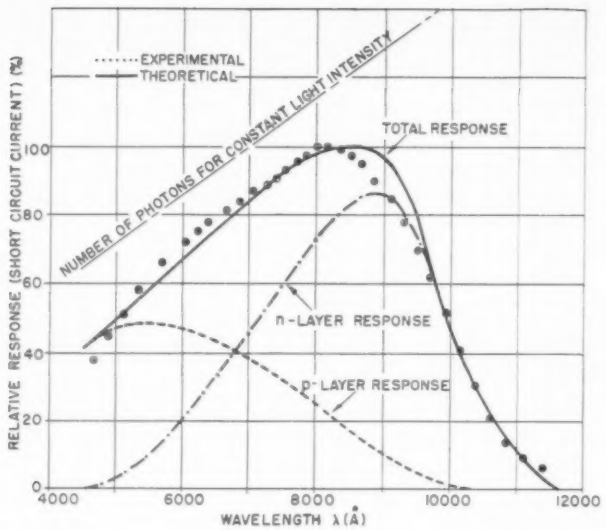

FIG. 3—Carrier creation within a solar cell. (Figure supplied by M. B. Prince from Reference 1)

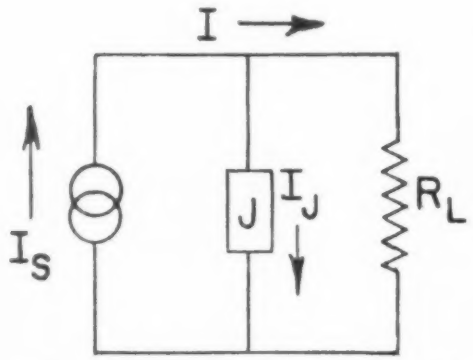

FIG. 4—Simplified equivalent circuit of illuminated cell.

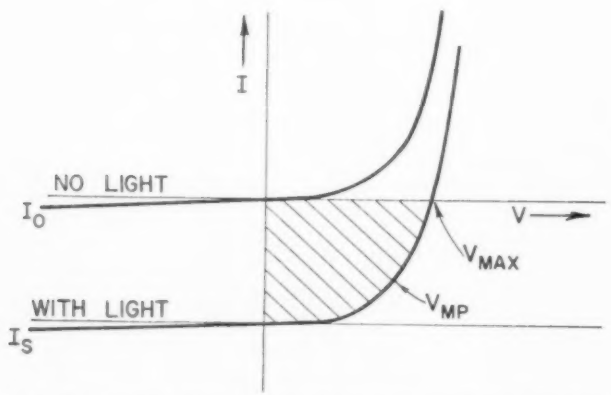

FIG. 5—Effect of light on current-voltage junction characteristic.

where the field exists. The field can be tailored to some extent to match the absorption of the light by varying the time and temperature of the boron diffusion process; however, because of the variation of absorption coefficient with λ a compromise must eventually be accepted. Fig. 3, kindly supplied by Dr. Prince of Hoffman Semiconductor Division, shows how the generation of carriers varies with wavelengths within the cell. Notice that the shorter wavelengths create carriers in the p region and the longer wavelengths create carriers in the n region. Since quite a large number are created in the n region, the diffusion length must be between 10^{-3} and 10^{-2} cm for good efficiency.

ELECTRICAL CHARACTERISTICS

The electrical characteristic of a photovoltaic cell can be understood from Fig. 5. Above, in Fig. 4, is the simplified equivalent circuit showing a constant current generator, a nonlinear junction impedance, and a load. Neglected is a shunting capacitance and resistance and a series resistance. In operation, light causes a current, I, to flow in the load which is the difference between the generated short circuit current, I_s, and what flows in the non-linear junction, I_j.

I_j is the usual junction current given by

$$I_j = I_o(e^{\lambda V} - 1) \qquad [1]$$

where I_o is the dark or reverse saturation current[10] and $\lambda \equiv e/kT$, k being the Stefan Boltzmann constant and T the absolute temperature. V is the voltage applied to the junction. Since

$$I_j + I = I_s \qquad [2]$$

$$I = I_s - I_o(e^{\lambda V} - 1) \qquad [3]$$

The maximum voltage, V_{max} is given when $I = 0$. From Equation [3] one obtains

$$V_{max} = \frac{1}{\lambda} \ln \left(\frac{I_s}{I_o} + 1 \right) \qquad [4]$$

Fig. 5 shows how the current voltage characteristic of a solar cell comes about. The dark current characteristic is given by Equation [1]. In the light the whole curve is given by Equation [3] as shown. Note that I_s can be many times the dark junction reverse current. The portion of the curve in the fourth quadrant is the region of power generation. The maximum power, P_{max}, delivered is represented by the largest rectangle that can be fitted into this area, and here can be seen one of the advantages of this type of generator. It can deliver almost 90 per cent of the power generated to a load, whereas in normal-type batteries 50 per cent of the power is so available. This was first pointed out by Lehovec in 1948.[11] Therefore, the squarer the i-V characteristic, the higher the efficiency will be. It is interesting to note that in a photovoltaic junction the current flows in the reverse direction and the voltage

VOL.
3
1959

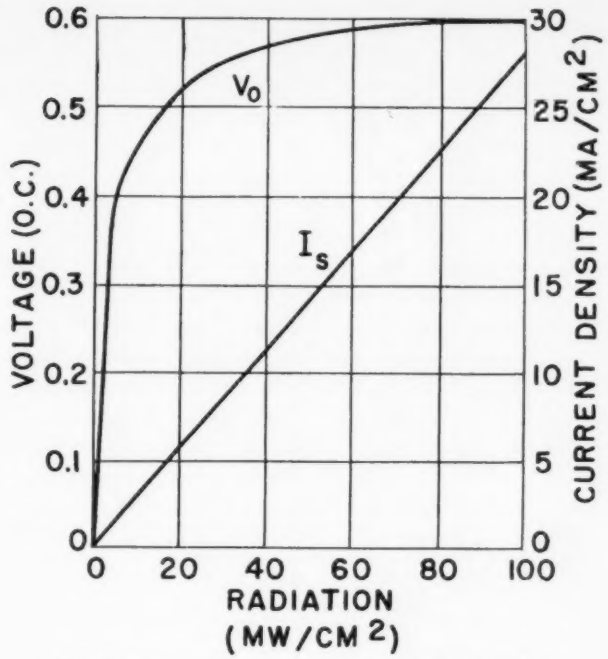

FIG. 6—V_{max} and I_s as a function of light intensity.

is in the forward direction for the usual p-n junction. Under conditions of low light level where $I_s/I_o < 10$ or where the series resistance becomes appreciable, the i-V characteristic can become linear. Examples of this will be shown later.

Fig. 6 shows how the voltage and current varies as a function of the flux density in silicon cells. Note that the current is directly proportional to the flux, while the voltage is dependent on the log of the flux according to Equation [4]. Note that the voltage characteristic shows a saturation value of voltage at high flux densities, which is quite convenient for charging storage batteries. Since the voltage is insensitive to the light level, charging can be maintained even though the light fluctuates considerably. To the right is shown the power as a function of voltage on the cell.

THEORETICAL CONSIDERATIONS

The expression for the maximum solar conversion efficiency of a solar photovoltaic cell is as follows:[12]

$$\eta_{max} = K\left(\frac{\lambda V_{mp}}{1+\lambda V_{mp}}\right)\frac{n_{ph}(E_G)V_{mp}}{N_{ph}\,E_{av}} \qquad [5]$$

where K is a constant depending on the reflection and transmission coefficients and the collection efficiency, V_{mp} is the voltage delivered at maximum power, $n_{ph}\ (E_G)$ is the number of photons that generate electron-hole pairs in the semiconductor of energy gap E_G, and $N_{ph}\,E_{av}$ is the input power where N_{ph} is the number of incident photons and E_{av} is their average energy in electron volts.

A number of interesting facts can be obtained from Equation [5], since λV_{mp} is usually much greater than 1, and $K \sim 1$, the equation can be written as follows:

$$\eta_{max} = \frac{n_{ph}(E_G)V_{mp}}{N_{ph}\,E_{av}} \qquad [6]$$

An estimate of the maximum theoretical efficiency for silicon can be obtained directly, since n_{ph} is about $\frac{2}{3}N_{ph}$ and V_{mp} is about $\frac{1}{3}E_{av}$, yielding about 22 per cent. Where monochromatic light is used with energy equal to the band gap, the efficiency can be well over 75 per cent since then $n_{ph} = N_{ph}$ and $V_{mp} \sim 0.75\,E_{av}$. Also, since $V_{mp} \propto V_{max} \propto \ln I_s$,

$$\eta_{max} \propto \ln I_s . \qquad [7]$$

Therefore at higher light intensities the maximum efficiency should increase.

Equation [6] also shows how η_{max} changes as the semiconductor energy gap is varied. Two effects take place: first the number of photons absorbed $n_{ph}(E_G)$ decreases as the band gap is increased. This is seen in Fig. 7, where the number of photons absorbed is plotted against the semiconductor energy gap. Second, the voltage increases as the band gap increases due to the reduction in I_o the dark current.[10] Fig. 8 shows the result of a calculation including these effects which shows how η_{max} varies with E_G.[12] The upper curve is calculated using standard p-n junction theory, and the lower curve shows the result if the junction reverse saturation departs from its theoretically predicted dependence on E_G. Note that these curves are for the solar spectrum that exists above the atmosphere. The optimum band gap is seen to be 1.6 ev; at that point the η_{max} is 20 per cent better than what it is for silicon. Note that in the lower curve there is little difference between materials.

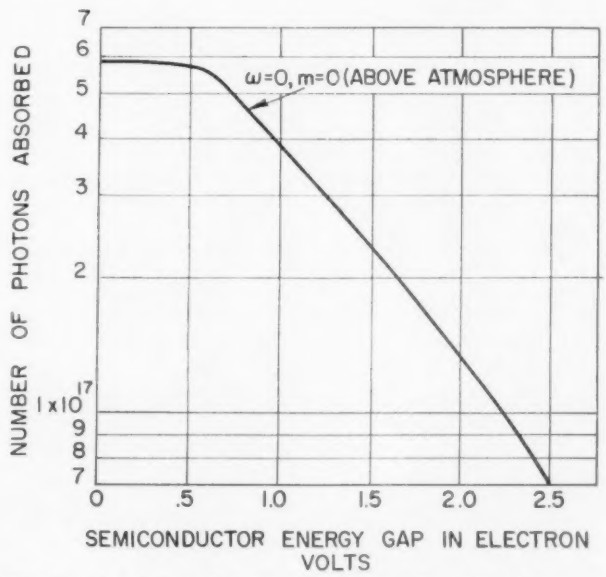

FIG. 7—Absorbtion of solar photons as a function of energy gap.

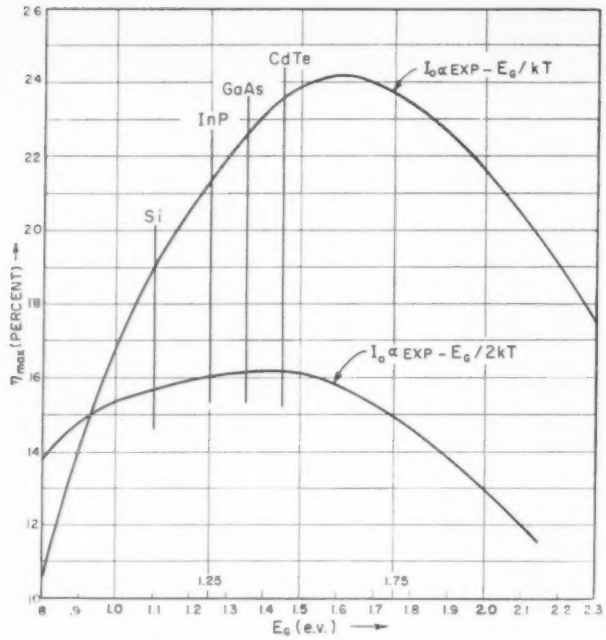

FIG. 8—Theoretical efficiency vs. semiconductor band gap.

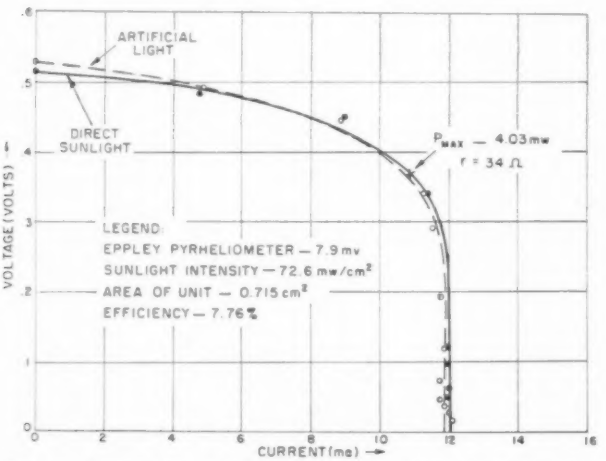

FIG. 9—Comparison of silicon current voltage characteristics in sunlight and in artificial light.

EFFICIENCY MEASUREMENTS, CALIBRATION AND SILICON RESULTS

Fig. 9 shows the *i-V* characteristic for a silicon photovoltaic cell. Note that for convenience the first quadrant is used for this plot instead of the fourth. This cell has an efficiency of 7.8 per cent, as measured in sunlight with a V_{max} of 0.52 v and an I_s of 12 ma. Note the rectangular characteristic of this curve. Also shown is the comparison of the cell's operation in sunlight and in artificial light. The purpose of this comparison is to show how efficiency is measured with an artificial light source. The major problem here is that one cannot easily duplicate the solar spectrum with an artificial light source and that the efficiency of a solar cell depends on the spectrum used. However, if one reproduces with an artificial source the same number of carriers or short circuit current in a solar cell, as the sun would produce, one can then say that the artificial source is effectively at the same solar intensity that one would measure with an absolute power measuring device such as a pyrheliometer. In the figure, the sunlight intensity was measured by the pyrheliometer to be 72.6 mw. The artificial light source was then adjusted to produce the same short circuit current, and as can be seen from the figure, the *i-V* characteristic was duplicated within a few per cent of the characteristic obtained in sunlight. Small deviations might be expected from cell to cell if the diffusion length varies by very much. This serves as a convenient laboratory method of measuring efficiency. The same technique can be used for other semiconductors; however, a separate light calibration is required for each material.

Presently available silicon solar energy converters have yielded efficiencies as high as 14 per cent; however, in production quantitites, efficiencies run between 7 per cent and 10 per cent. Such cells can be connected in series or parallel to increase the voltage or current. These cells are the easiest of all semiconductor devices to make, the major cost being that of producing the single crystal silicon wafers. Assuming a 10 per cent efficiency and a solar radiation flux of 100 mw per sq cm (the average sunlight intensity in the northeastern part of the United States during the summer), a 1-kw solar power supply would be 10 sq m in area, cost $200,000, and weigh 20 lb.

EXPERIMENTAL RESULTS ON GaAs, InP AND CdTe

Shown on Fig. 8 are three semiconductors, which, from the viewpoint of availability and stability, were selected to verify experimentally the theory described above. These materials are the III-V compound semiconductors GaAs and InP and the II-VI compound CdTe.

Two techniques were used to make *p-n* junctions on these new materials, namely, the diffusion process and the alloy process. These are similar to techniques employed with germanium and silicon. However, the scheme for doping the materials *n* or *p*-type is somewhat different. In general, a Column II element in the periodic table converts GaAs or InP into a *p*-type semiconductor, while a Column VI element converts it to *n*-type. For CdTe a Column I or VI element yields *p*-type and a Column VII or II element yields *n*-type. Fig. 10 shows the construction of a typical diffusion cell.

The major problems encountered in making efficient solar converters from these new materials has been the following:

(1) Making suitable ohmic contact to the *n* and *p*

VOL. 3 1959

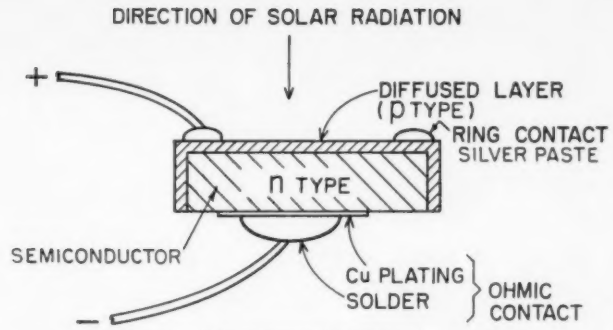

FIG. 10—Experimental photovoltaic cell.

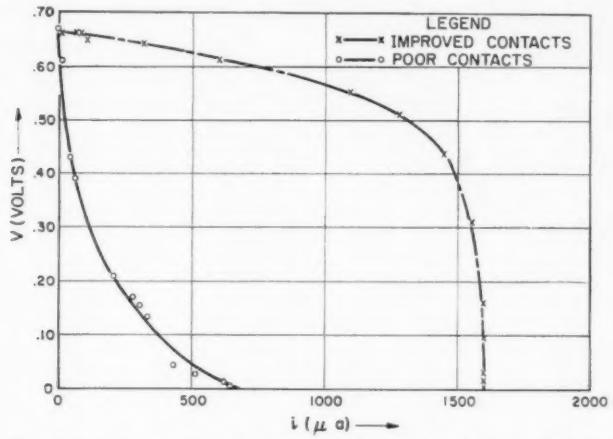

FIG. 11—Effect of contacts on i-V characteristics of GaAs solar cell.

regions. Rectifying or high resistance contacts lower the output voltage and current appreciably. In general, metallic plating and soldering or an indium alloy dot solves the problem. Fig. 11 shows the difference in i-V characteristics when poor contacts are improved in GaAs.

(2) Low resistivity in the p- and n-type regions. This is required to obtain the maximum voltage per junction and a low series resistance. This problem is solved by using highly doped original material and by controlling the alloy or diffusion process to get a maximum impurity concentration.

(3) The fact that the p-n junctions do not behave according to theory. This can be caused by poor crystal perfection, current leakage across the junction, or poor ohmic contact. The solution to this problem lies in better material, proper etching, lower diffusion temperature, and improved ohmic contacts.

Solar cells were successfully made on GaAs, InP and CdTe. Fig. 12 shows typical i-V plots in an artificial light equivalent to sunlight of about 100 mw per sq cm for a GaAs cells. The curves were obtained by varying the load resistance and measuring the voltage and current while the units were illuminated. The units were made by baking n-type GaAs in cadmium vapor for four hours (G34 and G41) and 40 hours (G49). Note that the open circuit voltage is as high as 0.9 v. This is a consequence of the large energy gap of GaAs and should be compared to a maximum voltage of 0.55 v in silicon. The impedance of these units at maximum power is about 100 ohms. The best efficiency yet obtained is 6.5 per cent in GaAs in small areas.[13] For cells about 1 sq cm in area efficiencies of 5 per cent have been obtained.

Fig. 13 shows the results obtained on InP. These units were made by the alloy process where a zinc indium dot was fired on to the InP at 500°C for 10 minutes. The zinc converts the n-type InP to p-type where it recrystallizes after having alloyed with the InP. The ohmic contact was alloyed indium. Because of the presence of the dot the exposed face was masked somewhat so that the effective area was about $\frac{1}{10}$ sq

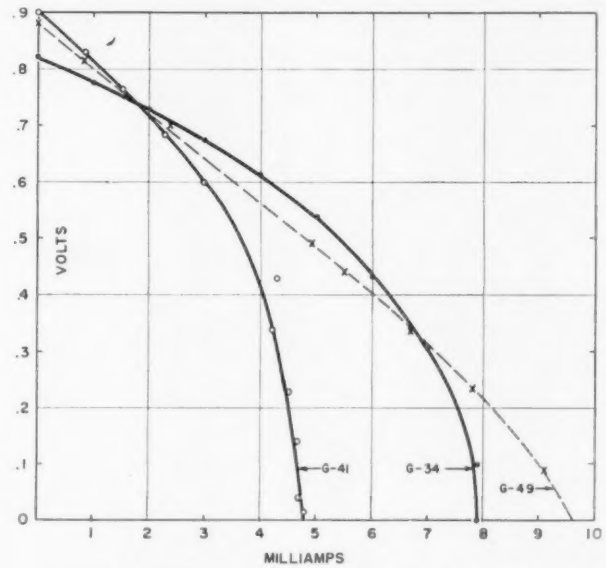

REPRESENTATIVE I-V CHARACTERISTICS OF GaAs DIFFUSION UNITS IN BRIGHT LIGHT (FML).

FIG. 12—Current-voltage characteristics of GaAs diffusion cells.

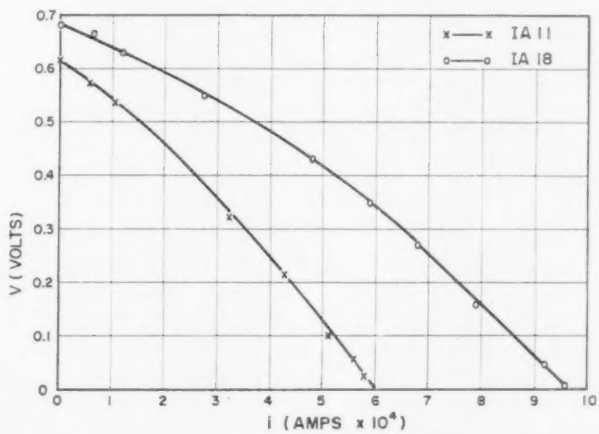

FIG. 13—Current - voltage characteristics of InP alloy junctions.

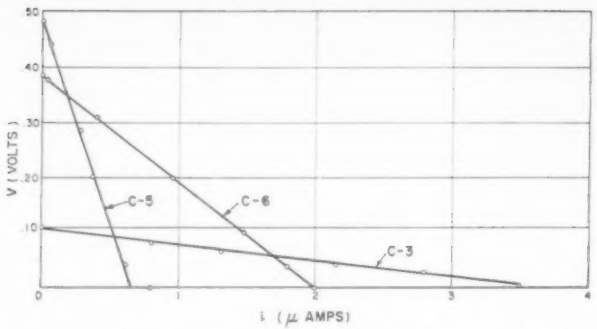

FIG. 14—Current-voltage characteristics of CdTe diffusion cells.

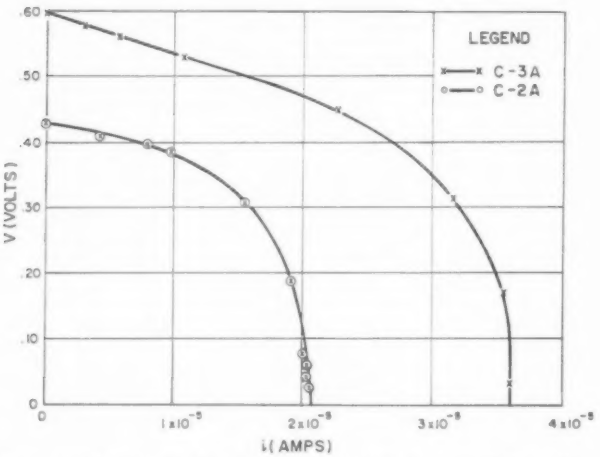

FIG. 15—Current-voltage characteristics of two CdTe alloy junctions.

cm. The maximum efficiency of IA-18 was 2 per cent. Note that the curves do not depart much from linearity. This implies the existence of a large internal resistance, about 1200 ohms for IA-11 and 700 ohms for IA-18. This is probably due to poor ohmic contact as supported by the low short circuit current, which is about 1 ma compared to about 10 ma for the GaAs.

The results for CdTe are shown in Figs. 14 and 15. With this material we were hampered by the lack of low resistivity crystals. In general, the technology of CdTe is behind that for GaAs and InP. Fig. 14 shows three current voltage curves for diffusion type junctions in CdTe. C-5 and C-6 were baked in iodine vapor at 800°C for 4 hours and C-3 in sodium vapor at 800°C for 4 hours. Indium was used as the ohmic contact to the *n*-type base wafer and silver paste to the diffused region. The output voltage is rather low considering the large band gap, i.e., 1.45 ev, and the short circuit current is quite low—about $\frac{1}{1000}$ of that in the other materials—thus reflecting a very high series resistance. This is also evident from the straight line characteristic of the curves. The resistance is given by the slopes of these lines for C-5, 10^6 ohms, C-6, 2×10^5 ohms, and C-3, 3×10^4 ohms.

Fig. 15 shows the results on the alloy-type CdTe units. The junction was prepared by alloying indium into *p*-type CdTe at 600°C for 10 minutes. Note that here the curves are rectangular, thus indicating considerably lower series resistance. The maximum conversion efficiency in CdTe has been achieved with the alloy-type junction and is 2.1 per cent.

RESULTS ON CdS AT WADC

The work on CdS solar cells under the general direction of D. C. Reynolds at WADC is quite interesting.[14] According to the theory CdS should be low on the efficiency scale. Because of its large band gap, 2.4 ev, only about $\frac{1}{5}$ of the solar photons should be absorbed. However, spectral response measurements show that a large absorption takes place in the region considerably beyond the cut-off at 0.8 ev where the crystal should be transparent, thus accounting for the high efficiencies which Reynolds reports to be up to 7.5 per cent.[15] This device does not obey the usual theory and to date is not understood. It may be possible that some ternary compound is formed near one of the contacts which has a considerably smaller band gap than CdS, thus accounting for the response at lower energy. Reynolds finds extremely long "diffusion lengths" in CdS. He finds the optimum thickness of a cell is about 0.9 mm and suggests this is due to exciton migration or a luminescence effect. A third explanation may be in the possibility of the formation of impurity bands in the heavily doped CdS.

A brief description of these cells is in order. CdS crystals grown by the vapor phase method and made *n*-type by indium doping to about 10^{-2} Ω cm are cut to about 1 x 1 x 0.09 cm. The surfaces are roughened and copper is plated onto one face and diffused into the

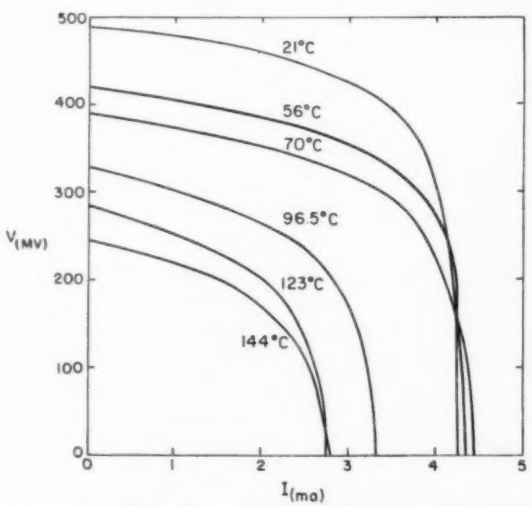

I – V CURVES FOR CdS AT VARIOUS TEMPERATURES

FIG. 16—Current-voltage curves for CdS at various temperatures.

VOL. 3 1959

interior at 460°C for less than one minute, making a p-type layer between 1 and 10 μ thick. Contact to this layer is made with a Hg-loaded expoxy resin. Contact to the n-region is made by soldering after zinc and copper plating. Note that this is a back-wall-type cell as contrasted to the front-wall cells made of silicon and GaAs, where the barrier is at the front surface.

Fig. 16 shows a series of i-V curves as a function of temperature on a CdS cell kindly supplied by Reynolds. This cell had an over-all η_{max} of 4 per cent as measured in sunlight. Note the excellent square shape of the i-V curve. The V_{max} is 490 mv and I_s is 4.5 ma. It could be expected that V_{max} should be well over 1 v in a $\delta/4$ per cent efficient CdS cell according to the usual theory. One disappointing characteristic here is the rapid fall off of I_s with temperature compared to the almost constant I_s of GaAs and silicon. Because of this and the usual decrease in V_{max} of about 2 mv per °C, the CdS η_{max} falls faster with temperature than either Si or GaAs. In fact, it appears that CdS behaves like a material with a band gap of 0.8 to 1.0 ev rather than 2.4 ev. At present there does not seem to be any high temperature advantage in using currently available CdS cells.

EFFECT OF INCREASED TEMPERATURE

One expects that any device utilizing semiconductors would be sensitive to temperature change, and photovoltaic cells are no exception. Calculations were made to see how the maximum efficiency as a function of band gap varies with temperature. It was assumed that the short circuit current was relatively independent of temperature, an assumption generally borne out experimentally and that the main variation that one observes is due to the fact that V_{max} is a function of I_o, a quantity quite sensitive to temperature.

Fig. 17 shows the results of these calculations.[16] Here, the efficiency is plotted as a function of the energy gap with the temperature as the parameter. There are two main points to be seen here, the first one being that the optimum semiconductor energy gap increases as the temperature increases. Thus at room temperature cadmium telluride is the optimum material, while at 300°C the optimum material is Z with an energy gap of 1.8 ev. The materials of Y and Z are ones that may be ternary compounds; as, for example, combinations of GaAs and GaP. The second point to observe is that the relative efficiency increases at higher temperatures when comparing a higher band gap material to silicon. For example, consider the comparison between silicon and GaAs at 150°C where it can be seen that GaAs would be almost twice as efficient a converter as silicon. However, at room temperature, GaAs is not quite 20 per cent better than silicon. Note that on these curves, CdS, although somewhat better than silicon at 150°C, is still not as good as GaAs would be. As a result of these calculations, GaAs is considered the most promising material as a high temperature (~200°C) solar converter.

Fig. 18 shows some specific temperature measurements on silicon. This is one of the early silicon devices with a somewhat lower efficiency than those made today; however, the temperature results are typical of all silicon devices. Note that the maximum voltage

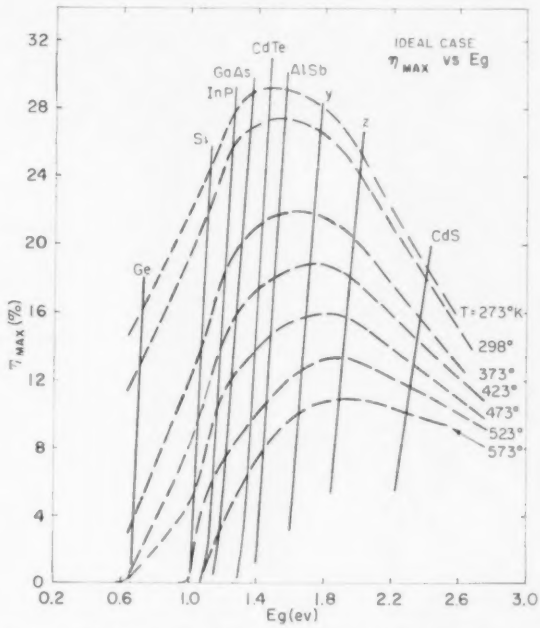

FIG. 17—Efficiency vs. energy gap for various temperatures.

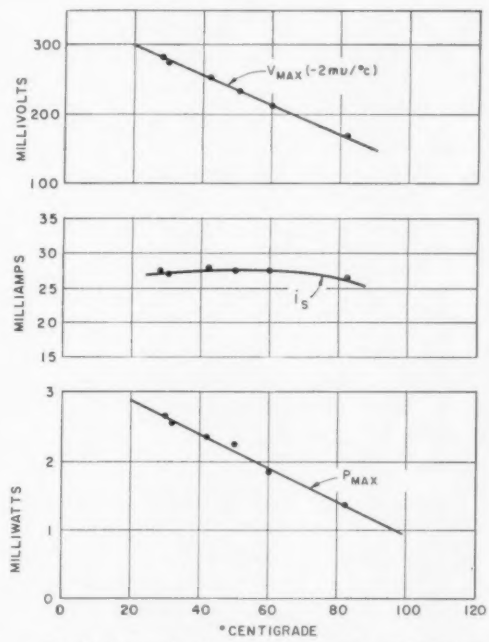

FIG. 18—Variation of silicon solar cell parameters with temperature.

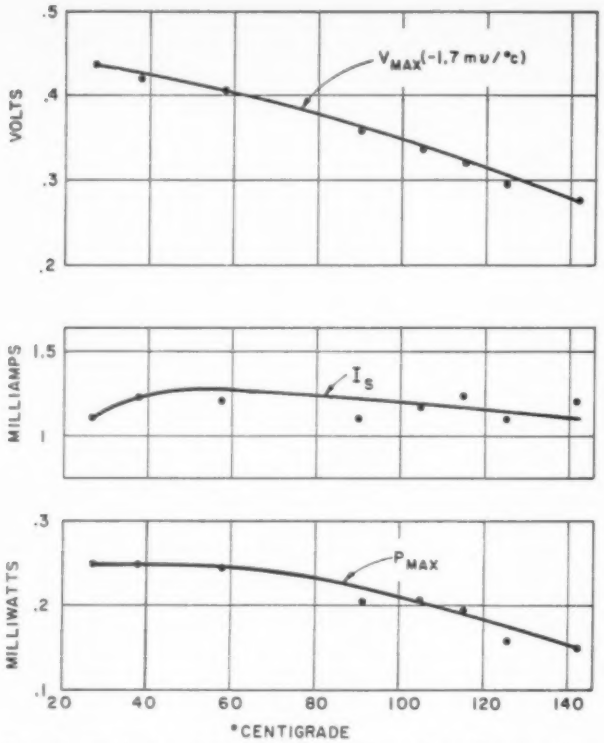

FIG. 19—Variation of GaAs alloy junction solar cell parameters with temperature.

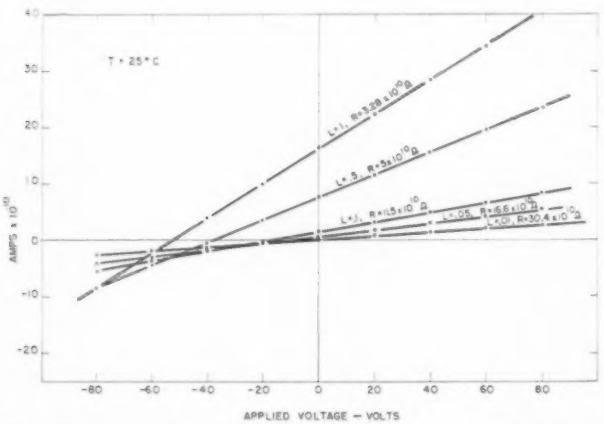

FIG. 20—Current-voltage characteristics for CdTe films at varying light intensities.

decreases with temperature at the rate of 2 mv per °C. The middle curve shows how the short circuit current remains relatively constant with temperature. The bottom curve shows how the maximum power decreases with temperature. The slope is approximately 0.02 mw per °C.

Fig. 19 shows similar results for GaAs. This represents one of the better cells. Many other cells have shown quite varied characteristics, many of which were poorer than the one shown. The voltage is seen to decrease at the rate of 1.7 mv per °C. The current is seen to be reasonably constant, and the power decrease is somewhat less than that of the silicon unit.

A NEW HIGH VOLTAGE PHOTOVOLTAIC EFFECT

Since the major expense in making silicon solar converters is in the production of the single crystal, possibilities of preparing cells by deposition methods such as evaporation, sputtering, etc., were studied. During this work a very interesting effect was discovered by Pensak and later worked on by Goldstein.[17] They found that, when cadmium telluride was evaporated at an angle onto a pyrex substrate at about 100–200°C to a thickness of about one micron and when suitable electrical contacts were made to the film, under bright light illumination such films could produce as much as 1500 v per cm.

Fig. 20 shows the *i-V* characteristic of the CdTe evaporated films. Note the high impedance and high voltages. Decreasing the temperature increases the voltage to about 300 v at liquid nitrogen temperatures. Such films exhibit high resistance on the order of 10^{13} ohms per square in the dark, and, as a result, the currents produced by such cells are quite low. As a matter of fact, at present, these cells have very low energy

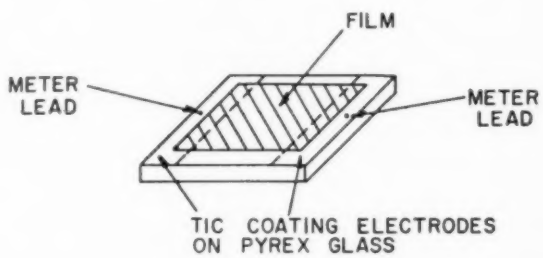

TYPICAL PHOTOVOLTAIC CELL

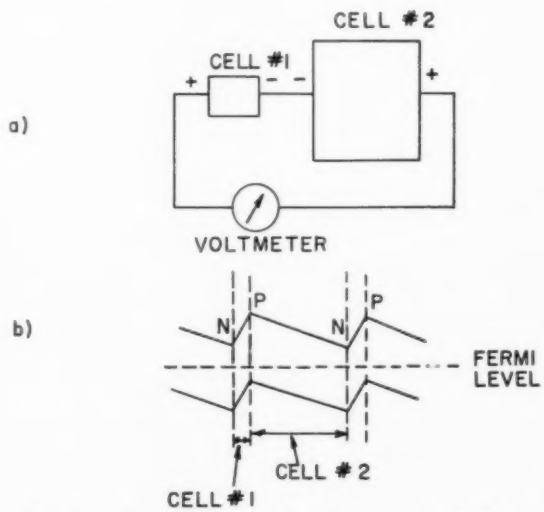

FIG. 21—Representations of series-connected cells.

VOL. 3 1959

conversion efficiencies, being on the order of 10^{-4} per cent. However, this is a breakthrough into a new and interesting type of photovoltaic converter which warrants further research.

Fig. 21 shows schematically what such films look like. At the top you see the film on glass. Contacts are made by using a transparent conducting coating and silver paste. In order to explain the extremely high voltages, one must assume that there are many *p-n* semiconductor barriers, possibly grain boundaries, that are somehow connected in a series chain. This would, however, not be enough to explain the results, since such a series connection would result in a voltage typical of just one barrier. The remaining barriers would cancel one another. In order to explain the present result, one must assume that the barriers are asymmetric. This is shown schematically at the bottom of the figure where a steep junction is shown between the *n-p* transition and a rather broad junction between the *p-n* transition. With light shining normally on such a configuration, assuming the lifetime to be small, it can be seen that carriers may be collected in the *n-p* region, but not from the *p-n* region, since those carriers generated in the *p-n* region would very easily recombine before being collected. These asymmetries may also be caused by impurity gradients, lifetime inhomogeneities, or stacking faults which are hexagon to cubic crystal structure transitions. Such stacking faults have been observed in II-VI compounds. Work in ZnS has shown correlations between a high voltage photovoltaic effect (produced by ultraviolet radiation) and stacking fault structures. Voltages of 50 to 100 v have been observed at room temperature, and 350–400 v at liquid nitrogen temperatures.

PROBLEM OF IMPROVED EFFICIENCY

There are five areas in which to seek higher efficiency in the single-crystal-type solar converters. Not all of the following areas can be optimized independently of the others. A good compromise is the best that can be expected.

(1) Spectrum matching. Here we have the problem of utilizing the maximum energy of the photons absorbed. Only for photons of band edge energy is this realized. At higher photon energies the excess energy beyond the band gap is imparted to the electron-hole pairs and is eventually dissipated as heat. A considerable improvement in efficiency could be realized if this problem were solved. Jackson has suggested[18] the possibility of using sandwich structures of differing band gap semiconductors. The sunlight is allowed to strike first the widest gap material, which absorbs part of the spectrum and transmits the rest to the next widest gap semiconductor. This material absorbs part of the spectrum and transmits the rest in turn to the next material, and so on. He calculates that for three semiconductors of 0.94, 1.34, and 1.91 ev band gap respectively a solar conversion efficiency of 69 per cent is possible and where ten different materials are used 86 per cent efficiency is theoretically possible.

Such devices would be difficult to construct mechanically, and each semiconductor would require a separate electrical connection. Series or parallel connection of the different semiconductors would either degrade the individual V_{max}'s or I_s's. The optical reflection from each interface would have to be reduced by special interference films. It has been suggested that such cells would be more expensive than the most valuable real estate, so that it would be much more economical to use more area and lower efficiency for most applications.

(2) Reflection and surface-recombination problems. These two problems are grouped together since it appears that the optimum condition exists when a compromise between the two is made. A surface with low optical reflection shows high surface recombination (loss of generated carriers by recombination at the surface) and vice versa. Prince has measured a 4 per cent reflection on 10 per cent efficient silicon solar cells whereas normal clean silicon surfaces have a 30 per cent reflection coefficient.[1] If a steep doping gradient or band gap gradient (i.e., GaP on GaAs) is built in very close to the surface even high surface recombination or a high absorption coefficient do little harm, since the carriers would be accelerated inward towards the junction before recombination can take place.

(3) Bulk recombination. This is a question of placing the junction at the optimum depth from the surface so that the greatest number of generated pairs are collected by the junction. A large diffusion length of about 10^{-2} cm is required to collect carriers generated by near band gap radiation. Such diffusion lengths are difficult to obtain where a semiconductor is highly doped and where it has first to be subjected to high temperatures in the fabrication procedure. In general, where a junction is shallow (limited by high series resistance), the carriers produced by high energy photons that do not get trapped by the surface are collected while the ones generated by longer wavelengths are lost due to bulk recombination. The opposite becomes true as the junction is made deeper.

(4) V_{max} limited to less than the band gap. The V_{max} for good silicon cells is about $\frac{1}{2}$ the value theoretically possible for a junction formed by highly doped *n*- and *p*-type regions. In GaAs this voltage has been as high as $\frac{2}{3}$ of the gap. While it is not possible to realize the complete band gap voltage higher doping should yield higher efficiencies.

(5) Series and shunt resistance. These parameters can reduce efficiency seriously, although in practice it

is not difficult to eliminate them entirely. Once the proper doping has been achieved, optimum contact arrangement can be employed to negate these two parameters. A shallow junction will add to series resistance, so that here again junction depth must be optimized.

CONCLUSIONS

In these conclusions the advantages and disadvantages of present solar cells as energy conversion devices are summarized.

The advantages are:

(1) Photovoltaic cells have given the highest over-all conversion efficiency from sunlight to electricity yet measured. The best value reported is 14 per cent.

(2) Such cells are easy to fabricate being one of the simplest of semiconductor devices in this category.

(3) Unlimited life.

(4) High power-to-weight ratio for satellite applications yielding 20 lbs per kw on the ground where 10 per cent cells are used in sunlight of 100 mw per sq cm and about 80 lbs per kw in satellite applications where 10 per cent cells are used in sunlight of 135 mw per sq cm but where tumbling, rotation, cell matching, higher temperature, light losses in cover, etc., are taken into account. A cell 15 mils thick with contacts is considered in the above.

(5) Photovoltaic cells are area devices that don't require high temperatures for high efficiencies, thus eliminating lenses and concentrators in all but very special applications.

(6) Where large scale application will one day be achieved the problems of power distribution by wires will be eliminated by using solar cells at the site where the power is required.

The two main disadvantages to date are the high cost and the need for a storage device.

In the near future silicon solar cells should be available with efficiencies in the 15 per cent range. Cells using other materials or combination of materials should be capable of 20 per cent conversion efficiency and large area polycrystalline films in the square foot range should yield 5 per cent efficiency. Such devices will represent very strong competition in the solar energy conversion field for the thermoelectric or thermionic devices which are showing promise.

ACKNOWLEDGMENTS

It is a pleasure to thank Mr. William Cherry of USARDL for his enthusiastic support of the work at the RCA Laboratories during the past four years. Dr. J. J. Loferski has been a major contributor to much of the work discussed. Messrs. Pensak, Wysocki and Dr. Goldstein have also contributed to the material used.

REFERENCES

1. M. B. Prince; M. Wolf. *J. Brit. IRE* **18:** 583, 1958.
2. E. Becquerel. *Compt. Rend.* **9:** 561, 1839.
3. W. G. Adams; R. E. Day. *Proc. Roy. Soc.* **A25:** 113, 1877.
4. B. Lange. *Zeit. Phys.* **31:** 139, 1930.
5. L. O. Grondahl. *Rev. Mod. Phys.* **5:** 141, 1933.
6. W. Schottky. *Zeit. Phys.* **31:** 913, 1930.
7. P. Rappaport. *Phys. Rev.* **93:** 246, 1954. Also Rappaport, Loferski, Linder. *RCA Review*, **17:** 100, 1956.
8. Chapin; Fuller; Pearson. *J. App. Phys.* **25:** 676, 1954.
9. Reynolds; Leies; Antes; Marburger. *Phys. Rev.* **96:** 533, 1954.
10. W. Shockley. *Electrons and Holes in Semiconductors.* D. Van Nostrand Co., New York, 1950, p. 314.
11. K. Lehovec. *Phys. Rev.* **74:** 463, 1948.
12. J. J. Loferski. *J. App. Phys.* **27:** 777, 1956.
13. D. A. Jenny; J. J. Loferski; P. Rappaport. *Phys. Rev.* **101:** 1208 1956.
14. D. C. Reynolds. (In: *Trans. Conference on the Use of Solar Energy*, Univ. of Arizona Pr., 1955, Vol. 5, p. 102.)
15. D. C. Reynolds. Private communication.
16. J. J. Wysocki; P. Rappaport. To be published in *J. Appl. Phys.* Apr. 1960.
17. B. Goldstein; L. Pensak. *J. App. Phys.* **30:** 155, 1959.
18. E. D. Jackson. (In: *Trans. Conference on Use of Solar Energy.* Vol. 5, p. 122.)

VOL. 3 1959

Selective Radiation Coatings. Preparation and High Temperature Stability

By Panos Kokoropoulos, Ehab Salam, and Farrington Daniels

Solar Energy Laboratory and Department of Chemistry, University of Wisconsin

Selective radiation coatings suitable for operation at high temperatures with focused sunlight are described. Coatings of CuO and Co_3O_4 on polished nickel, silver, and platinum have high absorptivity for solar radiation and low emissivity in the infrared when heated. They are stable at at high temperatures.

Selective radiation coatings are useful for heating by solar radiation. The development of efficient thermoelectric converters and proposals for utilizing solar energy in space vehicles call for increased research efforts in the development of surfaces which will absorb most of the sun's radiation (from 0.3 to 2.5 μ) and which will emit only a small fraction of the farther infrared radiation emitted by a heated black body. It is necessary that these surfaces withstand extended operation at high temperatures, above 500°C in boilers and thermoelectric generators, as well as operation in the neighborhood of 100°C.

Tabor[1] has shown that selective radiation surfaces can be made by placing a thin black coating on a bright polished metallic surface. Hottel and Unger[2a, b] have described an excellent selective surface obtained by spraying an aqueous solution of cupric nitrate on polished aluminum under controlled conditions and then heating to give a film of cupric oxide. The preparation, emissivity in the infrared and solar absorptivity of several selective radiation surfaces has been reported,[3] including an oxidized and chlorinated surface on copper, manganese dioxide on stainless steel, molydenum oxide compounds on aluminum, and other special coatings.

The object of the present investigation[4] was to prepare selective coatings by electroplating copper, cobalt, and other suitable metals on polished, reflecting metallic surfaces and oxidizing them by heating in air; to measure their emissivities and their absorptivities for solar radiation, and to investigate their stability at high temperatures.

It is planned to continue this work in an attempt to contribute to the theories involved and to find still better selective coatings.

EXPERIMENTAL PROCEDURES

Circular plates of metal 7.5 cm in diameter and 0.1 to 1 mm thick were treated with acid, highly polished with rouge and cleaned with carbon tetrachloride to remove grease until water gave a uniform film on the surface. They were then electroplated to give layers 10^{-5} to 10^{-4} cm in thickness. The thickness of the plated film was determined in two ways—by measuring the electric current and the time of plating, and by direct weighing on an analytical balance before and after plating. It was assumed that the density of the oxide film is the same as the bulk density of the oxide and the roughness of the surfaces has been neglected in these calculations.

Copper was electroplated from a solution of 2.25 per cent CuCN, 3.4 per cent NaCN and 1.5 per cent Na_2CO_3 at a current density of about 0.003–0.015 amperes per sq cm. Cobalt was electroplated from a hot solution of $CoSO_4 \cdot 7H_2O$ 50 per cent, NaCl 1.5 per cent and H_3BO_3 4.5 per cent at 40°C and at a current density of about 0.05 amperes per sq cm.

Extensive experiments were carried out with black coatings produced by dipping copper into a concentrated solution of 500 gm of sodium chlorite and 250 gm of sodium hydroxide per liter of water at 100°C. However, the work was discontinued because although the coating is adherent it is actually a mixture of oxides and chloride compounds.

The absorptivity of solar radiation was determined with an apparatus similar to the one described by Tabor.[5] It consists of a tube 9 cm in diameter and 16 cm long on a heliometer base, which can be rotated quickly so that either end may be pointed directly at the sun. The metal disc at the center has on one side the selective radiation coating and on the other side a coating of lamp black (camphor smoke) assumed to have an absorptivity of 0.95. The tube is insulated and each end is covered with a quartz window and a removable cap. A sensitive thermocouple is attached to the edge of the disc so that it is not directly radiated by the sun, and is connected to a recording potentiometer.

Absorptivity measurements were made only on

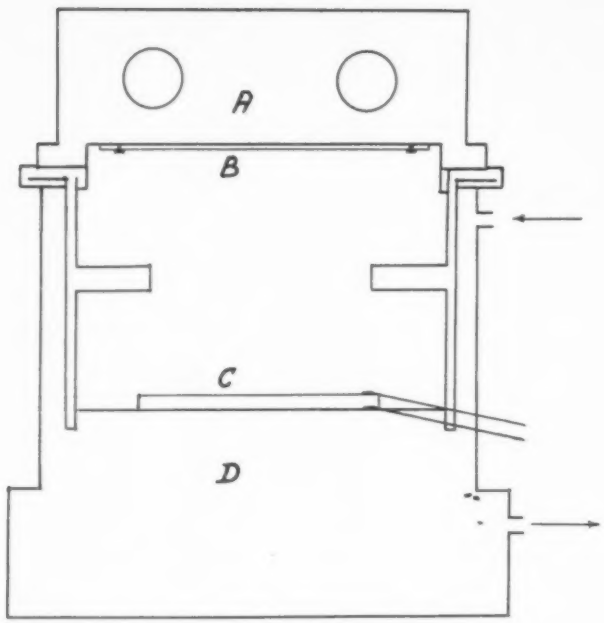

FIG. 1—Emissivity measurement apparatus.
A.—heating thermostat
B.—radiating sample
C.—radiometer
D.—cooling system

cloudless days, and a succession of cycles 150 seconds long was recorded, alternating between the lamp black coating and the selective radiation coating. The absorptivities were calculated from the temperature differences as recorded for the two sides using formulas described by Tabor[5] and Guild.[6]

The relative emissivities were determined on the same coated discs that were used for the absorptivity experiments. They were measured with an instrument similar to that described by Taylor et al,[7] as shown in Fig. 1. The coated metal disc is placed at one end of an insulated aluminum cylinder and thermostated at 110°, 140°C, or other temperature. A radiometer of 110 copper constantan junctions was placed 5 cm away at the other end of the cylinder and protected with radiation screens. It was made under the direction of Professor V. E. Suomi of the Department of Meteorology of the University of Wisconsin from a design described by Heilman.[8] The recorded radiometer readings were converted into emissivities by a calibration procedure in which a radiation emitter of bright aluminum foil, assumed to have an emissivity of 0.03, was covered tightly with sectors of black paper of various areas, assumed to have an emissivity of 0.95. The ratio of black and polished aluminum areas permitted a setting which agreed roughly with the emissivity recorded for the selective radiation coating, and the relative radiation received was compared with that from a known radiator. The instrument was further checked with the

TABLE I—Emissivity of Selective Radiation Coatings

CuO thickness	Co_3O_4 thickness	Underlying metal	Per cent black body 140°C	After second heating
2.4×10^{-5} cm		Ag	0.10	
2.8		Ag	.11	
4.9		Ag	.14	
2.4		Ni	.17	0.18
2.8		Ni	.19	.27
4.9		Ni	.25	.28
3.0		Pt	.13	
	6.8×10^{-5} cm	Ag	.27	
	12	Ag	.29	
	19	Ag	.30	

(Flat black paint, 0.95)

emissivity of polished iron at 0.52 and with the emissivity of polished copper, nickel, and brass.

RESULTS

Emissivity data are summarized in Table I and Fig. 2.

It is seen in Fig. 2 that the emissivity of the surface coated with thin layers of CuO or Co_3O_4 is directly proportional to the logarithm of the thickness of the layer.

The higher emissivity of cupric oxide on nickel than on silver at high temperatures is due to the fact that the nickel surface becomes oxidized and roughened by oxygen which diffuses from the air through the oxide coating. This explanation was confirmed as indicated in Table I by finding that a second period of heating increased the emissivity still more.

The measurements of solar absorptivity were less accurate. A coating of CuO (2.3×10^{-5} cm) on polished

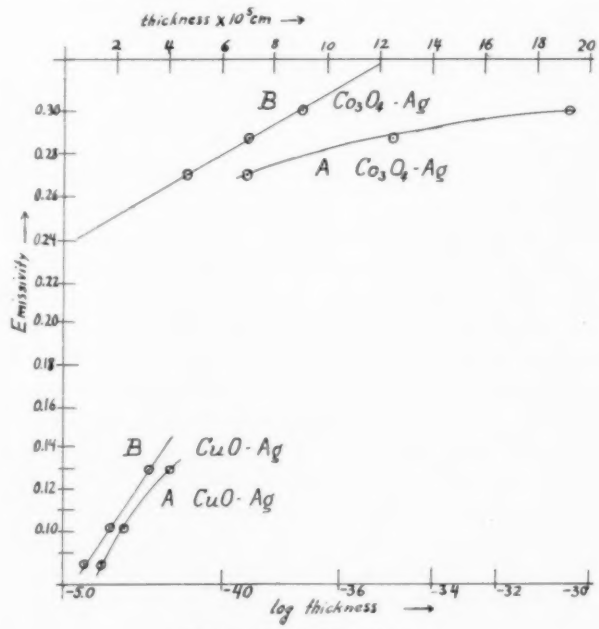

FIG. 2—Emissivity data.
A.—emissivity vs. thickness
B.—emissivity vs. log thickness

VOL. 3 1959

silver gave an absorptivity of 0.76, as much as that of a perfect blackbody absorber, a coating of CuO (2.4×10^{-5} cm) on nickel gave an absorptivity of 0.81 and a coating of Co_3O_4 (6.8×10^{-5} cm) on silver gave 0.90. In general the absorptivity increases with the thickness. With very thin coatings, the reflectivity of the underlying metal is an important factor in the absorptivity of solar radiation, but with thick coatings it is less important.

At temperatures in the neighborhood of 100°C, attainable with flat-plate collectors, many black coatings are stable and suitable for extended operation. At temperatures in the neighborhood of 500°C and above, only a few coatings are permanent. Black paint, organic matter, and sulfides will all be removed by oxidation. The black oxides are best, but at very high temperatures they will dissociate, and if there is a chance of removing the metal or the gaseous oxygen, they will not be permanent. Again, at high temperatures some metals will recrystallize and change the character of the surface and at still higher temperatures they will melt.

The results on the stabilities of coatings are summarized in Table II.

TABLE II—Stability of Selective Coatings in Air

Coating	Thickness	Underlying metal	Temperature °C	Properties
CuO	3×10^{-5} cm	Ag	Above 600° Above 800°	Ag crystallizes Cu alloys with Ag
CuO	3	Pt	600°	Excellent (at least 3 hr.)
			800°	Cu alloys with Pt
Co_3O_4	6	Ag	600°	Excellent coating but Ag crystallizes
	19	Ag	800° 900°	
Co_3O_4	7	Pt	1000°	Excellent

The emissivities for cobalt oxide films were considerably higher than those for cupric oxide, but part of the difference is due to the fact that the cobalt oxide coatings are thicker.

The nature of the surface of the underlying metal is extremely important in keeping the emissivities low. It was found essential to give the metals a high polish. In the case of chemically produced black coatings on copper or brass it was found possible to increase the emissivity of the selective radiation surface from 20 per cent to more than 40 per cent by sand-blasting the polished surface.

In the case of cupric oxide on silver the coating disappeared after 17 hours at 700°C. Similar results were determined with cupric oxide on platinum. The dissociation of CuO at this temperature is slight, but the metallic copper released by the dissociation appears to become alloyed with the metal and removed, so that the equilibrium is upset and the dissociation becomes complete. Cobalt oxide gave superior stability and did not alloy with either silver or platinum. After 12 hours at 900°C, the Co_3O_4 on silver was in excellent condition, but the underlying silver contained many small crystals. Cobalt oxide on platinum was heated at 1100°C for 26 hours and showed no alloying nor loss of blackness.

Various combinations of metals were tried. Copper is very unsatisfactory as an underlying metal at elevated temperatures because the oxygen of the atmosphere diffuses through the oxide film and attacks the bright copper surface, making the oxide coating thicker, so that it loses much of its selective radiation property. Eventually it becomes so thick that it peels off mechanically. Nickel oxidizes at still higher temperatures, but silver and platinum are inert toward oxygen, although oxygen dissolves in hot silver. Satisfactory results were obtained at 500° by electroplating nickel with silver, electroplating a thin coating of copper on the silver, and then oxidizing the outer copper layer. Unsatisfactory results were obtained when copper was plated with silver and then with a thin coating of copper, because atmospheric oxygen diffused through both the copper oxide and the silver layer and formed a coating of oxide on the underlying copper which then peeled off.

Thin coatings of copper oxide and cobalt oxide made from the electroplated films as described here were remarkably adherent and could not be easily scratched off. If the coatings were too thick, however, they were not mechanically satisfactory. Microscopic photographs showed the coatings to be finely crystalline, but extremely uniform. If the oxide exists in different crystalline forms there is a chance for instability over a temperature range. No such difficulty was detected with cobalt oxide, but nickel oxide with its green and black oxides was not studied for this reason.

Qualitative experiments were carried out with the oxide-chloride coating on copper. Reflectivity measurements were made at different wavelengths throughout the infrared with a Perkin and Elmer infrared spectrometer provided with a 45° prism reflector which intercepted the light beam from the source and reflected it at right angles to the coated copper surface, which in turn reflected it back into the spectrometer. Comparison of the intensity of radiation at each wavelength for the coated copper and a front-silvered mirror showed that the reflectivity is less with thicker coatings and that the specular reflectivity of polished copper is reduced (i.e., the absorption is increased) by the copper oxide coatings much more for the short wavelengths, around 3 μ, than for the longer wavelengths, around 9 μ.

These measurements support the direct measurements of absorptivity and emissivity previously recorded.

In another experiment, coated copper tubes, 18 cm long and 2.5 cm in diameter, heated to 250°C, were used as sources of radiation, and the radiation intensity was measured at different wavelengths with the infrared spectrometer, using a wide (2-mm) slit. The total area under the recorded emission curve was taken as a relative measure of the heat radiated by the tubes. Taking the copper surface coated with lamp black as unity, highly polished copper gave 0.10 and coated copper gave from 0.23 to 0.68, depending on the thickness of the black coating.

DISCUSSION

Many combinations of thin coatings of semiconductors on highly reflecting metals can give surfaces which absorb more than 85 per cent of the solar radiation at temperatures somewhat above 100°C and emit less than 20 per cent of the infrared radiation emitted by an ideal blackbody radiator.

For good selective radiation properties (i.e., high absorption in the solar region (0.3 to 2.5 μ) and high transparency and low emissivity in infrared in the general region of 5 to 10 μ) the coating must have a thickness ($10^{-5} - 10^{-4}$ cm) which is about equal to the wavelength of the radiation to be absorved and about $\frac{1}{10}$ or less of the infrared radiation which is emitted by the heated surface.

The thin coating must be a black semiconductor. There is a close relation between the electrical conductance and the optical properties which in turn are determined by the atomic number and the unfilled electronic shells. The oxides of the transition elements are suitable for such selective radiation coatings. The greater the electrical conductance, the lower is the emissivity. A thin film of cupric oxide has a lower emissivity than a thin film of cobalt oxide. The electrical properties of many of the semiconductors are well known, but the optical properties and the emissivity of thin films are less well known. The semiconductors, which increase in conductance as the temperature is raised, should give lower emissivities (in comparison with that of a perfect blackbody radiator) at higher temperatures.

Another factor which needs further study is the role of extra dissolved oxygen in the conductance and the emissivity of the semiconductor.

Another aspect of the problem which calls for further research is the practical production and engineering studies of these selective radiation surfaces. Small units can be placed in electrical ovens at 400°C and oxidized in air in a few hours. If they are too large or if they contain parts which cannot be heated to 400°C, other methods are needed. The heat conductance of large metal sheets is so good that it is difficult to bring the temperature high enough with small heating units or blasts of hot air. It has been found satisfactory to oxidize a surface electroplated with copper in air at high temperatures using focused sunlight from an army searchlight.

CONCLUSIONS

Selective radiation surfaces for operation in the neighborhood of 100°C can be made from thin coatings of semiconductors of black oxides on several different polished metals. For operation at higher temperatures, the number is quite limited on account of chemical or physical changes. Copper oxide on silverplated nickel is probably satisfactory at temperatures up to about 500°C. Cobalt oxide on platinum appears to be chemically and physically stable at 1000°C and is the most reliable selective radiation surface yet studied at these high temperatures. It has a somewhat higher emissivity than cupric oxide at 140° and experiments to measure its emissivity at 1000° are now underway. The actual temperature reached under equilibrium conditions with sharply focused sunlight will of course be the most significant measurement.

If the selective radiation surfaces are to be used in space vehicles, a further limitation may be placed on the stability of the oxide coatings. When the surfaces are heated to a high temperature in an exceedingly high vacuum such as exists in outer space, the few molecules of oxygen released by slight dissociation will be quickly removed from the surface and the equilibrium will be upset, so that the dissociation into metal and oxygen gas runs to completion, leaving only the metal and destroying the surface which absorbs the solar radiation. This difficulty can be overcome by keeping the temperature low, by using black oxides with very low dissociation pressures, or very slow rates of dissociation, or by enclosing the surface with extra oxygen in a gas-tight envelope of quartz or other transparent material. It is possible, too, that in a high vacuum the escape of oxygen, enclosed in the oxide as an impurity, may decrease the conductivity and increase the emissivity.

Further investigations of the absorptivities and emissivities of many oxides and metals at high temperatures are needed, together with a more complete understanding of the theories involved. The work is being continued in this laboratory.

VOL.
3
1959

ACKNOWLEDGEMENT

The authors are indebted to Mr. George Blytas for many conferences on theoretical material and calculations. They wish to acknowledge generous financial support from the Rockefeller Foundation and the Guggenheim Foundation. They wish to acknowledge

also support in the form of a Fulbright Fellowship and a Smith-Mundt Grant.

REFERENCES

1. H. Tabor. *Bull. Res. Council Israel* **5A:** 119 *Ibid.* **5C:** 5, 1955. Also in: *Transactions of the Conference on the Use of Solar Energy—the Scientific Basis, Tucson, 1955.* Vol. 2, Part 2, p. 24.
2. a. Proceedings of the Symposium on the Thermal Uses of Solar Energy, Montlouis, France, June, 1958. (In press)
   b. T. A. Unger. "The preparation of selectively black surfaces for use in the collection of solar energy." Thesis (Ph.D.)—Massachusetts Institute of Technology, 1958.
3. E. Salam and F. Daniels. Proceedings of the Symposium on the Thermal Uses of Solar Energy, Montlouis, France, June, 1958. (In press)
4. Reported at the meeting of the National Academy of Sciences, Bloomington, Indiana, Nov. 16, 1959. Also, P. Kokoropoulos and F. Daniels. *Science* 130, 419, 1959.
5. H. Tabor. *J. Sci. Instr.* **33:** 356, 1956.
6. J. Guild. *Proc. Roy. Soc.* **A161:** 1–38, 1937.
7. C. S. Taylor, L. A. Willey, D. W. Smith, J. D. Edwards. *Metals and Alloys* **9:** 989, 1938.

Optimum Storage of Heat with a Solar House

By Edward Speyer

Central Research Laboratory, American Machine & Foundry Company, Stamford, Connecticut

This paper reports calculations of the economic feasibility of solar house heating (and cooling) for different localities in the United States, and presents results in terms of maximum cost per square foot of solar collector which can be afforded if the solar system is to be competitive. Sunny mountainous regions, with cold winters (large fuel bills to be saved) are the most favorable areas.

Particular attention is given to the efficiency and capacity of energy storage and to the possibilities of saving summer heat for winter use. It is found that long-term storage is less economical than short-term storage. Storage costs of about a dollar per therm (10^5 Btu), or solar collectors built and installed for $1.50 per sq ft, would make solar houses commercially competitive.

INTRODUCTION

The two main parts of a solar house heating system are the solar energy collector (generally on the roof) and the energy storage facility. Collection and storage should each be considered in terms of capacity and efficiency. Collector capacity is the area perpendicular to the sun; collector efficiency is the percentage of incident solar energy which is stored or usefully employed. Storage capacity is the number of Btu's which can be released at night or on cloudy days; storage efficiency is the percentage of energy previously put in storage which is available after a certain period of storage time.

Solar house heating systems with short-term energy storage (for night use, and for two or three cloudy days in succession) use solar energy chiefly when it is least available, i.e. in winter. Long-term energy storage, which will substantially carry over summer heat for winter use, means that at least 50 per cent of the energy put into storage must be available three months later, and that the quantity of stored energy must be sufficient to reduce significantly the collector area needed. Long-term storage has generally been rejected as too expensive, the reasoning being that the extra storage capacity is needed only a small proportion of the time. However, long-term storage involves not only larger *capacity* but also improved *efficiency*; the solar heating system thus benefits *every* day from the reduction in energy leakage and loss. This report investigates energy storage as to both capacity and duration (efficiency) as functions of collector area and efficiency, climatic conditions (suitable geographical areas in the U. S.), auxiliary heating, air conditioning, and cost. The purpose is six-fold:

(1) To determine the optimum combination of collector area, heat storage capacity, and storage efficiency for solar houses in different parts of the U. S.

(2) To determine the effect on the above combination when auxiliary (non-solar) heat is furnished.

(3) To determine the cost per square foot of collector which would make solar house heating economically competitive with fossil fuels in the United States today.

(4) To determine the effect of possible future improved energy storage methods on the economic feasibility of solar house heating.

(5) To determine the feasibility of combining solar-powered air conditioning with solar house heating.

(6) To determine where, and by how much, breakthroughs in technology would make solar house heating economically feasible.

A number of investigations of solar house heating have appeared in the literature.[1-7] Four distinctive features of the present investigation may be noted:

(1) The optimum storage efficiency, and in particular when it should be long-term or short-term, is not decided in advance, but calculated.

(2) Storage capacity is taken as one of the variables in the calculation.

(3) In the solar house investigated in this paper, auxiliary (non-solar) heat is occasionally furnished, but only the hot water heater is used. The conventional furnace is eliminated.

(4) The collection efficiency is considered as varying with collection temperature and the collection temperature as varying with the amount of heat in storage.

PRINCIPAL CONCLUSIONS

(1) There is no general area in the United States where solar house heating is economically feasible today. To become competitive, one of four things must happen:

(a) Severe rationing of coal, fuel oil, and gas.

(b) The cost of fuel for house heating must go above

VOL. 3 1959

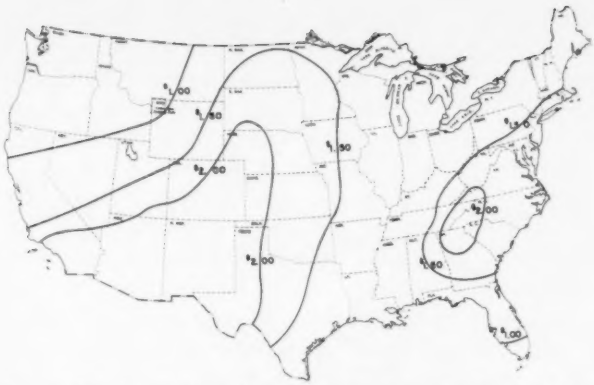

FIG. 1—Maximum allowable cost for each square foot of solar collector, assuming conventional energy storage and fossil fuels at 18¢/therm.

approximately 50 cents a therm. (This is somewhat less than the cost of electric heat today; a therm is 10^5 Btu.)

(c) An 80 per cent to 90 per cent reduction in the present cost of long-term energy storage of between 300 and 700 therms.

(d) Development of methods of building and installing solar energy collectors of 50 per cent efficiency under average conditions (See Fig. 3) for $1.50 per sq. ft. (See Fig. 1.)

(2) From an economic point of view, the most favorable regions for solar house heating, fuel costs being assumed equal, are mountainous regions and high plateaus (the Appalachian highlands and the Southwest plains). These regions have cold winter temperatures (large fuel bills to be saved) and large amounts of winter sunshine (relatively small collector area required). The least favorable regions are the Pacific Northwest, the Mississippi Valley, and the Gulf Coast (See Fig. 1).

(3) The relative feasibility of solar house heating in different parts of the United States varies by a factor of about three. That is, the maximum price that can be afforded per square foot of collector in the Southwest is three times that which can be afforded in the Pacific Northwest and in southern Florida (See Fig. 1).

(4) The collector area required to provide sufficient energy to heat a one-family dwelling varies from 450 sq ft in the Southwest to 2,000 sq ft in the North. This precludes the use of roof collectors for apartment buildings of more than two or three stories; thus, solar house heating is impractical in the heavily populated sections of cities.

(5) The required collector area depends strongly on the amount of winter insolation. A cloudy winter with 20 per cent less than average insolation, but average temperature, may increase the required collector area by more than a third. In order to provide for year-to-year weather variation without greatly increasing costs, an auxiliary heating unit should be used to make up the deficit during the less favorable winters.

(6) Although the stored energy may not reach its minimum until January or February, November and December are the critical months because they represent the greatest drain in stored energy. On the other hand, during the five or six warmest months of the year, the system will not be able to use, i.e., it will throw away, a considerable portion of the available solar

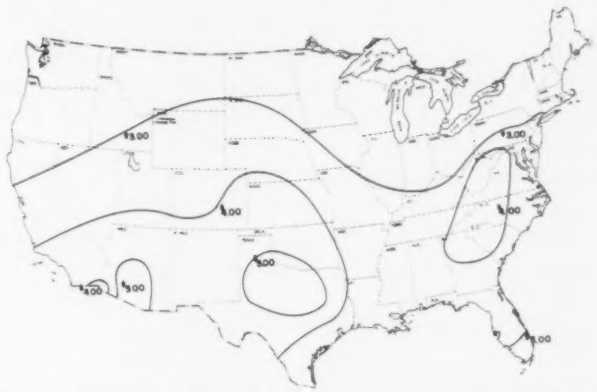

FIG. 2—Maximum allowable cost for each square foot of solar collector, assuming long-term energy storage cost at one dollar per therm and fossil fuels at 18¢/therm.

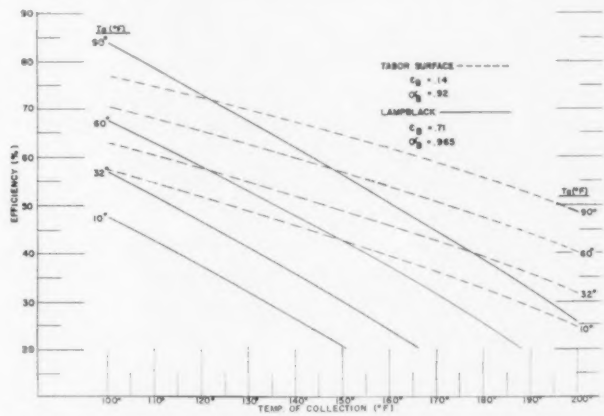

FIG. 3—Efficiency of collector and one glass plate vs. collection temperature for various ambient temperatures.

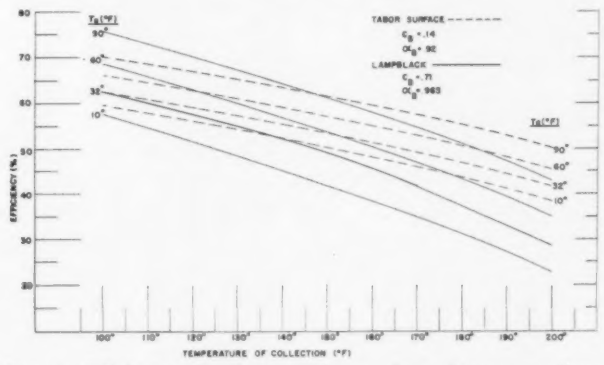

FIG. 4—Efficiency of collector and two glass plates vs. collection temperature for various ambient temperatures.

energy, unless the storage efficiency is very high (and expensive).

(7) The major determinant of the engineering requirements for a solar house in a given locality is the efficiency of the collector. The collector is more efficient when it has only to heat water (or air) to a moderate temperature than when it must heat a fluid to nearly the boiling point of water. (See Fig. 3 and 4.)

(8) If long-term energy storage is substituted for short-term storage, surprisingly little reduction in the required collector area is achieved. In some localities, the reduction is significant if storage *capacity* is increased, but nowhere is there much reduction as the *efficiency* is increased. (In some cases, because of a drop in collector efficiency, the required collector area may actually *increase* with storage efficiency.) In all localities, solar houses with short-term storage are more economical, even when the daily saving of heat with long-term storage is taken into account.

(9) If the energy storage is hot water, the most efficient maximum storage temperature is about 190°F. This assumes a Tabor surface collector similar to that of Fig. 3.

(10) The major cost of a solar heating system is the collector; however, even if there is no significant improvement in collector design or manufacture, a major breakthrough in the cost of high efficiency energy storage might make solar house heating economically feasible. Something like a 90 per cent reduction in energy storage costs for storage capacities between 300 and 700 therms would be required. Solar houses would then be designed with long-term storage instead of short-term storage.

(11) A major breakthrough in the cost of long-term energy storage would only slightly reduce the *relative* feasibility of solar house heating in different parts of the country; i.e., the ratio remains slightly more than double from the most to the least favorable areas. Moreover, the most favorable areas remain approximately the same, i.e., the Southwest and the Appalachian highlands. (Compare Fig. 1 and 2.)

(12) The maximum price that can be afforded per square foot of solar collector varies linearly with the cost of fossil fuel; that is, if the cost of fuel oil doubles, twice as much can be paid for the solar collector. (See Fig. 12.)

(13) If solar house heating as a whole is not economical, calculations will indicate that the greater the proportion of auxiliary heat furnished, the cheaper the over-all system. (This assumes, of course, that the solar equipment is scaled down as the demands on it are decreased.) The cheapest system will consist *entirely* of auxiliary heat, i.e., no solar heat at all. The optimum proportion of auxiliary heat, therefore, is dependent primarily on the point of view adopted. (In this paper most of the calculations assume that the auxiliary heat is to be furnished only to the domestic hot water drawn from faucets, not to the house itself.)

(14) Solar air conditioning by itself does not appear economical; solar heating and air conditioning combined in the same house may be more nearly economically feasible than solar heating alone, but the over-all prospects for solar air conditioning seem to stand or fall with the prospects for solar heating. (See section at the end of this paper.)

Further detailed conclusions are given in a later section, following explanation of the calculations on which they are based.

Orientation of Future Work

The idea of utilizing solar energy for space heating and cooling is not new. Practically any competently designed system will work, but none, so far, has been cheap enough to market. There are, broadly speaking, two ways of approaching the design problem: the handbook approach and the Einstein approach, i.e., intelligent use of materials, techniques, and principles which represent the most advanced state of the art, and an innovation based on a new and different concept. The past ten years have seen several competently designed solar houses built by the handbook approach and one new development—the silicon solar battery—embodying the Einstein approach. It does not seem likely that economical application of solar energy to heating and cooling will come about within the next 5 or 10 years by "successive approximations" of small improvements (and increases in the cost of fossil fuels), but only by an original "breakthrough" such as a different method of collecting solar energy (perhaps with a new type of fuel cell), or a practical means of dispelling winter overcast.

The difficulties encountered in applying solar energy economically indicate that research might more fruitfully be directed toward the basic physical processes than toward engineering projects. Applications of solar energy to date have taken the energy as it comes from the sun, and sought to use it efficiently. Perhaps progress can be made by modifying solar energy so that a transducer, like the silicon battery or an antenna, can use it more efficiently.

DESCRIPTION OF HEATING SYSTEM

The calculations are made for a house whose heating system is similar to that in the Massachusetts Institute of Technology solar house.[1, 2, 6] (See Appendix A.)

A. Collection

Solar energy is collected by fixed, flat-plate collectors tilted from the horizontal at 15° + the latitude, using water as the heat transfer medium. The absorbing

VOL. 3 1959

(blackened) surface of the collector has selective properties[8, 9] absorbing 92 per cent of the solar energy incident on it and re-emitting only 14 per cent as much energy (infrared) as would a Planckian radiator at the same temperature. The collector is covered with a single pane of glass. The efficiency to be expected from such a collector is shown in Fig. 3; the calculations follow the methods given by Hottel and Woertz.[10] Their exact simultaneous equations, rather than their approximation, must be used because of the selectivity of the absorber. Fig. 4 shows the results of similar calculations carried out for two glass cover plates. Further details are given in Reference 15.

The collector operates only when the sun heats it to a suitable temperature. When the sun sets, the pump stops and all the water runs back down into the storage tank. This prevents loss of heat and/or freezing the pipes on winter nights. The pump works faster when the sun is high than when the sun is low, so that the quantity of water heated per unit time is the variable, rather than the temperature to which the water is heated during a single day.

B. Storage

Energy is stored as hot, but not boiling, water. Water has 10 per cent higher thermal storage capacity per unit *volume* than iron, and at least 25 per cent higher than rocks. The superiority of water[15] is even greater when account is taken of the passages which must be provided for heat transfer to and from solid materials. Since the storage tank must be insulated, it must be at least fairly tight, so that not much additional expense is incurred in making it water-tight.

The water (or other liquid) should not be kept in vapor phase or under pressure. Pressure tanks are much more expensive, and the storage capacity per unit volume usually decreases rather than increases as the liquid passes to the vapor phase. Moreover, the boiling point must be kept low in order not to lower the collection efficiency, or less importantly, the storage efficiency.

C. Tank

A. cylindrical steel tank in the house or basement stores several thousand gallons of water. (See Appendix B.)

D. Insulation

Glass wool or other conventional insulation is used around the storage tank. This is preferable to burying the tank in the ground, which can be calculated as an infinitely thick insulation which absorbs the heat that leaks out of the tank. The mathematical solution for an infinitely buried tank has been given.[11] The temperature versus time curve is quite different from that for a conventionally insulated tank; the buried tank cools off much faster at first, but over a long period will hold the residual heat longer than the conventionally insulated tank. Poorly conducting clay, loam, or trap rock has a conductivity of about 4 Btu per sq ft per hr per °F for 1-in. thickness. A spherical 3,000-gal tank, filled with water at 207°F and buried in dry loam at 44°F, will cool down to 82°F in five weeks; the same initial and final temperatures, for a five week period, correspond to a mere 1.8 in. of glass wool with K factor of 0.3 Btu per sq ft per hr per °F for 1-in. Other methods of insulation are discussed in Reference 15.

E. Air Heat

The rooms are heated by convected hot air. People who live in one-family houses are divided in their preferences for hot water heat furnished via baseboard radiators and air heat furnished via ducts and gratings. In a solar-heated house, however, there is an overriding consideration in favor of air heat. If a room is to be satisfactorily heated by a radiator of normal size, the water in the radiator must not fall much below 140°F. On the other hand, if air is circulated through the house after being blown over hot-water coils, the water in the coils (circulated from the storage tank) can fall as low as 95°F and still heat the air sufficiently in a normal-sized heat-exchange device. If auxiliary heat is used for the air also, the storage tank water may be allowed to fall as low as 85°F, i.e., serve as first-stage heating of very cold air. Moving the minimum temperature from 140°F down to 85°F (using 207°F as maximum) increases the energy storage capacity of the tank by 82 per cent. Even more important, the efficiency of solar energy collection is improved during the most critical months of the year.

A person who is willing to go to the extra expense involved in solar heating is quite likely to want air conditioning in his house too. If a house is to have air conditioning, it should be designed for air heat, because the same ducts and blowers can be used for both systems.

F. Design Factors

The heating load is assumed to be 25,000 Btu per degree day for a house built for an outdoor design temperature of 0°F. The design temperatures used for the present calculations, based on data given in the *ASHAE Annual Guide*, are given in Table II.

The correction factors for the Btu per degree day rating of a house with design temperature different from 0°F are taken from the *ASHAE Annual Guide* and given in Table III. Its engineering significance is this: in localities with milder climates houses are generally built with less insulation and radiator area than the same size and style house would have if built in a

TABLE I—Boston Water Temperatures

Oct.	Nov.	Dec.	Jan.	Feb.	Mar.	Apr.	May	June	July	Aug.	Sept.
55°	50°	45°	40°	40°	45°	50°	55°	60°	65°	65°	60°

TABLE II

Locality	Outdoor design temperature °F	Latitude	Furnace cost	Annual house heat (Therms)	Annual water heat (Therms)
Blue Hill, Mass.	+4° F	42.0°	$800	1693.91	319.10
Central Mass.	0°	42.5°	800	1685.75	320.17
Ithaca, N. Y.	−10°	42.5°	800	1512.47	320.17
Madison, Wis.	−11°	43.1°	800	1600.21	321.32
Rhode Island	+4°	41.7°	800	1621.60	318.38
Columbus, Ohio	0°	39.9°	800	1403.75	315.09
Medford, Ore.	+20°	42.2°	600	1591.45	319.46
Lander, Wyo.	−13°	42.9°	800	1746.74	320.96
Rapid City, S. Dak.	−15°	44.0°	800	1544.71	322.75
N. Y. City and Long Island	+5°	41.8°	800	1342.03	318.74
Columbia, Mo.	−5°	38.9°	800	1193.89	313.23
Grand Jctn., Colo.	−10°	39.1°	800	1267.89	313.66
Nashville, Tenn.	+7°	36.1°	800	976.17	308.15
Atlanta, Ga.	+20°	33.8°	600	989.1	300.85
Fresno, Calif.	+30°	36.6°	600	1064.69	309.22
Albuquerque, N. M.	+8°	35.0°	800	1238.80	306.36
Los Angeles, Calif.	+35°	34.0°	600	922.35	304.50
Charleston, S. C.	+20°	32.8°	600	690.55	302.28
El Paso, Texas	+18°	31.8°	600	890.69	300.51
Ft. Worth, Texas	+10°	32.75	600	688.82	302.28
Phoenix, Ariz.	+27°	33.5°	600	677.08	303.43

TABLE III—Correction Factor (β) for Outside Design Temperature*

Design Temperature	−20° F	−10° F	0° F	+10° F	+20° F
Correction Factor	0.778	0.875	1.00	1.167	1.40

* Taken from *ASHAE Guide*.

colder area. Thus, the number of Btu needed to heat the house *per degree day* is greater in the South than in the North. As can be seen in Table XXVI, fuel costs (or savings) may be greater in a milder locality, like Rhode Island or southwestern Oregon, than in a locality with severer winters, like South Dakota.

G. Hot Water

Domestic hot water load is figured at 120 gal per day, heated to 140°F. To compute the heat load for this water, however, one must know the city water temperature. City water (underground) temperatures are not readily available in the published literature, so Whillier's figures for Boston are used with a correction made for difference of latitude. Boston and Blue Hill are taken as latitude 42° and the correction, plus or minus according to whether south or north, is one-half a degree Fahrenheit for each degree of latitude different from 42°. Whillier's figures for Boston are given in Table I.

H. Auxiliary Heat

Hottel[1] and Whillier,[2] who studied houses with short-term storage, have shown that the annual dollar return in fuel savings per square foot of collector is lower if the collector must provide *all* the house heat (and hot water) than if some auxiliary (non-solar) heat is provided in winter. This conclusion holds also for solar houses with long-term storage.

There are additional reasons for providing auxiliary heat in a solar house. First, a stand-by source of heat eliminates the need for designing the solar heating system against the worst winter on record. That is, auxiliary heat can be used during worse-than-average winters. Secondly, even if the house is unoccupied during the fall, the solar collecting and storage system would have to be kept operating, if there were no auxiliary source of heat which could be tapped in December and January to make up for the lack of stored heat. The same consideration applies if people want to move into a new solar house in winter.

The greatest dollar saving of conventional heat equipment is accomplished by eliminating the furnace. Since the auxiliary heating equipment is not planned to carry the full house heating load, i.e., it will provide hot water in winter and sometimes part of the house heat, a slightly oversized water heater using gas or oil or off-peak electricity, can suffice. Thus, two hot water tanks are to be provided in the solar house: a large energy storage tank, and a smaller tank (Whillier suggests 275 gal) for domestic hot water. Since the water in the solar system is circulated and stored for long periods it is kept completely separate from the domestic hot water, which should be of drinkable purity. A valve arrangement, however, permits filling the storage tank from the domestic hot water supply and another set of valves permits heat transfer from one water supply to the other. (Detailed design considerations are given by Whillier.)

The system for which the calculations have been made assumes that, with average weather conditions, the auxiliary heater provides the domestic hot water in December and January and half of February. Thus, the solar system provides all the house heat and 9½ months of domestic hot water, or about 96 per cent of the total annual heat load. If a calendar is prepared showing the temperature to be expected in the storage tank for each 3-day period during the first half of the winter, the auxiliary heater can be run whenever the storage tank temperature falls more than a few degrees below its average temperature for that date. The hot water heater would then be used for 12 or more hours a day during a cloudy winter month instead of only when needed to heat up the domestic hot water supply.

On the other hand, when more winter solar energy than usual is collected and/or the number of degree days is less than usual, the auxiliary heater may be relieved of the necessity of furnishing any heat at all. The variation in winters from year to year is different

VOL. 3 1959

for different parts of the country, but as a rule of thumb, one can assume a 50-50 chance that the monthly difference in collected energy, or in needed house heat, essentially, degree days) will vary plus or minus at least 10 per cent from the average. If the period taken is a year instead of a month, the percentage deviation with a 50-50 chance drops to about 5 per cent.[12-14]

I. Storage Temperature Limits

The temperature of the water used in heating the house is permitted to vary from a minimum of 85°F to a maximum of 207°F. (The minimum temperature would probably have been better chosen at 90°F, since 85°F water requires either a very large or very slow heat transfer to the air which is to be convected into the rooms.) The maximum temperature was determined by the stipulations that steam was not wanted and that at least a 5° differential is needed between the collection temperature and the temperature of the water in the storage tank.

SYMBOLS USED MORE THAN ONCE

A . . . . Area of solar energy collector (sq ft)
A_0 . . . Area of solar energy collector required when storage efficiency is perfect
B . . . . Auxiliary (non-solar) heat furnished to the house (Btu)
H . . . . House heating load per month (Btu)
I . . . . . Average monthly insolation (sunshine) falling on unit area of a horizontal collector (Btu/ft²/month)
i . . . . . Subscript for i^{th} month (i = 1 is October)
K/d . . Heat conductance per unit area through insulation d in. thick (Btu/ft²/hr/°F)
L . . . . Storage tank exponential heat loss rate factor (see Equations 7 and 8) (reciprocal minutes)
m_i . . . Number of days in i^{th} month
M . . . . Money (dollars)
ΔM Incremental capital investment in solar energy equipment
M_f . . . Annual fuel savings
Q . . . . Heat storage capacity (Btu)
S . . . . . Area of storage tank (sq ft)
T . . . . Temperature (degrees F). Subscripts: a = ambient; b = beginning of month; c = collection; e = end of month
V . . . . Volume of energy storage tank (gal)
W . . . Heat load of domestic hot water per month (Btu)
Y . . . . Amortization period in which solar equipment pays for itself in fuel savings (years)
α . . . . . Horizontal-to-tilt correction factor: ratio of insolation on south-facing surface tilted 15° plus latitude to insolation on horizontal surface, dimensionless (see Table IV)
β . . . . . Correction factor to heat load/degree day for outdoor design temperature different from 0°F, (See Table III) dimensionless
η . . . . . Efficiency of collection of solar energy, dimensionless (See Figs. 3 and 4)
σ . . . . . Shape factor of storage tank. Ratio of area to two-thirds power of the volume, dimensionless. (See Fig. 15)

SIMPLIFIED CALCULATION

The problem of designing a solar heating system with long-term storage is somewhat like that of calculating a bank balance: each month certain withdrawals and certain deposits are made, and the balance at the end of the month is carried over for the calculation of the next month's transactions. The difference between the heat collected and the heat furnished must be made up by (or, if it is positive, added to) the heat in the storage tank.

TABLE IV—Horizontal-to-Tilt Insolation Ratio
(Based On Data From Reference 14)

$$\alpha \equiv \frac{\text{Insolation on south-facing surface tilted 15° + latitude}}{\text{Insolation on horizontal surface}}$$

Latitude in Degrees	Jan.	Feb.	March	April	May	June	July	Aug.	Sept.	Oct.	Nov.	Dec.
30	1.60	1.38	1.14	0.92	0.78	0.71	0.76	0.85	1.04	1.29	1.53	1.68
35	1.77	1.48	1.21	.96	.80	.72	.77	.88	1.11	1.37	1.66	1.90
40	2.04	1.62	1.28	.99	.81	.73	.77	.91	1.17	1.50	1.91	2.18
45	2.31	1.82	1.37	1.03	.84	.74	.78	.94	1.23	1.64	2.16	2.51

The monthly heat collected consists of the product of four factors: the average monthly insolation on a horizontal surface (I), the horizontal-to-tilt correction (α) for the fact that the collector is not horizontal (see Table IV), the efficiency of collection η (see Figs. 3 and 4), and the area of the collector (A). The monthly heat furnished by the solar system consists of three parts: the house heating load (H), the domestic hot water heat (W), the heat leakage through the insulation of the storage tank. The house heat H is 25,000 times the number of degree days times the correction factor β. The degree days are reprinted in the *ASHAE Guide* from Weather Bureau publications. The correction factor can be read from a graph made from Table III. The difference between the heat collected and the heat furnished must be divided by the heat storage capacity (Q) per degree to give the change in temperature between the beginning and end of the month ($T_e - T_b$) in the stored water.

The insolation data (I) was obtained privately[15] from the Weather Bureau. Similar data are given in Reference 16. It may be remarked that to get its monthly 5-year averages, the Weather Bureau averages each month separately, with no regard for possible correlation between months. It might turn out, for example, that years with unusually high summer insolation might generally have unusually low autumn values, but such correlations are lost if one simply averages the values for each month in successive years. It would be better to plot for each station a curve for each year's values, month by month, and calculate the center of gravity or the maximum density of the curves.

In the simplified calculation, we assume that an as-yet-undiscovered method of energy storage provides perfect storage efficiency and permits energy collection at a constant efficiency of 50 per cent. Since there is perfect storage efficiency, there is no heat leakage.

Moreover, since the energy can be stored for as long as we please, no special arrangement need be made for the peak load in winter. Thus there is no need to supply auxiliary heat (except during colder-than-average years), and the total annual heat collected equals the total annual heat furnished. For the simplified calculation we can write,

$$\frac{Q(T_c - T_b)}{207 - 85} = I\alpha\eta A - (H + W) \qquad [1]$$

The calculation is begun by assuming that the temperature of the water in the storage tank on October 1st is 207° = T_b. We substitute into Equation [I] the appropriate values for October, and calculate T_c, which then becomes the T_b for November. We continue on through the year, making sure that the temperature in the storage tank remains always between 85° and 207°. If the temperature falls below 85°, we halt the calculation, assume a larger value for A, and begin with October again. The problem is to find the minimum collector area which will satisfactorily heat the house. The minimum value of collector area is found for each size of tank (heat storage capacity). As the storage capacity increases, a smaller collector area is required and less heat is thrown away in summer, until finally a capacity is reached beyond which no further decrease in collector area is possible. That is, all the available heat is used. The result of the calculation for 21 different localities in the United States is shown in Fig. 5; the sharp elbow in each curve represents the combination of minimum collector area with maximum useful storage capacity which will satisfactorily heat the standard house. The horizontal portion of each curve beyond its elbow indicates that further increase of storage capacity permits no concomittant reduction in collector area.

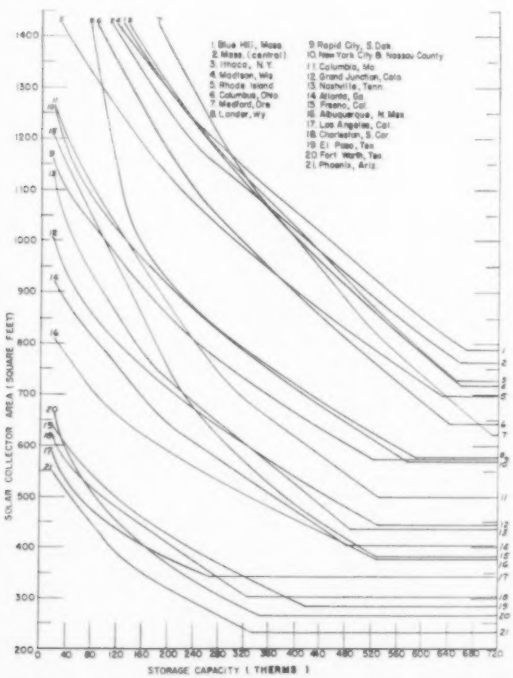

FIG. 5—Area of collector vs. storage capacity, assuming perfect storage insulation and 50 per cent constant collection efficiency.

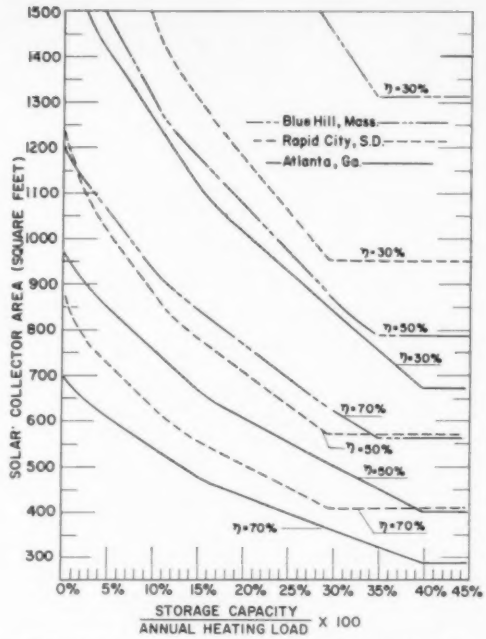

FIG. 6—Collector area vs. relative storage capacity for various efficiencies and localities.

Fig. 5 indicates that larger storage capacity can be utilized in the colder cities. To put it in terms of insolation instead of degree days, the less insolation a locality receives, the greater the saving in collector area that can be achieved with long-term storage. The curves with the steepest slopes—especially Medford, Lander, and Fresno—indicate that the ratio of the insolation per square foot of collector to the heat load per square foot of collector, falls unusually far in the late autumn and early winter. Medford, for example, although having mild winter temperatures, is in the Pacific Northwest where winter overcast typically blocks out more than 60 per cent of the possible sunshine.

Using 85°F as the base level, 1,000 gal of water at 207° represents a storage capacity of approximately 1,000,000 Btu. Thus the maximum useful storage capacity of the most even-climated city shown in Fig. 5—Los Angeles—requires a tank holding more than 26,000 gal. This would fit in one-half of a full basement, but it would be expensive. The practicality of a design based on Fig. 5, therefore, depends on the economics of our imaginary breakthrough in energy storage methods (which might not, for example, require a water-tight tank).

The figure of 50 per cent collection efficiency is a pure

VOL. 3 1959

guess, since we do not know the conditions under which the energy will be stored. If we assume other efficiencies, such as 30 per cent or 70 per cent, the results will be as shown in Fig. 6. It will be noted that the maximum useful storage capacity is independent of the collection efficiency; this is due to the constant value of the product of collection area times collection efficiency. In other words, graphs of collector area versus collection efficiency would be a family of hyperbolas, each hyperbola corresponding to a different storage capacity.

ECONOMIC FEASIBILITY

The solar collector and associated energy storage facility cost considerably more than the conventional heating equipment which is replaced. ΔM is defined as the difference, i.e., the incremental capital investment in solar equipment. Interest lost on the money invested, plus depreciation, maintenance, and repair of the solar equipment, are assumed to total 10 per cent. Then

$$Y = \frac{\Delta M}{M_f - 0.1\Delta M} \qquad [2]$$

where Y is the period required for the solar system to pay for itself, and M_f is the annual fuel saving, in dollars.

This formula is quite general. It applies to house heating or house cooling, or both, and holds whether or not auxiliary heat is supplied. Fig. 7 shows the amortization period Y plotted against the incremental investment ΔM for different dollar values for annual fuel saving. Fig. 7 provides sufficient reason for rejecting many plans for solar houses, such as those for providing heat on occasional cold nights in Florida. If we take 10 years as the maximum acceptable amortization period (mortgages customarily run longer, but money-saving equipment usually claims less), we see from

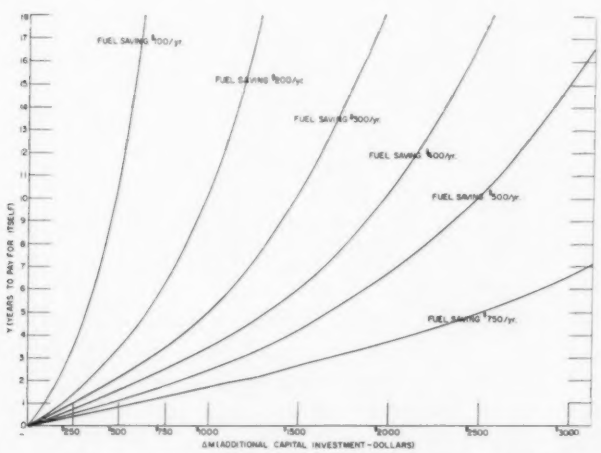

FIG. 7—Amortization period vs. incremental capital investment required for solar system, for various annual amounts of fuel saving.

Equation [2] that to be economically feasible on other than a novelty-luxury basis, the annual fuel savings M_f must exceed one-fifth of the incremental investment ΔM.

In fact, the equation

$$\Delta M = 5\ M_f \qquad [3]$$

is a good rule-of-thumb criterion for estimating economic feasibility.

The amortization period Y is not a suitable index for economic feasibility. We choose instead, the maximum allowable cost of the collector per square foot $\partial M/\partial A$ when the amortization period is 10 years.

Fig. 2 indicates the value of $\partial M/\partial A$ in different regions of the United States, using the simplified basis of calculation, i.e., the data shown in Fig. 5. The annual fuel saving M_f is calculated as the sum of the monthly heats furnished times the assumed fuel heat cost of 18 cents a therm. Fuel costs vary considerably, of course, with location, being cheaper near gas fields and coal mines and more expensive where transportation costs are higher. No attempt has been made to take this variation into account; the ratio of 18 to the actual number of cents/therm should be taken as a correction factor in using Fig. 2 (and also Fig. 1).

The cost of the furnace which is saved is taken as either $800 or $600 according to the location. (See Table II.) The cost of the solar heating system consists of the cost of the collector plus the cost of energy storage:

$$\Delta M = A\frac{\partial M}{\partial A} + Q\frac{\partial M}{\partial Q} - \begin{cases} 800 \\ 600 \end{cases} \qquad [4]$$

To calculate the data for Fig. 2, the cost of energy storage $\partial M/\partial Q$ was assumed to be one dollar per therm, which is only about 10 per cent of the actual present-day cost. We substitute Equation [4] into Equation [2]. read off the "elbow" values of Q and A from Fig. 5, and compute $\partial M/\partial Q$. The data used in computing Fig. 2 are given in the last column of Table XXVII.

The "elbow" figures, rather than a smaller storage capacity and larger collector area, represent the *maximum* $\partial M/\partial A$ because of the extremely low storage cost assumed. This can be checked readily by substituting values from Fig. 5 into Equation [4] with ΔM assumed constant.

No account has been taken of the cost of piping to and from the collector, or of the various valves and thermostats required. The cost of such solar equipment is certainly greater than the cost of the conventional equipment of this type, which is eliminated. This extra cost, which is independent of locality, is thus implicitly considered as part of the cost of the collectors. There is a slight inaccuracy introduced, because lump costs are considered as distributed over the collector area. The

result of the inaccuracy is to make solar heating in cold localities seem a little more nearly feasible (with large collector areas), and in warm localities a little less feasible, relative to each other, than would be the case if the lumped and distributed costs were accurately divided.

FULL CALCULATION

We now proceed to calculate the design data for our standard solar house using conventional methods of heat storage. We follow the same general procedure as in the simplified calculation except that we must also take into account:

(1) The heat leakage through the insulation of the storage tank.

(2) The thickness (and cost) of the insulation of the storage tank.

(3) The effect of furnishing auxiliary heat.

(4) The effect of the above three factors and the average outdoor daytime temperature on the collector efficiency.

The basic iterative equation, giving the change in storage tank temperature for the ith month is

$$(T_e - T_b)_i = \frac{I\alpha\eta_i A - (H + W - B)_i - 24\frac{K}{d}\sigma V^{2/3} m_i (T_b - T_a)_i}{8.337V + 12\frac{K}{d}\sigma V^{2/3} m_i} \qquad [5]$$

Equation [5] is essentially Equation [1], but includes an auxiliary heat term (B) and a heat leakage term,

$$24K/d\sigma V^{2/3} m_i \left(\frac{T_b + T_e}{2} - T_a\right)_i$$

The iteration starts with $i = 1$ (October) and $T_b = 207°$. T_a is the ambient temperature in the basement (around the storage tank), not on the roof. The temperature inside the storage tank is taken as the average temperature for the month $(T_b + T_e)/2$. The factor 8.337 is the number of pounds of water in one gallon: the specific heat of water, being unity, does not appear explicitly.

Long-term storage was defined in the opening paragraph as retaining at least 50 per cent of the energy for a period of three months. The three-month period is somewhat arbitrary, but it permits heat collected in the sunny months of August, September, and October to be used during the worst deficit months. Before carrying out the full calculations, we inquire as to the practicality of reducing the conductance through the walls of the storage tank so as to achieve long-term storage.

We first define a shape factor σ for the storage tank as the ratio of the area of the tank to the two-thirds power of the volume. (See Appendix B.)

$$\sigma = \frac{S}{V^{2/3}} \qquad [6]$$

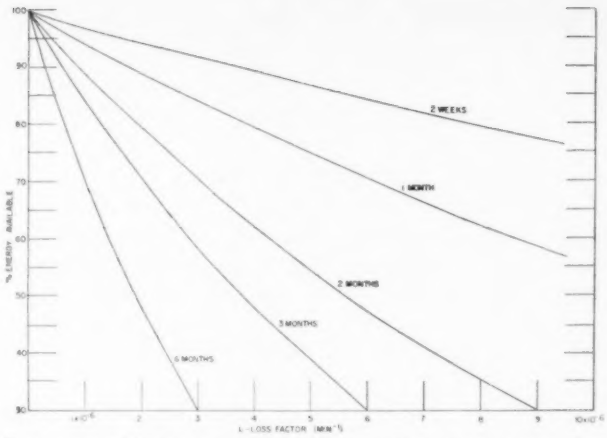

FIG. 8—Residual storage capacity vs. heat loss factor, for various storage periods.

We next define a decay factor L by the equation

$$(T - T_a) = (T_0 - T_a)e^{-Lt} \qquad [7]$$

where T is the temperature at time t, and T_0 is the temperature at time $t = 0$. L is in reciprocal minutes.

Equation [7] is the equation of a standard cooling curve when the heat absorbed by the insulation is neglected and the conductivity of the medium on each side of the insulation (water and steel inside and air outside) is infinite. These two simplifications tend to cancel each other, although for most of the situations dealt with here the latter is larger. This means that Equation [7] tends to show the tank as cooling more quickly than it actually would, i.e., the error is in the conservative direction. To calculate the cooling per month, we assume a standard-length month, i.e., 43,800 minutes.

It is not hard to show that

$$L = \frac{K/d}{1914V^{1/3}} \qquad [8]$$

where 1914 is a dimensional constant.

The insulation required for various percentages of energy retention and various periods of time is most conveniently expressed in terms of L. Fig. 8 shows this relationship, assuming T_0 as 206.6° and T_a as 44.6°. To interpret the L values in terms of tank capacity and insulation thickness, Table XXVIII is provided. The shape factor σ is taken as 5.54, which applies to a "square cylindrical tank," i.e., a right circular cylinder whose height equals its diameter. (See Appendix B.) From Fig. 8 it can be seen that if 50 per cent of the heat stored is to be available three months after storage, L must be 3.75×10^{-6} per minute. Table XXVIII shows that for 6,000-gal storage capacity this corresponds to a conductance of slightly more than 0.02 Btu per square ft per hour per °F.

Glass wool, which is a fairly typical and cheap insulation, has a conductivity of about 0.3 Btu per sq ft per hour per °F per in. thickness, at 190°F. This means that

VOL. 3 1959

for long-term storage the tank should be enclosed by at least 15 in. of insulation.

Equation [5] cannot be solved in a straightforward manner, because we do not know the proper value of A, nor of η_i. We start with a value of A obtained by approximation methods and from experience, and raise or lower it according as the calculation shows the minimum temperature in the storage tank goes below 85°, or does not ever go down to 85°. Five square feet is taken as the minimum significant increment of collector area.

Collection efficiency can be read off specially prepared graphs similar to Fig. 3, but with smaller increments of ambient temperature. This ambient temperature is out-doors at the collector, not in the basement. Since the collector is operative only during the warmest part of the 24-hour day, the ambient temperature is computed, as is done in the calculations for the M.I.T. solar houses,[6] as $\frac{7}{10}$ of the mean ambient temperature plus $\frac{3}{10}$ of the maximum temperature. All of these are daily temperatures averaged over the month. Unfortunately, the collection efficiency is different for each month, and in addition depends on the value chosen for A, since A controls the monthly change of the storage tank temperature. The collection temperature, it will be recalled, is 5° above the storage tank temperature. We use the average storage tank temperature for the month, which requires knowing the temperature at the end of the month, which is just what the iterative formula is supposed to find out.

The problem was programmed and run on an IBM 650. It was necessary to provide for a calculation of collection efficiency, rather than a graphical determination. This was accomplished to a satisfactorily close approximation (within a few tenths of a per cent) by regarding the curves of Fig. 3 as portions of the upper branches of a family of parabolas with axes parallel to the x-axis.

Some difficulty was encountered in running the program because successive iterations did not always form

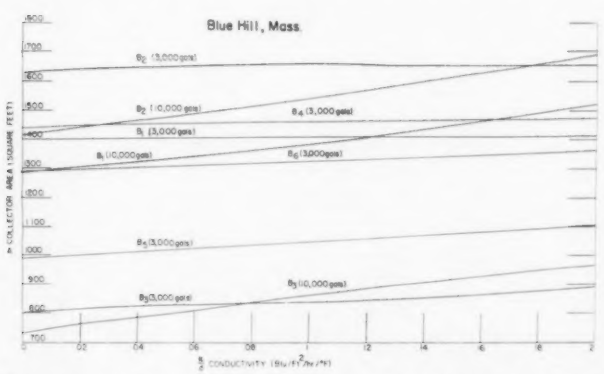

FIG. 9—Collector area vs. thermal conductivity of storage tank insulation, for various schedules of auxiliary heat (see Table XXIX) and 3,000-gal and 10,000-gal tank capacity.

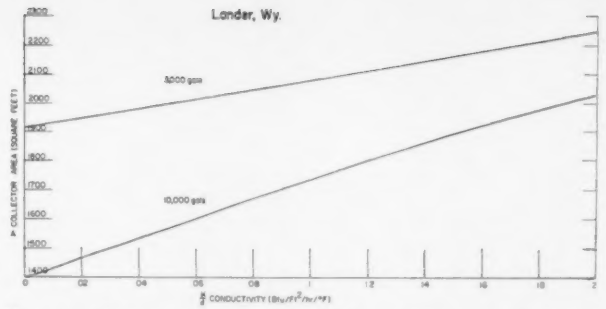

FIG. 10—Collector area vs. thermal conductivity of storage tank insulation, for 3,000-gal and 10,000-gal tank capacity.

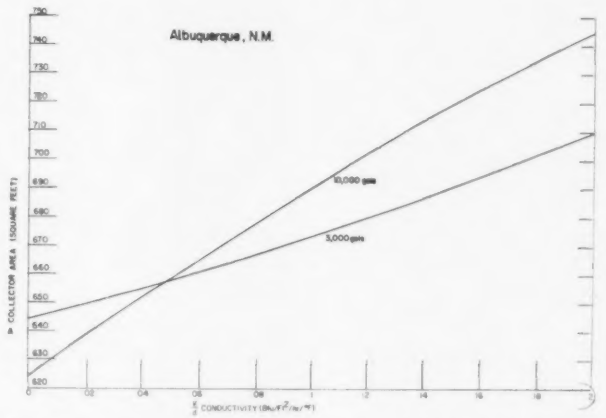

FIG. 11—Collector area vs. thermal conductivity of storage tank insulation for 3,000-gal and 10,000-gal tank capacity.

a sequence converging to vanishing terms. The trouble was traced to the unexpected sensitivity of the calculation to the value of the collection efficiency, and was overcome by having the computer determine if the differences between two successive pairs of computed collection temperatures have the same sign; if not, the terms may not be approaching a limit, and it is advisable to replace the third trial temperature by a temperature closer to the first temperature. In symbols, if

$$\frac{Tc_1 - Tc_2}{Tc_3 - Tc_4} < 0, \quad \text{then a new}$$

$$Tc_3' = Tc_3 + \frac{Tc_4 - Tc_3}{4} \qquad [9]$$

is formed. The former Tc_3 and Tc_4 become Tc_1' and Tc_2', respectively, and a new Tc_4' is computed.

The results of the calculations, together with the input data, are given in Tables IV to XXV. Figs. 9–11 are plotted from Tables V, XII and XX, respectively. These results are discussed in a later section.

Calculations were run for one place (Blue Hill) using different schedules of auxiliary heat. The "regular" schedule (B_1), it will be recalled, provides auxiliary heat during an average winter only for the domestic hot water, and then only for December, January, and half of February. The second schedule (B_2) assumed no

TABLE V—Blue Hill, Massachusetts

	Oct.	Nov.	Dec.	Jan.	Feb.	March	April	May	June	July	Aug.	Sept.
Insolation in therms/ft² (tilt correct incl.)	0.417	0.336	0.339	0.376	0.365	0.425	0.415	0.437	0.424	0.481	0.445	0.472
House heat (therms)	103.62	183.65	286.47	316.68	284.08	234.79	155.29	71.29	16.70	2.12	6.89	32.33
Water heat (therms)	26.35	27.00	29.45	31.00	28.00	29.45	27.00	26.35	24.00	23.25	23.25	24.00
Degree days	391	693	1081	1195	1072	886	586	269	63	8	26	122
Aver. ambient temp. (roof)	53.89°	43.16°	31.50°	28.18°	28.31°	36.77°	47.06°	58.85°	67.78°	72.71°	70.77°	64.50°
T_b for V = 3000 gal; K/d = 0; A = 1400 ft²	207°	207°	145.64°	86.27°	111.01°	108.49°	193.45°	207°	207°	207°	207°	207°
Efficiency η	34.28%	41.52%	57.23%	61.34%	58.21%	47.98%	34.48%	35.85%	38.58%	40.04%	39.47%	37.59%
T_b for V = 3000 gal; K/d = .02; A = 1400 ft²	207°	207°	140.57°	85.60°	108.89°	106.89°	190.38°	207°	207°	207°	207°	207°
Efficiency η	34.28%	42.39%	58.10%	61.75%	58.77%	48.70%	35.07%	35.85%	38.58%	40.04%	39.47%	37.59%
T_b for V = 3000 gal; K/d = 0.1; A = 1410 ft²	207°	207°	122.88°	85.03°	101.89°	102.53°	180.58°	203.24°	207°	207°	207°	207°
Efficiency η	34.30%	45.28%	60.71%	62.79%	60.40%	50.97%	37.38%	36.48%	38.58%	40.04%	39.47%	37.59%
T_b for V = 3000 gal; K/d = 0.2; A = 1410 ft²	207°	207°	102.54°	85.13°	92.07°	97.48°	168.33°	190.35°	207°	207°	207°	207°
Efficiency η	34.28%	48.54%	63.60%	64.17%	62.49%	53.63%	41.68%	38.66%	38.58%	40.04%	39.47%	37.59%
T_b for V = 10,000 gal; K/d = 0; A = 1290 ft²	207°	207°	158.71°	96.98°	85.81°	91.02°	150.52°	203.87°	207°	207°	207°	207°
Efficiency η	34.30%	39.31%	53.73%	63.37%	64.23%	57.25%	42.36%	36.35%	38.58%	40.04%	39.47%	37.59%
T_b for V = 10,000 gal; K/d = 0.02; A = 1310 ft²	207°	207°	152.49°	93.42°	85.38°	91.16°	148.92°	199.09°	207°	207°	207°	207°
Efficiency η	34.30%	40.38%	55.17%	63.93%	64.26%	57.46%	43.44%	37.18%	38.58%	40.04%	39.47%	37.59%
T_b for V = 10,000 gal; K/d = 0.1; A = 1390 ft²	207°	203.54°	131.57°	85.56°	85.63°	91.94°	143.34°	183.35°	207°	207°	207°	207°
Efficiency η	34.89%	44.43%	59.40%	64.97%	64.13%	58.14%	46.90%	39.83%	38.58%	40.04%	39.47%	37.59%
T_b for V = 10,000 gal; K/d = 0.2; A = 1520 ft²	207°	180.35°	119.02°	85.26°	89.89°	95.20°	140.65°	171.37°	207°	207°	207°	207°
Efficiency η	38.88%	50.12%	61.22%	64.41%	63.08%	58.07%	49.23%	41.83%	38.58%	40.04%	39.47%	37.59%

VOL. 3 1959

TABLE VI—Central Massachusetts

	Oct.	Nov.	Dec.	Jan.	Feb.	March	April	May	June	July	Aug.	Sept.
Insolation in therms/ft² (tilt correct incl.)	0.466	0.383	0.384	0.351	0.364	0.433	0.415	0.437	0.430	0.463	0.458	0.498
House heat (therms)	108.00	193.50	284.75	310.00	284.25	235.00	143.00	63.50	17.50	3.00	7.25	36.00
Water heat (therms)	26.44	27.09	29.54	31.09	28.08	29.54	27.09	26.44	24.09	23.34	23.34	24.09
Degree days	432	774	1139	1240	1137	940	572	254	70	12	29	144
Aver. ambient temp. (roof)	53.33°	41.94°	29.56°	26.76	26.56°	35.66°	47.01°	59.12°	68.58°	73.20°	71.28°	63.98°
T_b for V = 3000 gal; K/d = 0; A = 1425 ft²	207°	207°	162.13°	115.24°	85.50°	123.03°	191.72°	207°	207°	207°	207°	207°
Efficiency η	34.11%	38.56%	49.89%	60.49%	59.32%	45.66%	34.77%	35.93%	38.82%	40.19%	39.62%	37.43%
T_b for V = 3000 gal; K/d = 0.2; A = 1575 ft²	207°	207°	137.55°	121.28°	85.40°	128.05°	174.98°	207°	207°	207°	207°	207°
Efficiency η	34.11%	42.50%	52.69%	59.61%	58.63%	47.53%	37.74%	35.93%	38.82%	40.19%	39.62%	37.43%

TABLE VII—Ithaca, New York

	Oct.	Nov.	Dec.	Jan.	Feb.	March	April	May	June	July	Aug.	Sept.
Insolation in therms/ft² (tilt correct incl.)	0.445	0.292	0.259	0.283	0.369	0.402	0.398	0.455	0.439	0.514	0.491	0.493
House heat (therms)	98.66	168.44	246.97	270.38	252.88	213.94	132.56	63.88	18.16	3.72	8.75	34.13
Water heat (therms)	26.44	27.09	29.54	31.09	28.08	29.54	27.09	26.44	24.09	23.34	23.34	24.09
Degree days	451	770	1129	1236	1156	978	606	292	83	17	40	156
Aver. ambient temp. (roof)	55.37°	43.30°	31.14	28.26°	27.38°	36.27°	48.88°	60.70°	70.98°	75.68°	73.57°	66.52°
T_b for V = 3000 gal; K/d = 0; A = 1590 ft²	207°	207°	158.03°	85.04°	111.21°	173.31°	184.88°	207°	207°	207°	207°	207°
Efficiency η	34.75%	39.48%	55.54%	61.54%	48.14%	38.55%	36.54%	36.43%	39.54%	40.91%	40.30%	38.21%
T_b for V = 3000 gal; K/d = 0.2; A = 1680 ft²	207°	207°	121.15°	85.80°	101.41°	161.57°	164.20°	207°	207°	207°	207°	207°
Efficiency η	34.75%	45.59%	60.78%	62.77%	51.48%	43.99%	40.08%	36.43%	39.54%	40.91%	40.30%	38.21%

TABLE VIII—Madison, Wisconsin

	Oct.	Nov.	Dec.	Jan.	Feb.	March	April	May	June	July	Aug.	Sept.
Insolation in therms/ft² (tilt correct incl.)	0.467	0.321	0.302	0.374	0.369	0.491	0.437	0.461	0.431	0.481	0.502	0.523
House heat (therms)	99.03	192.23	280.91	307.01	260.41	217.48	124.92	58.68	17.69	2.80	6.69	32.36
Water heat (therms)	26.54	27.18	29.64	31.19	28.17	29.64	27.18	26.54	24.18	23.44	23.44	24.18
Degree days	459	891	1302	1423	1207	1008	579	272	82	13	31	150
Aver. ambient temp. (roof)	53.88°	37.31°	25.73°	21.77°	24.48°	35.74°	48.73°	60.71°	70.85°	76.57°	74.36°	65.94°
T_b for V = 3000 gal; K/d = 0; A = 1570 ft²	207°	207°	142.65°	85.63°	145.05°	140.60°	207°	207°	207°	207°	207°	207°
Efficiency η	34.28%	40.34%	56.24%	54.82%	47.19%	40.24%	32.62%	36.43%	39.50%	41.16%	40.52%	38.03%
T_b for V = 3000 gal; K/d = 0.2; A = 1600 ft²	207°	207°	104.02°	85.29°	124.39°	126.66°	207°	207°	207°	207°	207°	207°
Efficiency η	34.28%	46.67%	61.83%	57.84%	52.50%	42.57%	32.62%	36.43%	39.50%	41.16%	40.52%	38.03%

TABLE IX—Rhode Island

	Oct.	Nov.	Dec.	Jan.	Feb.	March	April	May	June	July	Aug.	Sept.
Insolation in therms/ft² (tilt correct incl.)	0.481	0.405	0.382	0.375	0.407	0.481	0.436	0.457	0.439	0.489	0.480	0.528
House heat (therms)	100.87	177.91	274.02	297.84	269.78	231.39	150.91	68.31	15.36	0	6.88	28.33
Water heat (therms)	26.29	26.94	29.39	30.94	27.94	29.39	26.94	26.29	23.94	23.19	23.19	23.94
Degree days	381	672	1035	1125	1019	874	570	258	58	0	26	107
Aver. ambient temp. (roof)	55.73°	45.15°	33.88°	31.49°	31.03°	39.23°	48.85°	59.86°	68.75°	74.18°	72.46°	65.76°
T_b for V = 3000 gal; K/d = 0; A = 1210 ft²	207°	207°	161.38°	88.06°	85.77°	127.92°	183.41°	207°	207°	207°	207°	207°
Efficiency η	34.87%	39.47%	55.31%	65.51%	59.76%	47.19%	36.84%	36.16%	38.87%	40.47%	39.97%	37.98%
T_b for V = 3000 gal; K/d = 0.2; A = 1310 ft²	207°	207°	130.09°	94.48°	85.15°	126.22°	166.13°	192.98°	207°	207°	207°	207°
Efficiency η	34.87%	44.66%	58.99%	64.68%	60.12%	50.16%	42.14%	38.53%	38.87%	40.47%	39.97%	37.98%

TABLE X—Columbus, Ohio

	Oct.	Nov.	Dec.	Jan.	Feb.	March	April	May	June	July	Aug.	Sept.
Insolation in therms/ft² (tilt correct incl.)	0.477	0.367	0.326	0.303	0.354	0.438	0.449	0.458	0.435	0.493	0.509	0.542
House heat (therms)	84.25	173.25	258.00	273.50	236.50	195.25	111.00	45.00	7.75	0	2.00	17.25
Water heat (therms)	26.01	26.67	29.11	30.66	27.69	29.11	26.67	26.01	23.67	22.91	22.91	23.67
Degree days	337	693	1032	1094	946	781	444	180	31	0	8	69
Aver. Ambient Temp. (roof)	57.65°	44.78°	34.16°	31.86°	33.75°	42.89°	53.17°	64.49°	74.21°	78.27°	76.21°	69.98°
T_b for V = 3000 gal; K/d = 0; A = 1380 ft²	207°	207°	170.91°	93.96°	85.16°	164.11°	204.41°	207°	207°	207°	207°	207°
Efficiency η	35.47%	37.69%	53.07%	64.88%	55.29%	38.79%	34.48%	37.59%	40.48%	41.65%	41.06%	39.24%
T_b for V = 3000 gal; K/d = 2; A = 1500 ft²	207°	207°	140.04°	97.10°	85.05°	155.75°	183.77°	207°	207°	207°	207°	207°
Efficiency η	35.47%	42.92%	57.21%	64.44%	56.52%	43.65%	38.05%	37.59%	40.48%	41.65%	41.06%	39.24%

TABLE XI—Medford, Oregon

	Oct.	Nov.	Dec.	Jan.	Feb.	March	April	May	June	July	Aug.	Sept.
Insolation in therms/ft² (tilt correct incl.)	0.537	0.347	0.262	0.306	0.413	0.539	0.573	0.583	0.551	0.561	0.660	0.630
House heat (therms)	114.10	218.40	287.70	301.70	219.45	193.20	133.35	72.45	24.15	0	0	26.95
Water heat (therms)	26.38	27.03	29.48	31.03	28.03	29.48	27.03	26.38	24.03	23.28	23.28	24.03
Degree days	326	624	822	862	627	552	381	207	69	0	0	77
Aver. ambient temp. (roof)	57.56°	47.29°	39.94°	39.63°	45.84°	49.66°	56.47°	62.69°	69.61°	76.81°	76.35°	69.68°
T_b for V = 3000 gal; K/d = 0; A = 1840 ft²	207°	207°	177.97°	85.16°	162.87°	207°	207°	207°	207°	207°	207°	207°
Efficiency η	35.45%	37.30%	54.86%	57.04%	39.44%	32.96%	35.10%	37.04%	39.13%	41.23%	41.10%	39.15%
T_b for V = 3000 gal; K/d = 0.2; A = 1970 ft	207°	207°	150.27°	85.52°	151.51°	207°	207°	207°	207°	207°	207°	207°
Efficiency η	35.45%	42.00%	58.94%	58.63%	41.36%	32.96%	35.10%	37.04%	39.13%	41.23%	41.10%	39.15%

Table XII—Lander, Wyoming

	Oct.	Nov.	Dec.	Jan.	Feb.	March	April	May	June	July	Aug.	Sept.
Insolation in therms/ft² (tilt correct incl.)	0.673	0.576	0.297	0.602	0.559	0.654	0.640	0.576	0.573	0.615	0.551	0.651
House heat (therms)	132.96	220.89	290.95	314.30	248.03	219.84	144.53	83.31	34.29	1.47	4.84	51.33
Water heat (therms)	26.51	27.15	29.61	31.16	28.14	29.61	27.15	26.51	24.15	23.41	23.41	24.15
Degree days	632	1050	1383	1494	1179	1045	687	396	163	7	23	244
Aver. ambient temp. (roof)	48.14°	33.03°	24.03°	20.46°	26.65°	35.20°	45.40°	55.28°	65.37°	74.84°	72.63°	61.64°
T_b for V = 3000 gal; K/d = 0; A = 1910 ft²	207°	207°	207°	85.54°	207°	207°	207°	207°	207°	207°	207°	207°
Efficiency η	32.45%	27.46%	45.93%	44.97%	25.31%	28.19%	31.54%	34.73%	37.86%	40.66%	40.02%	36.72%
T_b for V = 3000 gal; K/d = 0.02; A = 1940 ft²	207°	207°	207°	85.38°	207°	207°	207°	207°	207°	207°	207°	207°
Efficiency η	32.45%	27.46%	46.01%	45.01%	25.31%	28.19%	31.54%	34.73%	37.86%	40.66%	40.02%	36.72%
T_b for V = 3000 gal; K/d = 0.1; A = 2075 ft²	207°	207°	207°	85.38°	207°	205.78°	207°	207°	207°	207°	207°	207°
Efficiency η	32.45%	27.46%	45.97%	45.01%	25.48%	28.42%	31.54%	34.73%	37.86%	40.66%	40.02%	36.72%
T_b for V = 3000 gal; K/d = 0.2; A = 2240 ft²	207°	207°	207°	85.32°	207°	202.55°	207°	207°	207°	207°	207°	207°
Efficiency η	32.45%	27.46%	46.01%	45.02%	26.19%	29.02%	31.54%	34.73%	37.86%	40.66%	40.02%	36.72%
T_b for V = 10,000 gal; K/d = 0; A = 1400 ft²	207°	207°	195.67°	85.20°	190.10°	183.90°	207°	207°	207°	207°	207°	207°
Efficiency η	32.46%	29.59%	47.81%	47.68%	32.83%	32.46%	31.54%	34.73%	37.86%	40.66%	40.02%	36.72%
T_b for V = 10,000 gal; K/d = 0.02; A = 1470 ft²	207°	207°	194.60°	85.35°	194.56°	182.35°	207°	207°	207°	207°	207°	207°
Efficiency η	32.46%	29.80%	47.96%	46.95%	32.29%	32.70%	31.54%	34.73%	37.86%	40.66%	40.02%	36.72%
T_b for V = 10,000 gal; K/d = 0.1; A = 1735 ft²	207°	207°	189.98°	85.66°	207°	175.07°	207°	207°	207°	207°	207°	207°
Efficiency η	32.43%	30.62%	48.63%	44.95%	31.34%	34.02%	31.54%	34.73%	37.86%	40.66%	40.02%	36.72%
T_b for V = 10,000 gal; K/d = 0.2; A = 2025 ft²	207°	207°	184.04°	85.13°	207°	169.87°	207°	207°	207°	207°	207°	207°
Efficiency η	32.46%	31.74%	49.64%	45.05%	32.31%	34.95%	31.54%	34.73%	37.86%	40.66%	40.02%	36.72%

VOL. 3 1959

Table XIII—Rapid City, South Dakota

	Oct.	Nov.	Dec.	Jan.	Feb.	March	April	May	June	July	Aug.	Sept.
Insolation in therms/ft² (tilt correct incl.)	0.601	0.491	0.429	0.449	0.484	0.625	0.565	0.494	0.449	0.518	0.576	0.613
House heat (therms)	102.50	182.66	249.69	279.01	235.96	214.23	126.08	73.19	30.34	6.56	4.92	39.57
Water heat (therms)	26.66	27.30	29.76	31.31	28.28	29.76	27.30	26.66	24.30	23.56	23.56	24.30
Degree days	500	891	1218	1361	1151	1045	615	357	148	32	24	193
Aver. Ambient Temp. (roof)	51.95°	38.48°	29.63°	24.46°	27.62°	34.69°	47.50°	57.40°	67.09°	76.71°	74.62°	64.64°
T_b for V = 3000 gal; K/d = 0; A = 975 ft²	207°	207°	143.44°	90.19°	85.01°	146.57°	189.62°	207°	207°	207°	207°	207°
Efficiency η	33.66%	40.54%	56.51%	63.44%	56.26%	41.81%	35.29%	35.40%	38.38%	41.20%	40.60%	37.64%
T_b for V = 3000 gal; K/d = 0.2; A = 1070 ft²	207°	207°	116.55°	96.91°	85.77°	141.76°	173.47°	207°	207°	207°	207°	207°
Efficiency η	33.68%	44.97%	59.45%	62.38%	56.84%	45.29%	38.14%	35.40%	38.38%	41.20%	40.60%	37.64%

Table XIV—New York City and Long Island

	Oct.	Nov.	Dec.	Jan.	Feb.	March	April	May	June	July	Aug.	Sept.
Insolation in therms/ft² (tilt correct incl.)	0.512	0.415	0.395	0.395	0.462	0.502	0.468	0.477	0.461	0.509	0.499	0.533
House heat (therms)	67.25	146.87	244.25	266.85	243.98	204.44	120.24	37.93	2.69	0	0	7.53
Water heat (therms)	26.32	26.97	29.42	30.97	27.97	29.42	26.97	26.32	23.97	23.22	23.22	23.97
Degree days	250	546	908	992	907	760	447	141	10	0	0	28
Aver. ambient temp. (roof)	59.73°	48.60°	37.17°	34.77°	34.46°	42.48°	52.74°	64.18°	73.55°	78.42°	76.80°	70.71°
T_b for V = 3000 gal; K/d = 0; A = 1030 ft²	207°	207°	172.33°	86.53°	91.03°	147.00°	174.01°	207°	207°	207°	207°	207°
Efficiency η	36.12%	38.64%	54.76%	65.87%	57.15%	46.54%	39.58%	37.50%	40.29%	41.69%	41.23%	39.46%
T_b for V = 3000 gal; K/d = 0.2; A = 1095 ft²	207°	207°	131.44°	87.70°	85.72°	137.69°	152.56°	207°	207°	207°	207°	207°
Efficiency η	36.14%	45.47%	60.62%	66.41%	59.29%	51.38%	43.20%	37.50%	40.29%	41.69%	41.23%	39.46%

Table XV—Colombia, Missouri

	Oct.	Nov.	Dec.	Jan.	Feb.	March	April	May	June	July	Aug.	Sept.
Insolation in therms/ft² (tilt correct incl.)	0.570	0.503	0.360	0.376	0.408	0.535	0.419	0.472	0.472	0.537	0.538	0.614
House heat (therms)	61.18	152.71	230.93	254.75	204.55	162.98	76.12	31.52	3.27	0	1.40	14.48
Water heat (therms)	25.85	26.52	28.95	30.50	27.55	28.95	26.52	25.85	23.52	22.75	22.75	23.52
Degree days	262	654	980	1091	876	698	326	135	14	0	6	62
Aver. ambient temp. (roof)	61.19°	45.93°	35.77°	32.41°	36.55°	45.74°	57.05°	66.78°	75.78°	80.92°	79.89°	72.39°
T_b for V = 3000 gal; K/d = 0; A = 1130 ft²	207°	207°	207°	85.05°	116.80°	170.37°	207°	207°	207°	207°	207°	207°
Efficiency η	36.60%	31.75%	49.27%	61.83%	50.26%	38.08%	35.28%	38.28%	40.93%	42.39%	42.10%	39.95%
T_b for V = 3000 gal; K/d = 0.2; A = 1280 ft²	207°	207°	180.56°	85.20°	123.83°	187.87°	207°	207°	207°	207°	207°	207°
Efficiency η	36.58%	36.39%	53.33%	60.80%	51.13%	40.27%	35.28%	38.28%	40.93%	42.39%	42.10%	39.95%

Table XVI—Grand Junction, Colorado

	Oct.	Nov.	Dec.	Jan.	Feb.	March	April	May	June	July	Aug.	Sept.
Insolation in therms/ft² (tilt correct incl.)	0.689	0.545	0.520	0.512	0.494	0.622	0.546	0.519	0.539	0.542	0.624	0.691
House heat (therms)	72.84	173.25	247.63	278.03	202.13	161.44	87.94	31.72	5.03	0	0	7.88
Water heat (therms)	25.89	26.55	28.99	30.54	27.58	28.99	26.55	25.89	23.55	22.79	22.79	23.55
Degree days	333	792	1132	1271	924	738	402	145	23	0	0	36
Aver. ambient temp. (roof)	57.31°	40.91°	31.35°	26.40°	34.40°	44.14°	55.13°	65.46°	75.43°	82.07°	79.23°	71.74°
T_b for V = 3000 gal; K/d = 0; A = 870 ft²	207°	207°	154.54°	110.39°	85.89°	166.77°	207°	207°	207°	207°	207°	207°
Efficiency η	35.39%	39.37%	52.29%	61.04%	54.95%	38.26%	34.68%	37.88%	40.83%	42.71%	41.92%	39.76%
T_b for V = 3000 gal; K/d = 0.2; A = 960 ft²	207°	207°	127.06°	115.13°	85.39°	158.47°	188.97°	207°	207°	207°	207°	207°
Efficiency η	35.37%	43.94%	55.71%	60.41%	56.25%	42.72%	37.77%	37.88%	40.83%	42.71%	41.92%	39.76%

Table XVII—Atlanta, Georgia

	Oct.	Nov.	Dec.	Jan.	Feb.	March	April	May	June	July	Aug.	Sept.
Insolating in therms/ft² (tilt correct incl.)	0.635	0.563	0.543	0.539	0.484	0.562	0.515	0.443	0.393	0.411	0.493	0.530
House heat (therms)	38.50	137.55	214.90	221.20	179.20	141.40	46.55	7.00	0	0	0	2.80
Water heat (therms)	24.80	25.50	27.90	29.45	26.60	27.90	25.50	24.80	22.50	21.70	21.70	22.50
Degree days	110	393	614	632	512	404	133	20	0	0	0	8
Aver. ambient temp. (roof)	65.98°	54.39°	47.99°	47.03°	49.19°	55.25°	64.91°	72.76°	80.46°	82.50°	81.75°	76.71°
T_b for V = 3000 gal; K/d = 0; A = 605 ft²	207°	207°	151.73°	87.43°	94.80°	104.31°	181.67°	207°	207°	207°	207°	207°
Efficiency η	38.04%	43.82%	60.54%	68.35%	66.54%	55.47%	41.89%	40.06%	42.26%	42.83%	42.62%	41.20%
T_b for V = 3000 gal; K/d = 0.01; A = 605 ft²	207°	207°	148.44°	86.35°	93.84°	103.07°	179.40°	207°	207°	207°	207°	207°
Efficiency η	38.04%	44.36%	61.17%	68.67%	66.88%	55.99%	42.28%	40.06%	42.26%	42.83%	42.62%	41.20%
T_b for V = 3000 gal; K/d = 0.02; A = 605 ft²	207°	207°	144.98°	85.34°	92.72°	101.73°	177.14°	207°	207°	207°	207°	207°
Efficiency η	38.04%	44.86%	61.78%	68.95%	67.22%	56.50%	42.65%	40.06%	42.26%	42.83%	42.62%	41.20%
T_b for V = 3000 gal; K/d = 0.05; A = 615 ft²	207°	207°	138.82°	86.44°	93.21°	101.57°	173.77°	207°	207°	207°	207°	207°
Efficiency η	38.07%	45.86%	62.55%	68.71%	67.14%	57.03%	43.19%	40.06%	42.26%	42.83%	42.62%	41.20%
T_b for V = 3000 gal; K/d = 0.1; A = 620 ft²	207°	207°	126.32°	85.11°	89.98°	98.03°	166.07°	207°	207°	207°	207°	207°
Efficiency η	38.06%	47.87%	64.50%	69.36%	68.11%	58.73%	44.43%	40.06%	42.26%	42.83%	42.62%	41.20%
T_b for V = 3000 gal; K/d = 0.2; A = 640 ft²	207°	207°	108.13°	88.18°	86.38°	95.76°	155.45°	207°	207°	207°	207°	207°
Efficiency η	38.06%	50.74%	66.64%	69.44%	68.91%	60.62%	46.14%	40.06%	42.26%	42.83%	42.62%	41.20%

TABLE XVIII—Nashville, Tennessee

	Oct.	Nov.	Dec.	Jan.	Feb.	March	April	May	June	July	Aug.	Sept.
Insolation in therms/ft² (tilt correct incl.)	0.551	0.418	0.383	0.345	0.409	0.482	0.489	0.509	0.458	0.497	0.506	0.570
House heat (therms)	42.79	130.88	201.46	216.19	176.73	138.38	51.68	11.95	0	0	0	6.11
Water heat (therms)	25.42	26.10	28.52	30.07	27.16	28.52	26.10	25.42	23.10	22.32	22.32	23.10
Degree days	154	471	725	778	636	498	186	43	0	0	0	22
Aver. ambient temp. (roof)	64.62°	52.12°	44.36°	42.45°	44.88°	52.71°	62.97°	71.62°	79.81°	83.27°	82.15°	75.75°
T_b for $V = 3000$ gal; $K/d = 0$; $A =$ 935 ft²	207°	207°	179.80°	112.72°	85.67°	179.40°	207°	207°	207°	207°	207°	207°
Efficiency η	37.65%	38.42%	51.57%	64.92%	55.90%	38.70%	37.13%	39.72%	42.08%	43.04%	42.73%	40.93%
T_b for $V = 3000$ gal; $K/d = 0.2$; $A =$ 1045 ft²	207°	207°	143.71°	111.46°	85.80°	169.02°	179.92°	207°	207°	207°	207°	207°
Efficiency η	37.63%	44.46%	57.23%	65.10%	57.40%	44.93%	41.63%	39.72%	42.08%	43.04%	42.73%	40.93%

TABLE XIX—Fresno, California

	Oct.	Nov.	Dec.	Jan.	Feb.	March	April	May	June	July	Aug.	Sept.
Insolation in therms/ft² (tilt correct incl.)	0.618	0.578	0.389	0.424	0.522	0.650	0.608	0.633	0.598	0.638	0.599	0.623
House heat (therms)	36.16	145.07	243.89	264.49	168.20	127.83	60.97	18.08	0	0	0	0
Water heat (therms)	25.51	26.19	28.61	30.16	27.24	28.61	26.19	25.51	23.19	22.41	22.41	23.19
Degree days	86	345	580	629	400	304	145	43	0	0	0	0
Aver. ambient temp. (roof)	67.85°	57.13°	48.61°	47.55°	53.01°	58.83°	65.55°	72.47°	80.47°	87.14°	84.78°	78.24°
T_b for $V = 3000$ gal; $K/d = 0$; $A =$ 1040 ft²	207°	207°	207°	85.08°	136.71°	207°	207°	207°	207°	207°	207°	207°
Efficiency η	38.61%	35.34%	52.74%	62.91%	45.85%	35.88%	37.91%	39.97%	42.27%	44.09%	43.46%	41.64%
T_b for $V = 3000$ gal; $K/d = 0.2$; $A =$ 1255 ft²	207°	207°	207°	85.10°	158.28°	207°	207°	207°	207°	207°	207°	207°
Efficiency η	38.63%	35.34%	52.74%	59.80%	42.33%	35.88%	37.91%	39.97%	42.27%	44.09%	43.46%	41.64%

TABLE XX—Albuquerque, New Mexico

	Oct.	Nov.	Dec.	Jan.	Feb.	March	April	May	June	July	Aug.	Sept.
Insolation in therms/ft² (tilt correct incl.)	0.741	0.640	0.623	0.636	0.630	0.710	0.671	0.628	0.607	0.610	0.646	0.719
House heat (therms)	61.53	177.82	253.74	273.78	201.53	166.25	81.57	19.76	0	0	0	2.82
Water heat (therms)	25.27	25.95	28.37	29.92	27.02	28.37	25.95	25.27	22.95	22.17	22.17	22.95
Degree days	218	630	899	970	714	589	289	70	0	0	0	10
Aver. ambient temp. (roof)	61.32°	46.91°	39.45°	36.43°	42.77°	49.51°	59.64°	69.23°	79.46°	83.17°	80.50°	74.31°
T_b for $V = 3000$ gal; $K/d = 0$; $A =$ 645 ft²	207°	207°	132.10°	91.35°	85.58°	163.40°	186.85°	207°	207°	207°	207°	207°
Efficiency η	36.64%	44.82%	60.61%	66.39%	57.71%	43.78%	39.49%	39.02%	41.42%	43.01%	42.27%	40.51%
T_b for $V = 3000$ gal; $K/d = 0.02$; $A =$ 650 ft²	207°	207°	128.42°	91.82°	85.51°	161.74°	183.55°	207°	207°	207°	207°	207°
Efficiency η	36.64%	45.45%	61.08%	66.33%	57.96%	44.56%	40.03%	39.02%	41.42%	43.01%	42.27%	40.51%
T_b for $V = 3000$ gal; $K/d = 0.1$; $A =$ 675 ft²	207°	207°	116.41°	95.99°	86.08°	157.55°	173.33°	207°	207°	207°	207°	207°
Efficiency η	36.64%	47.35%	62.20%	65.68%	58.50%	46.90%	41.74%	39.02%	41.42%	43.01%	42.27%	40.51%
T_b for $V = 3000$ gal; $K/d = 0.2$; $A =$ 710 ft²	207°	207°	105.68°	102.40°	86.10°	154.89°	163.53°	207°	207°	207°	207°	207°
Efficiency η	36.64%	49.08%	62.81%	64.77%	58.89%	48.88%	43.35%	39.02%	41.42%	43.01%	42.27%	40.51%
T_b for $V = 10,000$ gal; $K/d = 0$; $A =$ 625 ft²	207°	207°	157.56°	107.52°	85.22°	125.82°	170.73°	207°	207°	207°	207°	207°
Efficiency η	36.64%	40.63%	54.45%	64.20%	63.21%	52.30%	42.17%	39.02%	41.42%	43.01%	42.27%	40.51%
T_b for $V = 10,000$ gal; $K/d = 0.02$; $A =$ 640 ft²	207°	207°	152.09°	104.59°	85.25°	126.07°	167.93°	207°	207°	207°	207°	207°
Efficiency η	36.64%	41.54%	55.70%	64.56%	63.17%	52.68%	42.62%	39.02%	41.42%	43.01%	42.27%	40.51%
T_b for $V = 10,000$ gal; $K/d = 0.1$; $A =$ 690 ft²	207°	207°	132.42°	96.64°	85.36°	124.57°	156.79°	203.87°	207°	207°	207°	207°
Efficiency η	36.64%	44.79%	59.77%	65.66%	63.38%	54.62%	44.96%	39.50%	41.42%	43.01%	42.27%	40.51%
T_b for $V = 10,000$ gal; $K/d = 0.2$; $A =$ 745 ft²	207°	192.40°	115.86°	93.14°	85.55°	121.55°	145.84°	184.98°	206.26°	207°	207°	207°
Efficiency η	39.10%	49.78%	62.66%	66.13%	63.78%	56.74%	49.71%	42.74%	41.50%	43.01%	42.27%	40.51%

VOL. 3 1959

Table XXI—Los Angeles, California

	Oct.	Nov.	Dec.	Jan.	Feb.	March	April	May	June	July	Aug.	Sept.
Insolation in therms/ft² (tilt correct incl.)	0.593	0.534	0.515	0.523	0.578	0.670	0.543	0.559	0.480	0.570	0.592	0.606
House heat (therms)	39.82	91.55	137.78	173.03	139.61	124.97	84.68	55.39	25.63	14.19	10.07	25.63
Water heat (therms)	25.11	25.80	28.21	29.76	26.88	28.21	25.80	25.11	22.80	22.01	22.01	22.80
Degree days	87	200	301	378	305	273	185	121	56	31	22	56
Aver. ambient temp. (roof)	65.74°	61.97°	58.66°	55.33°	56.17°	58.93°	61.27°	64.14°	66.95°	69.91°	70.69°	69.10°
T_b for V = 3000 gal; K/d = 0; A = 475 ft²	207°	207°	171.49°	137.40°	86.65°	156.04°	174.37°	191.81°	207°	207°	207°	207°
Efficiency η	38.00%	42.76%	52.84%	64.54%	62.07%	49.57%	44.53%	40.01%	38.34%	39.22%	39.45%	38.98%
T_b for V = 3000 gal; K/d = 0.2; A = 550 ft²	207°	199.72°	130.40°	125.79°	85.87°	151.57°	150.73°	162.48°	196.43°	201.47°	207°	207°
Efficiency η	39.19%	50.45%	60.75%	66.32%	62.83%	53.94%	52.88%	46.51%	41.00%	40.10%	39.45%	38.98%

Table XXII—Charleston, South Carolina

	Oct.	Nov.	Dec.	Jan.	Feb.	March	April	May	June	July	Aug.	Sept.
Insolation in therms/ft² (tilt correct incl.)	0.562	0.529	0.461	0.547	0.484	0.559	0.543	0.530	0.476	0.489	0.513	0.483
House heat (therms)	18.20	94.50	159.60	165.20	132.65	98.35	22.05	0	0	0	0	0
Water heat (therms)	24.92	25.62	28.02	29.57	26.71	28.02	25.62	24.92	22.62	21.82	21.82	22.62
Degree days	52	270	456	472	379	281	63	0	0	0	0	0
Aver. ambient temp. (roof)	69.56°	59.54°	54.04°	53.57°	55.02°	60.11°	68.14°	74.22°	80.48°	82.83°	82.63°	78.73°
T_b for V = 3000 gal; K/d = 0; A = 505 ft²	207°	207°	173.12°	85.89°	136.30°	126.91°	196.85°	207°	207°	207°	207°	207°
Efficiency η	39.14%	41.79%	59.18%	64.37%	58.77%	50.97%	40.35%	40.48%	42.27%	42.92%	42.87%	41.78%
T_b for V = 3000 gal; K/d = 0.2; A = 575 ft²	207°	207°	127.80°	85.15°	131.10°	111.37°	172.72°	207°	207°	207°	207°	207°
Efficiency η	39.15%	49.06%	65.80%	65.23%	61.84%	56.98%	44.28%	40.48%	42.27%	42.92%	42.87%	41.78%

Table XXIII—El Paso, Texas

	Oct.	Nov.	Dec.	Jan.	Feb.	March	April	May	June	July	Aug.	Sept.
Insolation in therms/ft² (tilt correct incl.)	0.725	0.670	0.649	0.661	0.654	0.745	0.679	0.648	0.587	0.592	0.658	0.706
House heat (therms)	23.61	131.53	211.12	225.96	150.08	111.29	37.10	0	0	0	0	0
Water heat (therms)	24.77	25.47	27.88	29.42	26.57	27.88	25.47	24.77	22.47	21.67	21.67	22.47
Degree days	70	390	626	670	445	330	110	0	0	0	0	0
Aver. ambient temp. (roof)	68.08°	55.30°	48.88°	46.91°	52.82°	58.10°	66.88°	75.35°	84.13°	84.93°	83.25°	78.65°
T_b for V = 3000 gal; K/d = 0; A = 495 ft²	207°	207°	155.53°	86.56°	89.07°	179.32°	207°	207°	207°	207°	207°	207°
Efficiency η	38.70%	43.46%	60.34%	69.25%	57.44%	40.29%	38.31%	40.81%	43.28%	43.50%	43.04%	41.75%
T_b for V = 3000 gal; K/d = 0.2; A = 535 ft²	207°	207°	114.07°	90.00°	86.51°	158.92°	174.12°	207°	207°	207°	207°	207°
Efficiency η	38.69%	50.07%	65.77%	69.12%	60.85%	48.97%	43.70%	40.81%	43.28%	43.50%	43.04%	41.75%

Table XXIV—Fort Worth, Texas

	Oct.	Nov.	Dec.	Jan.	Feb.	March	April	May	June	July	Aug.	Sept.
Insolation in therms/ft² (tilt correct incl.)	0.674	0.577	0.542	0.483	0.541	0.617	0.573	0.549	0.555	0.581	0.623	0.669
House heat (therms)	16.92	87.23	155.50	181.47	130.12	89.86	26.26	1.46	0	0	0	0
Water heat (therms)	24.92	25.62	28.02	29.57	26.71	28.02	25.62	24.92	22.62	21.82	21.82	22.62
Degree days	58	299	533	622	446	308	90	5	0	0	0	0
Aver. ambient temp. (roof)	71.41°	58.32°	51.49°	48.09°	52.47°	58.52°	68.42°	75.85°	84.34°	88.28°	88.67°	81.47°
T_b for V = 3000 gal; K/d = 0; A = 555 ft²	207°	207°	207°	134.87°	86.12°	188.94°	207°	207°	207°	207°	207°	207°
Efficiency η	39.66%	35.72%	45.69%	63.14%	56.35%	38.86%	38.78%	40.95%	43.34%	44.40%	44.50%	42.54%
T_b for V = 3000 gal; K/d = 0.2; A = 635 ft²	207°	207°	162.35°	123.43°	85.76°	175.35°	181.72°	207°	207°	207°	207°	207°
Efficiency η	39.68%	43.15%	54.50%	64.86%	58.42%	45.25%	42.90%	40.95%	43.34%	44.40%	44.50%	42.54%

TABLE XXV—Phoenix, Arizona

	Oct.	Nov.	Dec.	Jan.	Feb.	March	April	May	June	July	Aug.	Sept.
Insolation in therms/ft² (tilt correct incl.)	0.737	0.632	0.594	0.616	0.674	0.727	0.680	0.668	0.612	0.596	0.628	0.717
House heat (therms)	8.77	88.92	159.50	189.01	123.21	78.16	29.51	0	0	0	0	0
Water heat (therms)	25.02	25.71	28.12	29.67	26.80	28.12	25.71	25.02	22.71	21.92	21.92	22.71
Degree days	22	223	400	474	309	196	74	0	0	0	0	0
Aver. ambient temp. (roof)	73.92°	62.18°	56.30°	52.40°	57.78°	63.56°	71.15°	79.43°	88.37°	93.58°	91.60°	87.14°
T_b for V = 3000 gal; K/d = 0; A = 445 ft²	207°	207°	191.86°	112.78°	89.80°	203.24°	207°	207°	207°	207°	207°	207°
Efficiency η	40.40%	39.41%	52.85%	66.85%	55.01%	37.97%	39.59%	41.97%	44.42%	45.79%	45.28%	44.09%
T_b for V = 3000 gal; K/d = 0.2; A = 485 ft²	207°	207°	136.98°	100.04°	85.22°	177.20°	179.40°	207°	207°	207°	207°	207°
Efficiency η	40.40%	48.34%	62.92%	69.28%	59.60%	46.70%	44.06%	41.97%	44.42%	45.79%	45.28%	44.09%

auxiliary heat at all. Six different schedules were assumed and calculated. The schedules are given in Table XXIX and the results shown in Fig. 9. The third schedule is based on the figures given by Whillier[2] for the M.I.T. house, which—as explained in Appendix A—was built "tight" so as to reduce drastically the convection losses generally found in a residential house. If one regards the decrease in heat demand due to the tight construction as though it were auxiliary heat furnished to our standard house of average tightness, the third schedule (B_3) is the result.

The fourth, fifth, and sixth schedules are chosen to ascertain the effect of different amounts of auxiliary heat on the required collector area together with the other parameters.

FURTHER ECONOMIC CONSIDERATIONS

A. Cost of storage

The cost of energy storage is conveniently separated into cost of the tank and cost of insulation. Steel tanks are more practical than wooden tanks, and, in the larger sizes, cheaper as well. (See Appendix B.) A 3,000-gal tank of diameter 5 ft 4 in. and 18 ft long can be built of $\frac{3}{16}$-in. steel, and costs $350. Larger diameter tanks must be built of $\frac{1}{4}$-in. steel. An 8 ft x 8 ft tank (3,000 gal) costs $500; a 10 ft x 10$\frac{1}{4}$ ft tank (6,000 gal) costs $750; a 10$\frac{1}{2}$ ft x 15$\frac{1}{2}$ ft tank (10,000 gal) costs $982; a 12 ft x 12 ft tank (10,000 gal) costs $1,300. These prices are not for quantity orders, but the saving can be considered canceled out by the additional cost, not figured in the above, of rust prevention treatment. (Data from the Buffalo Tank Corp.)

In the 3,000-gal tank size, the longer tank is more economical than the square tank. The shape factors are 6.36 and 5.54 respectively—a 13 per cent disadvantage for the long tank, but 13 per cent increase in insulation cost is significantly less than the $150 difference in tank price. The same conclusion holds *a fortiori* for the case of the two 10,000-gal tanks; the long tank has a shape factor of 5.625, an increase of only 1$\frac{1}{2}$ per cent, while the insulation cost which is to be increased by this amount is not quite double that for the 3,000-gal tank.

A plot of the different tank capacities against cost does not result in a smooth curve; moreover, for lowest cost, tanks must be purchased in stock sizes. Thus, it is better to consider tank costs as quantized, rather than as so many dollars per gallon capacity.

The cost of insulation is figured on the basis of data furnished by the Pittsburgh Plate Glass Co. on their Superfine Fiber Glass of 1 lb per cu ft density and K factor at 137°F of 0.27 Btu per sq ft per hr per °F for 1-in. thickness. It comes in batts either 3 in. thick or 5 in. thick and the price for quantity orders for either thickness figures out to 6.7 cents per sq ft per in. thickness. This means, for example, that the 18 ft long, 3,000-gal tank mentioned above can be swathed in 15 in. of insulation for about $400, 15 per cent allowance being made for the fact that the outer batts must cover a larger area than the innermost batt.

In determining the most economical combination of collector area, tank capacity, and insulation, it is convenient to express the insulation cost as 1.8 cents per sq ft for an insulating value of 1 Btu per sq ft per hour per °F. The change in K factor with temperature is neglected.

B. Optimizing the Parameters

On a strictly economic basis it is cheaper in most localities to save some $400 invested in insulating the house when it is constructed and pay perhaps $35 more per year for fuel oil. (See Fig. 7). However, such a house will be less comfortable in extremely cold or extremely hot weather, which is the reason people are willing to pay for the insulation. Similarly, instead of making a "tight" house at an extra construction cost of $500 or $1,000, a solar heating system, since it requires an extra capital outlay in the best of cases, should aim at ways to *reduce* the construction costs of the house.

In this report we are not concerned with optimizing the proportions spent on different items in house construction but only with optimizing the items, or parameters, used in the present calculations, i.e., the cost

VOL. 3 1959

of collectors and of storage. The calculations are made for the standard house described above. The measure of economic feasibility is again taken as the amount which can be afforded for each square foot of collector, assuming a 10-year amortization period, and Equations [2] and [3] are used to calculate $\partial M/\partial A$. Equation [4], however, is no longer adequate; instead we use:

$$\Delta M = A\frac{\partial M}{\partial A} + V\frac{\partial M}{\partial V} + \frac{1}{K/d}S\frac{\partial M}{\partial S}\bigg|_{K/d=1} - \begin{Bmatrix}800\\600\end{Bmatrix} \quad [10]$$

The third term on the right is the cost of insulation; the partial derivative is the cost of insulation per unit area for a thickness and material of 1 Btu per sq ft per hr per °F. The value of K/d is thus one of the variables, or rather f is, since K is fixed at 0.27 Btu per sq ft per hr per °F in. thickness.

The problem is to find the set of values for A, V, $\partial M/\partial V$, S, and d which will minimize ΔM, or rather which will maximize $\partial M/\partial A$. We thus need not only Equation [10] but also the relation

$$\frac{\Delta M}{5} = M_f = 0.18\sum_{1}^{12}(H + W - B)_i \quad [11]$$

where the factor of 0.18 is our assumed fossil fuel rate of 18 cents a therm, and B is the B_1 Schedule of Table XXIX. The first step is to assume a value for V of either 3,000, 6,000 or 10,000 gal. Then, from the storage tank cost and dimension information given in Part A of this Section, we get $\partial M/\partial V$ and S. We next pick a value of K/d and interpolate the corresponding value of A from the calculated data, and, substituting into Equations [10] and [11], compute $\partial M/\partial A$. The process is then repeated for different pairs of K/d and A values until a maximum value of $\partial M/\partial A$ is obtained. Then a different choice is made for V, and the whole process again repeated.

This trial and error procedure was used for only three localities: Lander, Blue Hill, and Albuquerque. It then became obvious that the optimum storage tank size for all localities is 3,000 gal. We cannot consider tanks much smaller than 3,000 gal or the storage will not be able to supply house heat during several days of successive cloudy weather, i.e., there is a minimum even for short-term storage.

In Albuquerque, $\partial M/\partial A$ is \$2.52 for a 3,000-gal tank, and about 70 cents for a 10,000-gal tank. As can be seen from Fig. 11, the 10,000-gal tank must be well insulated (long-term storage) in order to reduce the required collector area. In Lander, which can be seen from Fig. 10 to be a much more favorable place for large storage tanks, $\partial M/\partial A_{max}$ is \$1.06 for a 3,000-gal tank, and 86 cents for a 10,000-gal tank. Lander is probably the best place of the twenty-one for large-capacity storage; when the smallest tank turned out to be the cheapest there too, further calculations were limited to houses with 3,000-gal storage tanks. Accordingly, $V\,\partial M/\partial V$ was taken as \$350, and S as 400 sq ft.

Thus, Equations [10] and [11] reduce to

$$\frac{\partial M}{\partial A} = \frac{1}{A}\left(5M_f - \frac{400\times 0.018}{K/d} + \begin{Bmatrix}450\\250\end{Bmatrix}\right) \quad [12]$$

Figs. 9–11 led to a further simplification in calculating the optimum values of the parameters. It became clear that a sufficiently good approximation could be obtained by assuming a linear relationship between A and K/d.

$$A = \frac{\Delta A}{0.2}K/d + A_0 \quad [13]$$

where A_0 = required collector area when $K/d = 0$ and ΔA = difference in required collector area for $K/d = 0$ and $K/d = 0.2$.

The optimum value of K/d can then be found directly by setting equal to zero the derivative of $\partial M/\partial A$ with respect to K/d. Thus we get

$$\frac{K}{d}\bigg|_{opt.} = \frac{1.44 + \sqrt{2.0736 + 0.288\left(M_f + \begin{Bmatrix}50\\90\end{Bmatrix}\right)A_0/\Delta A}}{M_f + \begin{Bmatrix}50\\90\end{Bmatrix}}$$

The results of these calculations are tabulated in Table XXVI. Fig. 1 is drawn on the basis of the values (maxima) found for $\partial M/\partial A$. The insulation costs, $S\,\partial M/\partial S$ are found simply by dividing the optimum

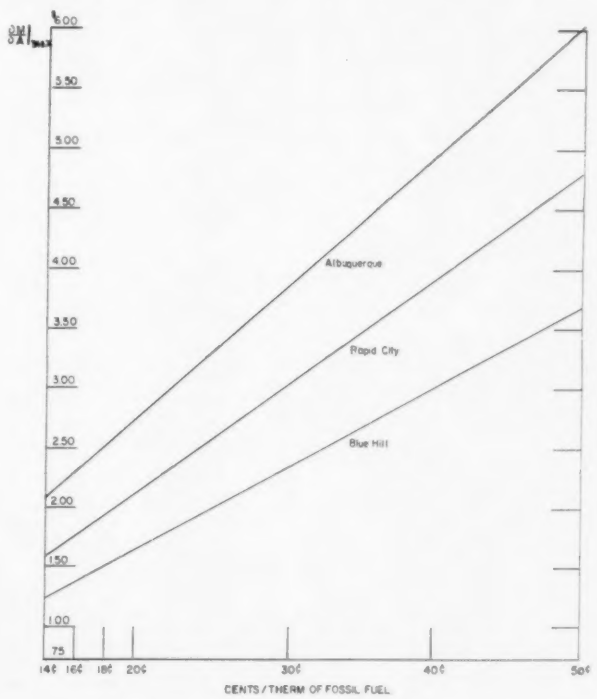

FIG. 12—Maximum allowable cost for each square foot of solar collector vs. cost of heating fuel.

TABLE XXVI—Optimum Parameters

$V = 3000$ gal $\quad V\frac{\partial M}{\partial V} = \$350 \quad S\frac{\partial M}{\partial S}\Big|_{\frac{K}{d}=1} = \$7.20$

Location	Fuel saving at 18¢/therm (M_f)	Insulation factor K/d (Btu/ft²/hr/°F)	Insulation costs $S\frac{\partial M}{\partial S}$	Collector area A (ft²)	$\frac{\partial M}{\partial A}\Big\|_{max.}$
Blue Hill, Mass.	$349	0.08	$88	1401	$1.50
Central Mass.	348	.08	87	1487	1.41
Ithaca, N. Y.	316	.12	62	1641	1.20
Madison, Wis.	332	.19	39	1598	1.30
Rhode Island	336	.09	77	1256	1.63
Columbus, Ohio	296	.10	75	1438	1.29
Medford, Ore.	331	.11	67	1909	0.96
Lander, Wyo.	359	.06	120	2010	1.06
Rapid City, S. D.	323	.09	81	1017	1.95
New York City & Long Island	286	.11	65	1063	1.71
Columbia, Mo.	258	.08	86	1192	1.38
Grand Jctn., Colo.	271	.09	79	910	1.90
Nashville, Tenn.	218	.09	76	985	1.49
Atlanta, Ga.	219	.14	53	626	2.07
Fresno, Calif.	234	.08	95	1121	1.18
Albuquerque, N. M.	265	.10	76	674	2.52
Los Angeles, Calif.	208	.09	81	505	2.39
Charleston, S. C.	165	.10	69	540	1.86
El Paso, Texas	202	.12	58	517	2.32
Ft. Worth, Texas	166	.10	70	592	1.70
Phoenix, Ariz.	164	.12	61	466	2.16
$V = 10{,}000$ gal	$V\frac{\partial M}{\partial V} = \$982$		$S\frac{\partial M}{\partial S}\Big|_{\frac{K}{d}=1} = \$14.15$		
Lander, Wyoming	359	.07	202	1640	0.86

TABLE XXVII—Simplified Calculation

Locality	Annual degree days	Correction factor beta	Fuel savings (No auxil. heat) $0.18\sum_{1}^{12}(H+W)_i$	Collector area (ft²)	Cost of energy storage @ $1/therm	$\frac{\partial M}{\partial A}\Big\|_{max}$ $/ft²
Blue Hill, Mass.	6392	1.06	$362	785	$672	$2.47
Central Mass.	6743	1.00	$361	760	$662	$2.56
Ithaca, N. Y.	6914	.875	$330	725	$652	$2.48
Madison, Wis.	7417	.863	$346	715	$660	$2.61
Rhode Island	6125	1.059	$349	695	$632	$2.75
Columbus, Ohio	5615	1.00	$309	640	$644	$2.66
Medford, Ore.	4547	1.40	$344	615	$712	$2.61
Lander, Wyo.	8303	.842	$372	575	$596	$3.59
Rapid City, S. D.	7535	.82	$336	570	$528	$3.43
N. Y. City and Long Island	4989	1.076	$299	565	$570	$3.05
Columbia, Mo.	5113	.934	$271	495	$536	$3.27
Grand Jctn., Colo.	5796	.875	$285	440	$536	$3.84
Nashville, Tenn.	3513	1.112	$231	430	$488	$3.41
Atlanta, Ga.	2826	1.40	$232	400	$484	$4.31
Fresno, Calif.	2532	1.682	$247	380	$532	$3.43
Albuquerque, N. M.	4389	1.129	$278	375	$532	$4.42
Los Angeles, Calif.	2015	1.831	$221	340	$268	$4.22
Charleston, S. C.	1973	1.40	$179	300	$332	$3.87
El Paso, Texas	2641	1.349	$214	280	$420	$4.47
Ft. Worth, Texas	2361	1.167	$178	265	$348	$5.07
Phoenix, Ariz.	1698	1.595	$176	230	$316	$5.07

K/d values into $7.20, i.e., 400 sq ft times 0.18 dollars per sq ft for 1 Btu per sq ft per hr per °F.

C. Changes in Fuel Cost

Waiting for conventional fuel to become expensive (while presumably the cost of building and installing solar equipment remains unchanged) is a sad method of "improving" solar house heating. However, it is worthwhile investigating the effect of such an increase in fuel costs. Fig. 12 shows the permissible cost per square foot of collector plotted against the cost per therm for fossil fuel used in three different cities. Where the graph crosses 18 cents per therm corresponds to the data given in Table XXVI.

The calculation is made the same way as that described in Part B of this section, but with the fuel savings proportional to the value assumed for the cost of fossil fuel. It is not hard to show that the curves should be approximately linear. They can be represented with fair accuracy by the equation:

$$\frac{\partial M}{\partial A} \doteq \frac{5M_f}{A_0}\,p + \frac{450K/d - 7.2}{A_0 K/d} \qquad [15]$$

where p is the ratio of the cents per therm paid for fossil fuel to the assumed value of 18 cents per therm.

DISCUSSION OF RESULTS

One's first instinct when confronted with the mass of data presented in the tables and figures is self-preservation; i.e., reduction of the data to a few simple general equations. This can be done only on a limited basis, but it is not worthwhile, for example, to try to fit the annual insolation or heat load data with sinusoidal expressions.

It can be seen from Figs. 9–11 that, for a given storage capacity, there is a nearly linear relationship between collector area (A) and insulation (K/d), as expressed in Equation [13]. But if we try to extend the idea to include storage capacity and find a relation such that the constants hold for all localities, we can expect disappointment. For example, a relation of the form

$$A = C_1 V^{C_2} K/d + C_3 \frac{M_f}{V^{C_2}\sum_{1}^{4} I_i} \qquad [16]$$

where the C's are constants, was investigated and found not worthwhile. Instead it seems better to be content with observing:

(1) The slope of A vs. K/d curves increases with V.

(2) A_0 with 10,000-gal storage is always less than A_0 with 3,000-gal storage.

(3) A increases with the severity of the winter (degree days) and decreases with the amount of winter insolation. Summer insolation makes no difference because heat is thrown away in the summer anyway unless the storage capacity is very large and the storage efficiency

VOL. 3 1959

very high. (See section on "Simplified Calculation," above.)

Inspection reveals the great sensitivity of the calculation to collector efficiency (Fig. 3). For example, in Table V the temperature in the 3,000-gal storage tank on January 1st is 85.03° when the insulation leaks 0.1 Btu per sq ft per hour per °F, but 85.13° when the insulation leaks heat twice as fast. In both cases, the collector area is taken as 1410 sq ft, although it is clear that a very slightly smaller collector area, 1408 or 1409 sq ft, would suffice in the second case. The chief reason for this paradox—that *lower* storage efficiency makes the over-all system *more* efficient—is indicated in the lines immediately below the temperatures, i.e., the collector efficiencies. When the heat leaks out faster, the collector temperature is lower; in November and December, which are the critical months, the gain of 3 per cent in collector efficiency more than outweighs the greater heat wastage of the less thickly insulated storage tank.

Another striking example is afforded by Figure 9. As shown by Table XXIX, the B_4 schedule supplies more auxiliary heat than the B_1 schedule in November, February and March, and the same auxiliary heat in December and January. Yet the B_4 schedule requires a *larger* collector area, for all storage efficiencies, than does the B_1 schedule. As with the first example, the computer calculation (not given for B_4) was checked by desk calculator and the paradox traced to the higher storage tank temperature (due to the auxiliary heat supplied in November) causing a lower collection efficiency. These two examples illustrate the value of carrying out the calculations to four significant figures, even though agreement with measurements would not be expected to be better than the second significant figure.

It is clear that auxiliary heat should be furnished with caution, since it may not give real assistance to the solar heating system. To calculate the optimum auxiliary heat schedule would be very tedious, but the superiority of B_1 over B_4 suggests that it should be small. Auxiliary heat furnished before the minimum tank temperature is reached, i.e., January 1st, lowers the collection efficiency. Auxiliary heat furnished after January 1st is generally unnecessary. However, if no auxiliary heat at all is furnished, as in schedule B_2, the result—as can be seen from Fig. 9—is a substantial increase in the required collector area. It is probable that B_1 is quite close to the optimum. (As pointed out in Principal Conclusion No. 13, this does not mean the most economical.)

The extreme sensitivity of the system to collection efficiency means that the maximum temperature at which the water is stored should, in an optimized system, be carefully determined. The paradoxes indicated above strongly imply that 207°F is too high a temperature. The optimum maximum storage temperature should probably be about 190°F. This would reduce the energy storage capacity of the tank, but the gain in collection efficiency would (especially in November) reduce the required collector area and thus the cost.

The optimum maximum temperature was not calculated, however, because the result would be considerably in error as long as the calculation is made on a month-to-month basis, i.e., the collection efficiency does not vary with the day-to-day temperature in the storage tank, but is taken as constant over an entire month. It is even possible that neither of the above paradoxes would appear, i.e., actual cross-overs from the expected result, if collection efficiency were not quantized monthly. However, the conclusions drawn would probably remain valid.

No calculations were run for collectors with efficiencies different from those shown in Fig. 3. To a first approximation, however, the required collector areas can be taken as inversely proportional to the collection efficiencies under certain more-or-less average conditions:

$$\frac{\eta_1}{\eta_2} = \frac{A_2}{A_1} \qquad [17]$$

Equation [17], it will be recalled, holds accurately for the simplified calculation. (See Fig. 6.)

One other paradox deserves mention. In Table V, line 1, it can be noted that the insolation for December exceeds that for November, although the December sun is lower in the sky and the days are shorter. The chief reason is indicated in Table IV, i.e., the horizontal-to-tilt ratio. A secondary reason is that December has one more day than November.

We turn now to the results of the calculations of economic feasibility. The significance of the values computed for $\partial M/\partial A$ depends on the actual present-day costs of building and installing collectors. Reasonable estimates seem to be: custom-made collectors would cost more than $10 per sq ft; if collectors were mass-produced, the cost could probably be brought below $5, perhaps below $3. In the next decade fuel costs will probably rise, but so will materials and labor, so that little change in feasibility is to be expected from this direction. A breakthrough, on the other hand, that would permit collectors to be built and installed for $1.00 or $1.50 per sq ft, would make a decisive change in feasibility prospects.

This means that a breakthrough in cost of collectors, to make solar house-heating competitive, must accomplish a price improvement by a factor of two or three. A breakthrough in storage costs to accomplish the same thing would have to be more extreme. In the simplified calculation above, a factor of 10 was assumed, i.e., 90 per cent reduction of cost. The fact, mentioned above,

that the "elbow" values in Fig. 5 are the most economical on each curve means that 90 per cent reduction is somewhat greater than that necessary. In other words, a factor of 7 or 8 in storage cost reduction might suffice. This assumes, of course, that the collector costs indicated in Fig. 2 are realistic. The minimum factor which would do the trick depends, however, not only on collector costs ($\partial M/\partial A$) but also on the collector efficiency, which was assumed in the simplified calculation to be a constant 50 per cent.

A breakthrough in storage costs would almost automatically make long-term storage more economical than short-term storage. As indicated in Fig. 5, large reductions in collector area (A) are achieved only by using very large storage capacities; such large capacities are advantageous only if summer heat is saved for winter use, i.e., long-term, high efficiency storage. Thus, if storage reduces collector area to where present collector costs can be met, the storage would be both of high efficiency and large capacity.

The similarity between Fig. 1 and Fig. 2, e.g., the relatively favorable areas being in the Southwest and the Appalachians, show that the areas suitable for solar house-heating are nearly independent of the cost of energy storage. In other words, whether or not there is a breakthrough in cost of energy storage, the same sections of the country remain the most favorable sections, and the same sections of the country remain the most unfavorable.

It should be noted that the accuracy of Figs. 1 and 2 is quite poor; not only were they drawn chiefly on the basis of 21 points, but the significant variations in climate known to occur within short distances (e.g., between Blue Hill and Boston) were ignored. In several cases, such as Tables VI and XIV, degree-day data for a locality was combined with isolation data for an adjacent area to complete the set of input data.

Both Figs. 1 and 2 show the southern tip of Florida as an uneconomic place for solar house heating. The chief reason is that the annual fuel savings (M_f) are too small. (See Fig. 7.) Since we have stipulated that the furnace is to be eliminated, some importance attaches to what might be called the "furnace line," i.e., the geographical line south of which the better class one-family houses do *not* have central heating. Inquiry as to where this line should be drawn indicates that it is moving southward; that is, in new houses along the Gulf Coast there is a growing tendency to include central heating. Even in Miami, the electric company is propagandizing for central heating because the electric load on cool evenings, when everyone turns on their electric room heaters, constitutes a utility problem. The line passing through places having an average January containing between 300 and 330 degree days hits San Diego, Yuma, Corpus Christi, and Jacksonville. New

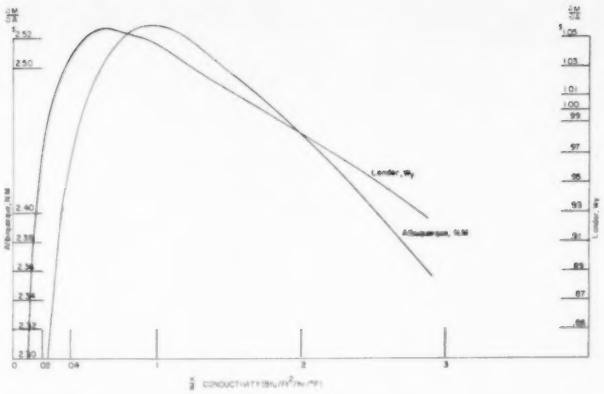

FIG. 13—Cost for each square foot of solar collector vs. thermal conductivity of storage tank insulation for 3,000-gal tank costing $350 and insulation costing $7.20/$(K/d)$.

Orleans, Mobile, and Thomasville (Georgia) have slightly more.

In this connection it may be noted that the widely reproduced feasibility map by Siple (Reference 6, page 15), considers only "mechanical feasibility," i.e., "economic considerations were not included." Some writers on solar energy have not been too careful about observing the distinction.

It was shown above that the dividing line between long-term and short-term storage is about 0.02 Btu per sq ft per hr per °F. Thus, it can be seen from the column of insulation factors in Table XXVI that short-term storage is cheaper than long-term storage. This means that the idea of storing summer heat for winter use does not pay at the present cost of energy storage.

It can be noted that the variation in the economically optimized insulation factor for different parts of the United States is quite small, averaging about one-fifth the insulation required for long-term storage. However, the thickness of insulation is not critical as far as overall expense is concerned; using Equation [10], $\partial M/\partial A$ goes through a flat maximum when graphed against K/d. The curve falls more steeply on the side of the thicker insulation because the cost of insulation becomes infinite as K/d approaches zero. Two examples, for Albuquerque and Lander, are shown in Fig. 13.

It is difficult to draw general conclusions from Table XXVI. For example, there is no correlation between the insulation costs ($S\ \partial M/\partial S$) and the optimized collector area or the optimized collector cost. There is a slight correlation between the latter two; that is, a small collector area is usually associated with a high permissible collector cost, but there are exceptions even to this qualitative formulation. Compare, for example, Blue Hill and Rhode Island with Nashville, Columbia, and Fresno.

If the storage tank is placed inside the house instead

VOL. 3 1959

of in the basement, the ambient temperature is higher and the heat leakage rate per inch thickness of insulation is less. Moreover, the heat that leaks out in winter is not lost but helps to heat the house, thus providing almost 100 per cent efficiency. Löf[3] and Telkes[4] have each built a solar house embodying this idea. If there is a full basement, extra lolly columns may be needed to support the tank. The tank itself could be part of the structure of the house, preferably at an inside corner, so that only a half or a quarter of the cylindrical surface protrudes into a room or closet. However, only about 15 per cent saving on insulation is achieved because the heat must still be stored for the same length of time. If the house is designed for short-term storage, the percentage saving in insulation is greater, but there is not much insulation cost to begin with. Moreover, the heat leakage in summer will probably be objectionable. In such cases, *cold* can be stored in the tank. (See the following section.)

No consideration was given in the calculations to the collection of solar energy through south-facing windows. As indicated by Anderson[6] the losses for a sunny winter day (in New England) calculated for a 24-hr period, will exceed the solar radiation transmitted into the house unless the window is double-paned and/or curtained at night.

AIR CONDITIONING

The most expensive part of the solar equipment is the collector, and it would be advantageous if the same collector could be used to operate a cooling system in summer as well as the heating system in winter. Since there is considerably more solar energy available to the collector in the summer than the heating system can make use of, no additional collector area is required if a solar-powered air-conditioning unit is added. Moreover, some parts of the country, particularly the Southwest, where air conditioning is needed, are also the most favored for solar house heating. (These areas sometimes have such low humidity that the air can be satisfactorily cooled by simple water-spray devices rather than refrigeration machinery.)

However, in most parts of the United States, the annual cost of air conditioning is too small for a solar system to pay for itself as a fuel (i.e., electricity) saver. Almost any one-family house of 2,000 sq ft or less can be cooled with a 2-ton or 3-ton unit. In southernmost United States, the cost of electricity for a season of air conditioning is generally less than $150, and in most parts of the country it is less than $75.[17, 18] This is despite the fact that the cost of removing a Btu may be more than double the cost of furnishing a Btu. Fig. 7 shows that such a small fuel saving can be justified only if the cost of the solar equipment does not exceed that of the conventional equipment by more than $200 or $300.

Secondly, flat-plate collectors which are quite satisfactory for heating houses do not, under usual weather conditions, yield high enough temperatures to be suitable for a refrigeration system. Thus, if collectors are to be used for both heating and cooling, the more expensive kind needed for cooling must be installed (at least, *some* of the collector area must have the higher temperature type.)

Higher temperatures are needed whether one uses a solar-powered compressor with a mechanical air conditioning system or an absorption-type refrigeration cycle. Tabor, who made a theoretical comparison between these two alternative methods, has expressed the opinion that there is not much to choose between them. From the standpoint of considering economic feasibility, it is easier to consider the solar compressor. Although in practice there is a complicated engineering problem involved, in principle the solar compressor consists chiefly in replacing an electric motor with a cyclical heat engine, the rest of the air conditioning system being similar in the conventional and the solar system. Between the difficulties of building a cheap substitute for a simple electric motor and the high temperature requirement on the solar collector, solar air conditioning does not appear very promising.

However, solar house heating can make possible a saving if the house is air-conditioned. If the storage tank is used to store *cold* water, a conventional refrigeration unit can be run more or less continually during the hot season cooling the water. The required capacity of the refrigeration unit is thereby reduced from perhaps 3 tons to 1 ton or even $\frac{3}{4}$ ton. The kilowatt hours of electricity consumed are about the same, but the difference in initial cost between the large and small unit represents a one-shot saving made possible by the solar storage tank. The small second tank can be used to provide house heat on occasional cool evenings. However, this may not be satisfactory in many regions where the seasons change irregularly and "unseasonable" temperatures are common.

The question of economic feasibility for solar cooling involves two questions: (1) Does the additional capital investment involved in adding solar cooling to a solar-heated house justify the additional savings achieved? As indicated, this question can be answered from Fig. 7. (2) Is combined solar cooling and heating more or less nearly economically feasible than solar house heating alone? Even if solar heating and cooling are economically infeasible when considered separately, is the combination any better?

If we compute $\left.\frac{\partial M}{\partial A}\right|_{\max}$ for each case, certain costs

for the equipment must be assumed. This can be avoided, however, by turning the problem around and calculating instead the maximum extra capital investment (that is, the cost of the solar cooling equipment minus the cost of installing equivalent conventional air conditioning) that the solar house owner can pay without increasing the collector cost per square foot. It can be shown from Equations [2] and [10] that $\partial M/\partial A$ remains unchanged if the extra capital investment required to add solar air conditioning to a solar-heated house equals five times (assuming 10-year amortization period) the annual savings accomplished by the solar air conditioning unit. For example, an annual electric bill saving of $50 justifies an extra expenditure up to $250; if the solar air conditioner can be made and installed for less than $250 extra, then combined solar heating and cooling is more nearly economically feasible than solar heating alone. Whether or not this figure is attainable at today's prices was not investigated.

ACKNOWLEDGEMENTS

I am indebted to Dr. Lloyd Shaffer for many stimulating discussions and suggestions; Miss Cathy May of the AMF Computer Group programmed the problem and ran the calculations. Most of all, I am indebted to Miss Mildred Loeffler for painstakingly carrying out most of the hand calculations, including those on which Figs. 3–6 are based.

REFERENCES

1. H. C. Hottel. "Residential uses of solar energy." *Proc. World Symposium on Applied Solar Energy, Phoenix, Arizona, November, 1955.* p. 103–112.
2. A. Whillier. Contribution to "Solar House Heating—a Panel Discussion." *Proc. World Symposium on Applied Solar Energy, Phoenix, Arizona, November, 1955.*
3. G. Löf. *Ibid.*
4. M. Telkes. *Ibid.*
5. R. W. Bliss. *Ibid.*
6. *Space Heating with Solar Energy: Proceedings of a Course-Symposium at M.I.T., August, 1950.* M.I.T., 1954.
7. A. Whillier. "Principles of solar house design." *Prog. Archit.* **36:** 122–126, (May 1955).
8. H. Tabor. *Bull. Res. Counc. Israel* 5A: 119–134, 1956. 5C: 5–27, 1955. **6C:** 155–176, 1958.
9. T. A. Unger "The preparation of a selectively black surface for use in the collection of solar energy." Ph. D. Thesis, M.I.T., 1958.
10. H. C. Hottel and B. B. Woertz. *Trans. ASME* **64:** 91–104, 1942.
11. J. Crank, *The mathematics of diffusion.* Oxford, 1956.Ch. 3.
12. S. S. Visher, "Relative heating requirements for American homes." *Sci. Monthly* Oct. **1945:** 313–316. "Relative cooling requirements for American homes." *Sci. Monthly* **1946:** 209–212.
13. J. L. Threlkeld and R. C. Jordan. *Heat. Pip. Air Cond.* **29:** 135–144, Dec., 1957.
14. C. F. Becker and J. S. Boyd. *J. Solar Energy* **1:** 13–21, Jan., 1957.
15. E. Speyer. American Machine & Foundry Co., Report CRL-T-20.
16. M. Telkes. *Heat. & Vent.* Apr., 1954.
17. S. F. Gilman, L. A. Hall, and E. P. Palmatier. *ASHVE Trans.* **60:** 525–42, 1954.
18. T. N. Willcox. "Annual utility cost operating residential cooling system" *Fuel Oil News* June, 1954.

TABLE XXVIII

$\sigma = 5.54$ L (per min)	V = 3000 gal K/d (Btu/ft²/hr/°F)	V = 6000 gal K/d	V = 10,000 gal K/d
1×10^{-6}	0.499×10^{-2}	0.628×10^{-2}	0.745×10^{-2}
2	0.997	1.257	1.490
3	1.496	1.885	2.235
4	1.995	2.513	2.980
5	2.493	3.142	3.725
6	2.992	3.770	4.470
7	3.491	4.398	5.215
8	3.989	5.026	5.960
9	4.488	5.655	6.704
10	4.987	6.283	7.449

TABLE XXIX—Auxiliary Heat Schedules

	B_1	B_2	B_3	B_4	B_5	B_6
October	—	—	.3H	—	—	—
November	—	—	.4H	.5W	W	.5W
December	W	—	.5H	W	W+ ·5H	W+ ·25H
January	W	—	.5H	W	W+ ·5H	W+ ·25H
February	.5W	—	.5H	W	W+ ·5H	W
March	—	—	.4H	.5W	.5W	.5W
April	—	—	.3H	—	—	—

May thru Sept.—None required

W = water heat; H = house heat.

APPENDIX A: THE M.I.T. SOLAR HOUSES

The standard house assumed in this report is similar to the solar houses built by Massachusetts Institute of Technology at or near Blue Hill, Massachusetts. This report is much indebted to the published reports[1, 2, 6] on these houses. However, several differences in point of view may be noted:

1. The M.I.T. houses are "tight," with air change in winter reduced to $\frac{1}{3}$ change per hour, as compared with $1\frac{1}{2}$ or 2 changes per hour in a normal house. The extra construction cost involved in sealing all air leaks should be added to the solar house heating costs. Not knowing what this extra cost is, I have not made the calculation, but the B_3 schedule in Table XXIX and Fig. 9 is calculated for a house whose solar heat requirements are proportional to those of an M.I.T. house. The B_3 schedule amounts to 34 per cent of the annual heating load (house heat plus hot water) being supplied by an auxiliary heating unit.

2. The M.I.T. houses are small, about 1,200 sq. ft. in floor area. This is understandable in an expensive experiment. I have assumed for calculation, however, that since solar heating requires a substantial capital investment, a house for an above-average income level is indicated.

3. Heat storage is not considered in the M.I.T. studies as a means of reducing the necessary collector area because only overnight storage (or storage for two or three days) is contemplated. The M.I.T. reports

VOL. 3 1959

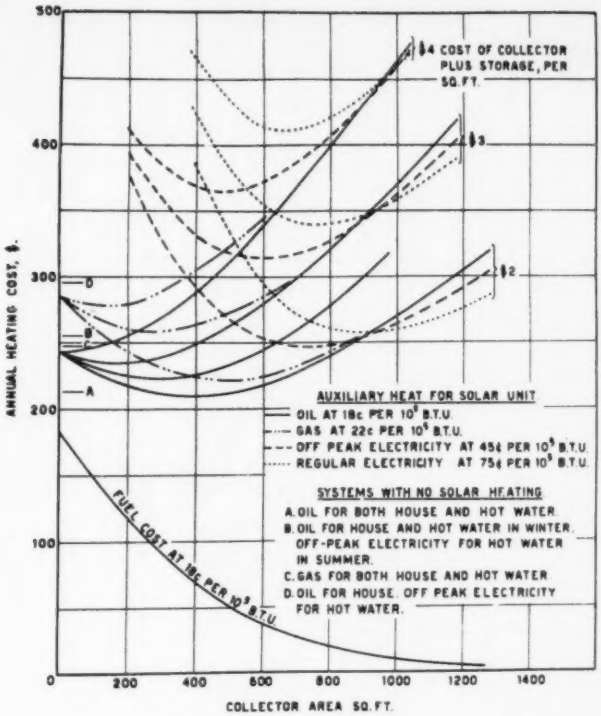

FIG. 14—M.I.T. Solar House cost analysis (from Whillier).

refer to storage capacity as proportional, rather than in inverse proportion, to collector area. The houses reported on at Phoenix[1, 2] had storage tank capacities of 1,200 and 1,500 gal.

4. In the M.I.T. calculations the parameters are optimized by calculating the effect of different percentages of auxiliary heat on the dollar value of the annual heat collected per square foot of collector. The value declines monotonically, (starting with a maximum, for collector areas of less than 200 sq ft, of about 33 cents per sq ft.) Since solar house heating is not economically competitive at an assumed fuel saving of 18 cents per therm, they could not take for their criterion of optimization the maximum dollar value earned figured on the *total* collector area. They used, instead, maximum dollar value earned figured on the *incremental* area; that is, a *relative* law of diminishing returns. They found then that between 25 per cent and 50 per cent of the heat load should be auxiliary (non-solar) heat. This, combined with the smaller house considered, explains the fact that the optimum collector areas indicated in Fig. 14, taken from Whillier's paper[2] are only about half that indicated for B_3 in Fig. 9 (about 850 sq ft). In other words, the M.I.T. houses, *considered in the terms of this paper*, have auxiliary heating of about 65 per cent, 34 per cent being "built in" by the tight sealing of the house.

5. The auxiliary heat is furnished by a conventional furnace. In the house described above, the furnace is eliminated and the auxiliary heat furnished by a hot water heater. This changes the economic calculation somewhat, since the elimination of the furnace is figured, in New England, as a saving of $800 in favor of solar heating.

6. Long-term storage is rejected flatly. Hottel[1] states that it "is undesirable, because of the very poor load factor on it." Whillier[7] states: "The load factor on that part of the storage system which exceeds 1, 2 or, 3 days' capacity is too low." This judgment does not take account of the fact that good insulation makes the system more efficient all through the year by reducing *daily* heat leakage, not just during exceptionally long periods of cold, cloudy weather. However, as the calculations show, the collector area reduction achieved by efficient storage is quite modest. This is especially true in Blue Hill, Massachusetts. (See Fig. 9.)

A direct comparison between the M.I.T. results and those presented in this paper cannot be fairly made because of the above-mentioned differences. In addition, there are slight differences in the calculated solar energy collected per square foot in each month. However, Fig. 14, reproduced from Whillier's paper,[2] shows satisfactory agreement. The annual fuel oil bill, when there is no solar heating (collector area zero) is seen to be about $180; at $2 per sq ft, solar heating never reduces the annual heating bill below about $210.

The break-even point would seem from Fig. 14 to be about $1.50 per sq ft, as compared with $1.86 which was calculated for B_3 by the optimizing method explained above.

APPENDIX B: STORAGE TANKS

We define a dimensionless shape factor, σ as the ratio of the surface area of the tank to the $\frac{2}{3}$ power of the volume. (See Equation [6].) A spherical tank, which has, of course, the lowest value of σ (4.836) costs ap-

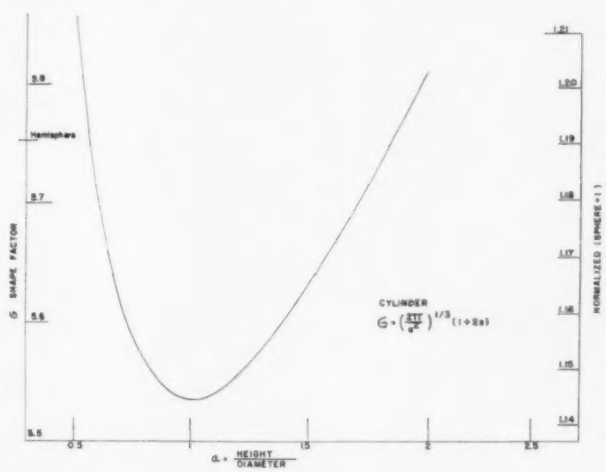

FIG. 15—Shape factor vs. ratio of height to diameter of right circular cylinder.

proximately twice as much as a cylindrical tank. A "square" cylinder, i.e., one whose diameter equals its height, has a σ value of 5.536; thus for the same storage efficiency a cylindrical tank requires about 15 per cent greater thickness of insulation than a sphere.

To avoid the expense of on-site assembly of the tank, the diameter must be kept below the maximum which can conveniently be shipped, i.e., about 11 ft. Thus, tanks larger than 10,000 gal are usually made longer than they are wide. Fig. 15 shows the effect of the shape factor of varying the proportions of the cylinder; the abscissa is the ratio of height to diameter. On the right hand margin the shape factor has been normalized, with the sphere taken as unity, so that one can read directly the percentage penalty for cylinders of different proportions. The sphere falls too far below the curve to appear, but the hemisphere is indicated.

The larger the capacity of the tank, the larger the surface area, and hence the greater the heat leakage per day for the same thickness of insulation. The question arises whether storage efficiency increases or decreases with tank capacity. Storage efficiency *increases* with tank capacity, the period of useful storage being longer for a 10,000-gal tank than for a 3,000-gal tank. Fig. 8 shows that storage efficiency, i.e., percentage energy available along any constant time line, increases monotonically as L decreases. As can be seen in Equation [8], the L factor varies inversely as the one-third power of the volume. The same conclusion can be drawn from Table XXVIII where the same insulation factor, say 3×10^{-2}, corresponds to lower L values as one moves across the table from left to right.

Steel tanks, lap-welded and painted with a rust-inhibitor-like calcium plumbate, are preferable to wooden tanks. Tidewater red cypress is the best wood for water tanks; prices are not quite competitive with steel tanks. If one insulates the outside of a wooden tank so that it cannot "breathe," the life of the tank is seriously shortened. Moreover, with wooden tanks there is a need—from time to time—to tighten the hoops which hold it together in order to prevent water leakage.

VOL.
3
1959

Design of a Sea Thermal Energy Power Plant

By Asa E. Snyder

USI Clearing Division of U. S. Industries, Inc.

A unique 8000-kw gross power and sea water conversion plant is described which uses the temperature difference of the ocean to produce usable energy and fresh water. This plant has been designed by the research and development department, Clearing Division of U.S. Industries, Inc., for installation along coastlines in a semi-tropical area. Estimated cost for the sea thermal energy plant is 2.5 to 3 million dollars, including building and erection costs. This is equal to $310 to $375 per kw, amounts which are competitive with fossil-fuel burning plants in remote areas.

INTRODUCTION

The thermal energy of the sea is actually latent solar energy which has been stored within the large bodies of water upon the earth's surface. Almost 35,000 times the existing annual energy consumption of the world is delivered annually to the earth in the form of solar radiation. Over seventy per cent of the earth's surface is covered by the oceans; thus, a major percentage of the world's supply of solar energy is deposited in the seas.

Actually, however, only the surface water or top layers of the ocean are warmed. At relatively shallow depths in the ocean, no more than 1200 ft, the sunlight does not penetrate, and the ocean water temperature is 40°F or less, but surface water temperatures of 80° to 90°F are quite common in the tropic regions.

Based upon our existing knowledge of thermal power cycles, we know that any such system requires:

(1) a source of heat, or a hot body,

(2) a receiver of heat, or a cold body,

(3) a working medium,

(4) a means of abstracting or adding heat and a method of producing work.

The temperature difference between the surface and the depths can be utilized as the source and receiver respectively and is therefore a potential means of obtaining almost unlimited amounts of energy. The water itself can be utilized as a working medium, and only an economical and practical means for extracting work is required. The objective of this paper is to describe the fundamentals of a plant designed by the Research and Development Department of Clearing Division of U.S. Industries, Inc., that will utilize the temperature difference of the oceans to produce useable energy and fresh water.

Brief Background of S.T.E.

The initial impetus to the study of sea thermal energy was given by Monsieur Georges Claude between 1925 and 1935 when he carried out tests on the installation of a submarine cold water pipe from a coastal power station in Cuba, and of a vertical submarine cold water pipe beneath the floating "Tunisia" power station. The accomplishments of his experiments were:

(1) The successful operation of a steam turbine with a difference of 27°F.

(2) The design of an efficient air extractor.

(3) The demonstration of the problems in protection from wave action and laying the cold water inlet pipe in the open ocean.

In 1941 the French Government created an interministerial organization to continue the research of Claude. In 1948 the semi-official company "Energie des Mers" was formed by the French Government to continue research and study in this field.

In the United States, the Office of Saline Water, U.S. Department of Interior, has sponsored design studies of flash-type evaporators which might utilize energy in bodies of water. The basic studies for work of this nature were conducted under the Sea Water Conversion Program at the University of California.

The Research and Development Department, Clearing Division of U.S. Industries, Inc., has actively entered into a program of design research and study in the field of sea thermal energy and desires to stimulate interest in this form of energy conversion for use in the semitropical coastal areas of the world.

Distribution of Temperature and Suitable Areas for Installation of S.T.E.

The general distribution of surface temperatures of the oceans is given in Table I.

Analysis of the data given in Table I shows that the 25°C (77°F) clime falls within the belt of 20° North and South latitudes. As stated earlier, at depths of 1200 ft or more the temperature is sufficiently low,

TABLE I—Surface Temperature of the Ocean[1]

Latitude	Atlantic (°C)	Pacific (°C)	Indian (°C)
70°–60° N	5.60		
60°–50° N	8.66	5.74	
50°–40° N	13.16	9.99	
40°–30° N	20.40	18.62	
30°–20° N	24.16	23.38	26.14
20°–10° N	25.81	26.42	27.23
10°–0° N	26.66	27.20	27.88
10°–0° S	25.18	26.01	27.41
20°–10° S	23.16	25.11	25.85
30°–20° S	21.20	21.53	22.53
40°–30° S	16.90	16.98	17.00
50°–40° S	8.68	11.16	8.67
60°–50° S	1.76	5.00	1.63
70°–60° S	1.30	1.30	1.50

with minimal variations, in all oceans. Therefore, the appropriate areas for consideration of the feasibility of installation of S.T.E. Plants is established by the world's water temperature distribution.

Countries or areas which can reasonably expect to utilize this type of power plant can be listed as follows:

(1) Central America and the Caribbean Islands

(2) Northern Coast of East and West South America

(3) West Coast of Africa—from Mauritania South to the Congo

(4) East Coast of Africa—from Somaliland South to Madagascar

(5) South Coast of Arabia

(6) Ceylon

(7) Indonesia, New Guinea, and Borneo

(8) Phillipine Islands

(9) Taiwan

(10) Australia

More detailed studies of suitable locations have been made and are contemplated by Clearing R&D, and are available for discussion with interested parties.

Geological Considerations in Plant Location

The power plant must be close to deep water which has unrestricted communication with the oceans. A steep shore, such as that usually found along a volcanic or coral island, spits of land, natural peninsulas, or bars of river-borne silt are desirable. If at all possible, a

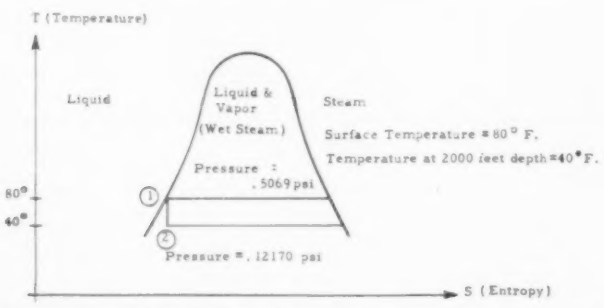

FIG. 1—Available energy of sea thermal energy (S. T. E.) plant.

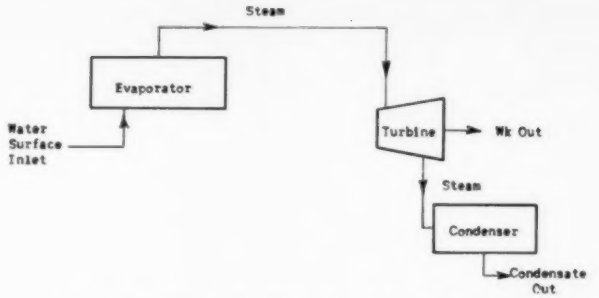

FIG. 2—Simplified schematic of S. T. E. plant.

near-by submarine canyon which is approximately at right angles to the shore line is desirable. Excessively rugged or rocky profiles along the bottom are to be avoided, but are not limiting. Fig. 4 illustrates a plan for a typical plant.

Principle of Sea Thermal Energy

Fig. 1 illustrates a simple temperature entropy diagram for water. Observe that cooling the temperature of water vapor already heated to 80°F (Point 1) to 40°F (Point 2) lowers the vapor pressure to that obtainable at 40°F. The vapor pressure at 80°F is 0.5069 psi, whereas the vapor pressure at 40°F is 0.1217 psi. We thus have a small but decided pressure drop, which can be used to extract power from the seas.

Fig. 2 schematically illustrates a simplified basic system for extracting sea thermal energy in the form of useful mechanical work. Referring to that figure the process is described as follows:

(1) Heated surface water is lead into a chamber where the water is evaporated at the higher temperature.

(2) This chamber is connected to a turbine, which extracts mechanical work as the pressure drops through the turbine.

(3) The exhaust from the turbine then enters a condenser where the vapor is condensed into liquid.

THE CLEARING SEA THERMAL ENERGY POWER AND SALT WATER CONVERSION PLANT DESIGN

As part of a long-range program, the Research and Development Department, Clearing Division of U.S. Industries, Inc., has investigated and designed an 8000-kw gross power and sea water conversion plant suitable for location along a coast line in a semitropical area of the world.

The sea thermal energy power and sea water conversion plant described in this paper is a unique type of plant; no installation exactly similar to the proposed system exists in the world today. The development of this type of power plant has awaited the advent of industrialization of those tropical land areas where

VOL. 3 1959

favorable thermal differentials exist in the nearby oceans. As mentioned earlier, a sizable backlog of academic and industrial programs on components for the sea thermal energy (S.T.E.) plant does exist today; and one similar installation located on the African Ivory Coast was actually carried into a construction phase before being discontinued by the French Government because of the close proximity of low-cost hydroelectric power. No extensive development of component hardware is required today to put a sea thermal energy design into practice.

Purpose and Scope of Described Design

A set of hypothetical requirements is assumed for this paper. The installation is assumed to be part of a process-type facility situated in a desirable location (close to deep water) along a shore line on open ocean. This installation will be required to produce large quantities of power, fresh water, and brine; a 5000-kw net output is required as part or all of the output of the facility.

Other sizes of power plants could be studied, producing any preselected combination of power, fresh water and brine, depending upon the requirements of the specific installation.

Design Objectives

The plant is designed for a constant net output of 5000-kw, and the potable water and brine production rate is to be established by this. Design emphasis for the entire installation is placed upon high rates of availability and reliability. Maintenance costs are to be minimal with major overhaul periods of two years. Initial cost of the power plant, including all structures, power generation, piping, and storage facilities will not exceed $375 per kw based on the gross kw output. In order to accomplish this, efficiency is to be sacrificed in favor of design simplicity and low initial cost. Whenever possible in the basic design, consideration is to be given to manufacture or subassembly of components at erection site to reduce freight differentials and to utilize effectively local labor rates in remote areas.

General Description of System

A simple schematic of the proposed system is illustrated in Fig. 3. The water is initially gravity fed through an inlet open to the ocean, which is essentially a ditch cut by bulldozer leading into a solar heating flat. The solar heating flat is a scientifically designed "black body" heat collector, where the inlet water is heated by solar radiation to a maximum temperature. The basic design of the system is such, however, that under adverse atmospheric conditions it will continue to work at reduced efficiencies, i.e., night or cloudy days.

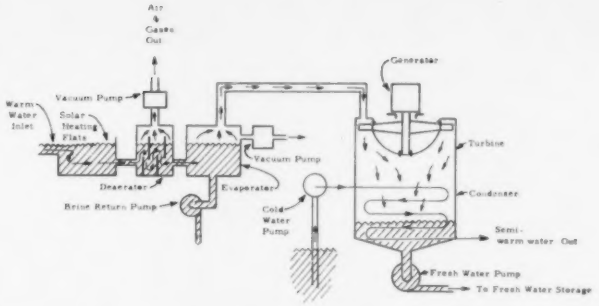

FIG. 3—Schematic of S. T. E. installation.

The water then flows to the deaerator which extracts air and other dissolved gases, which would decrease the efficiency of the plant, from the sea water. The deaerated sea water passes into the evaporator and is partly flashed into steam because of a high evaporator vacuum. A brine-return pump holds the salinity in the evaporator to a level that prevents salt precipitation.

The vapor then flows through a reaction turbine, which drives a generator, and then passes to the lower pressure zone in the condenser, where cold sea water circulating through the condenser tubes cools and condenses the steam to potable water. The condensate pump distributes the fresh water to suitable storage basins.

The cold sea water is pumped from an approximate depth of 2000 ft. A specially designed intake pump is

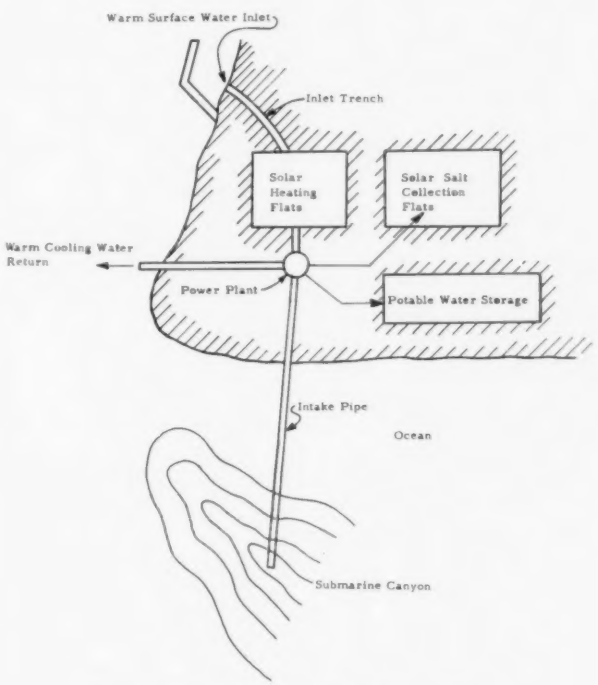

FIG. 4—Plan view of S. T. E. installation.

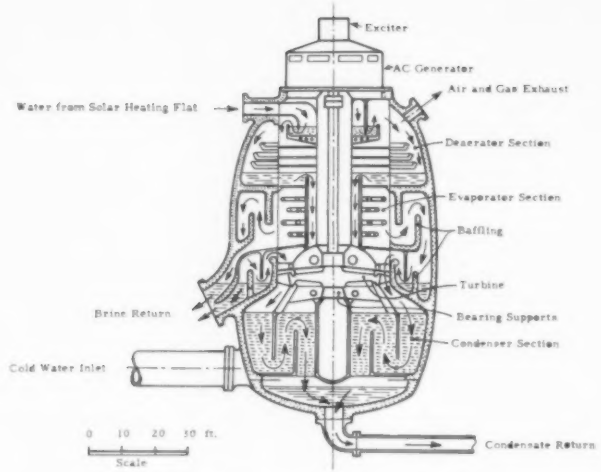

FIG. 5—Cross-section of S. T. E. installation.

installed from the bay to the inlet depth. The pipe is designed in sections and is manufactured from several different materials. The sections passing through the surf are corrosion-proof steel welded pipe, encased in concrete protective jackets, and buried under a surf-breaking rock fill. The next sections of the pipe are constructed from fiberglass and epoxy resins with intermittent flexible rubber bellows sections. The inlet to the pipe consists of a special water-ballasted tank-like device with foul-proof inlet screening.

Description of the Plant

A cross-section view of the proposed power plant is shown in Fig. 5. Fig. 4 is a plan view of the total installation. Table II lists the assumptions used in making the calculations, and Table III shows the calculated results.

The solar heating flats are large black-topped recessions where water is heated by solar radiation under

TABLE II—Assumptions for Technical Calculations of S.T.E. Power Plant

(1) Net power	5000 kw
(2) Inlet sea water temperature	80°F.
(3) Solar heating flat outlet temperature	90°F.
(4) Evaporator steam temperature	84°F.
(5) Cooling water inlet temperature	40°F.
(6) Condensate temperature	50°F.
(7) Density of fresh water @ 50°F	62.4 lb/cu.ft.
(8) Density of sea water @ 40°F	64.0 lb/cu.ft.
(9) Specific heat of water	1.0 B/lb.°F.
(10) Deaerator steam loss	1% of Gross Steam Flow
(11) Intake pipe (total length)	4000 ft.
(inlet depth)	2000 ft.
(12) Assumed component efficiencies	
AC generator efficiency	95%
Turbine mechanical efficiency	90%
Turbine stage efficiency	85%
Coolant pump efficiency	90%
Condensate pump efficiency	80%
Brine return pump efficiency	90%

TABLE III—Specifications for 5000-kw Net S. T. E. Power Plant

Fluid qualities	
Inlet flow to evaporator	192,000 gpm
Brine return	190,900 gpm
Vapor loss in deaerator	11 gpm
Potable water flow	1,123 gpm
Cooling water flow	140,600 gpm
Pumping and auxilary power requirements	
Cooling water pump	1,660 kw
Condensate pump	22 kw
Brine return pump	1,300 kw
Vacuum pump	18 kw
Total	3,000 kw
Gross kw output	8,000 kw
Electric generator	
Speed	450 rpm
Voltage	4160
Type	3 Phase—60 cycles
Steam flow	
Enthalpy drop (Ideal)	66.0 Btu/lb
Enthalpy drop (Actual)	51.2 Btu/lb
Net flow	156 lb/sec (9357 lb/min)
Condenser	
Heat extracted	9.63×10^6 Btu/min
Log mean temperature difference	4.97°F
Friction head loss	56.1 ft
Area	188,000 sq ft
Tubing size	3″ OD x 049 Gage
Tubing total length	239,000 ft
Tubing spacing	5″ centers stag.
Condenser Dimensions	
Inner diameter	10 ft
Outer diameter	50 ft
Height	19 ft
Condenser weight with baffling	192 tons
Turbine	
Speed	450 rpm
Hub diameter	30.8 ft
Tip diameter	33 ft
Mean diameter	31.9 ft
Bucket height	1.08 ft
Maximum tip velocity	776 fps
Inlet Pipe	
Inside diameter	6.30 ft
Total length	4000 ft
Inlet depth	2000 ft
Solar Heating Flat	
Total area	Approximately 9 million sq ft (3000 ft x 3000 ft)

favorable conditions. At night the water is received at ocean surface temperatures, and the entire plant operates at reduced outputs.

As may be seen from Fig. 5, the heated water from the solar flats enters the deaerator chamber through a simple vacuum seal, after which it is cascaded over a series of vertically spaced, perforated circular trays. The water is broken into fine droplets in passing through the perforations, which assures complete deaeration because of the large wetted area exposed. The pressure in the chamber is maintained by a vacuum pump at a value somewhat above the steam vapor pressure to minimize the steam loss. This is estimated to be 1 per cent of the net steam flow.

The deaerated water next flows into the evaporator, where it partially flashes into steam due to the lower

VOL. 3 1959

pressure in the evaporator. Mechanical baffling separates the vapor from the liquid and assures that only dry steam reaches the turbine. The unflashed liquid is returned to the solar flats for reheating by the brine return pump, which, of course, works against an atmospheric head.

After expansion in the turbine, which may be constructed of lightweight metal or inexpensive plastic materials because of the low temperatures, the steam passes into an annular condenser consisting of tubes arranged normal to the steam flow and baffled to force the steam to take repetitive passes through the tubes. The annular condenser represents the most economical construction for the large heat-transfer value required.

The condensate is collected in the bottom of the condenser and removed by the condensate pump, which also works against an atmospheric head.

In the event that potable water is not desired, a mixing type of condenser can be incorporated in the design instead of the surface condenser at some saving in initial cost.

The turbine is vertically mounted, supported within simple water-lubricated bearings. The bearing housing supports are rigidly mounted to the main shell. The turbine shaft connects to the generator, which is independently mounted and isolated on the top of the shell and connected to the turbine by means of a flexible coupling. A rotary vacuum seal maintains the vacuum within the shell.

Design of Intake Piping

The inlet piping system is illustrated in Fig. 6. The first section of the pipe, extending from the shore to a depth of 50 ft, is constructed of corrosion-resistant welded steel pipe encased in a protective concrete jacket. This pipe is laid in an excavated trench and then covered with stone fill as a surf breaker. The next section of the pipe is a flexible pipe designed to follow the ocean floor to a depth of 2000 ft.

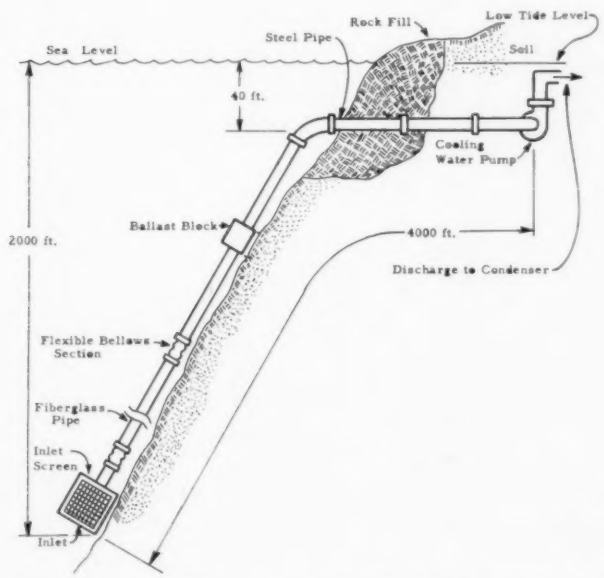

FIG. 6—Inlet piping system of S. T. E. installation.

The cooling water inlet pump is a Kaplan-type pump designed to handle 140,600 gpm. In order to operate efficiently this pump must have a positive head and is therefore located below the low-tide mark.

The second section is composed of alternate sections of flanged fiberglass pipe and steel and rubber bellows. The fiberglass sections are anchored to the floor by means of cast concrete ballast blocks, except for the initial sections which consist of controlled buoyancy steel tanks. The inlet consists of a specially designed controlled buoyancy steel tank, containing nonfouling screens with self-cleaning features.

At the time of final construction, the entire assembly is floated into position using the buoyant tanks and special rafts. The first section is connected to the second section or deep part of the piping by skin divers using scuba gear, and the assembly is sunk and lowered into position. Cables from the raft convoy permit a gradual positioning of the final assembly into place.

Design for Prevention of Marine Fouling

The growth of marine microörganisms, both plant and animal, could be a continual source of trouble unless special precautions are taken by the designer to prevent this from occurring. Very little is actually known about the degree of fouling to be expected in deep water inlets. We propose that antifouling measures based upon existing power plant practices be incorporated in the design. Two basic control measures will be incorporated:

(1) use of velocity to control growth,

(2) control by chlorination.

Actual results of operating steam power plants indicate these provisions will offer adequate control at a minimum of cost.

Starting and Control of the Plant

If the proposed plant is to be used as a part of a power installation, i.e., an additional steam or diesel generation installation is available, then the generator of the S.T.E. power plant may be converted to a motor, and at the same time additional power may be supplied to the auxiliaries in order to start the plant. After the plant becomes self-supporting, the outside power supply is cut off, and the plant continues operating.

Should the S.T.E. plant be the sole power source, then a small standby auxiliary plant, either diesel or steam, will be required to start and activate the system

and also to act as an emergency energy source during maintenance intervals.

The S.T.E. power plant, once started, can operate at constant maximum output during daylight hours and at reduced outputs during evenings, rainfall, or other adverse solar conditions. If the power requirements fluctuate and the S.T.E. is the sole power source at the mill, a special governor will be built into the turbine to hold speed constant over a varying load. Essentially, therefore, the addition of control features is dependent upon the over-all requirements of the installation.

ECONOMICS OF SEA THERMAL ENERGY POWER AND SEA WATER CONVERSION

The size of equipment required for a power plant of the type described in this paper is relatively large, but the low temperatures of the cycle permit the use of very low-cost materials The initial capital investment of a S.T.E. power plant will not exceed that of an equivalent fossil fuel-burning thermal power plant, and the operating and maintenance costs of a sea thermal energy installation will be minimal.

In addition to producing electrical power, the S.T.E. power plant produces two by-products which make the investment additionally attractive. As shown in Table III, the potable water by-product will approximate 1,123 gpm for an 8000-kw gross installation. Furthermore, the installation will produce salts at various production rates depending upon the size of available evaporating flats. The true value of the potable water and salts must be considered in establishing the actual operating expense of the plant.

The estimated cost for the 8000 gross kw Clearing S.T.E. installation is 2.5 to 3.0 million dollars, including building and erection costs. On a dollar per installed kilowatt basis this amounts to $310 to $375 per kw, which is competitive with installation costs of a comparable fossil fuel-burning thermal power plant installed in a remote area.[4,5]

The Clearing S.T.E. 8000-kw power and salt water conversion plant produces 1.62×10^6 gal of fresh water per day. In order to compare the basic cost of the S.T.E. plant with a more conventional water conversion plant, a simple present-worth engineering economy study has been made comparing the S.T.E. plant with a multistage flash plant heated by steam.

For the Clearing S.T.E. plant installed at a site in an underdeveloped area for a 20-year life:

First cost (estimated)	$2,480,000
P.W. of annual disbursements based on 40,000 per year at 4% (40,000 × 13,590)	543,000
P.W. of all disbursements for 20 years	$3,023,000

However, the Clearing S.T.E. plant also produces 5000-kw of power, which can be sold. Then:

P.W. of all receipts for electrical sales based on $.05 per kw hour at 4% ($2,190,000 × 13,590)	$29,800,000

The present worth of net receipts is therefore $29,800,000 minus $3,023,000, or $26,777,000.

Referring to Reference 2, the first cost of a multistage flash steam heated plant for 1.0×10^6 gpd is $1,534,900 with disbursements of $1015 per day. For a basis of comparison (1.62×10^6 gpd plant of the same design), the cost and disbursements are assumed to be increased by 25 per cent; thus, the first cost is $1,920,000, and the disbursements are $1270 per day.

Then on a present worth basis:

First cost	$1,920,000
P.W. of annual disbursements at 4% ($261,000 × 13.59)	3,540,000
P.W. of all disbursements for 20 years	$5,460,000

There is therefore a large advantage for the S.T.E. installation of ($26,777,000 plus $5,460,000) $32,237,000 over the more conventional type of distillation process. Such economic advantages cannot easily be ignored.

REFERENCES

1. H. U. Sverdup; M. W. Johnson; R. H. Fleming. *The Oceans, Their Physics Chemistry, and General Biology.* 1st ed. New Jersey, Prentice-Hall, 1942.
2. F. A. Lobel. "The future in sea water conversion." *Plant & Power Services Engr.* June **1959:** 18–20, 50.
3. J. H. Keenan; F. G. Keyes. *Thermodynamic properties of steam.* 1st ed. New York, Wiley, 1936.
4. "Energy in Latin America". United Nations, Department of Economic and Social Affairs, E/CN. 12/384/Rev. 1, Nov. 1957.
5. *Electric Power Bulletin for Asia* ST/ECAFE/SER.L/2, 1956. Commission for Asia and the Far East.

VOL. 3 1959

The Derivations of Several "Plate-Efficiency Factors" Useful in the Design of Flat-Plate Solar Heat Collectors*

By Raymond W. Bliss, Jr.

Solar Energy Laboratory, Institute of Atmospheric Physics, University of Arizona, Tucson

All variables influencing the efficiency of a flat-plate solar heat collector as a heat exchanger can be combined into a single "efficiency factor." These efficiency factors are more or less design constants of the particular collector design, and are only slightly influenced by operating conditions. Consequently they are extremely convenient for use in accurate design and performance calculations. The full mathematical derivations are presented for several of these efficiency factors for various types of collectors, together with graphical data and examples of their use.

PRINCIPAL SYMBOLS USED

A ..... Intensity of atmospheric radiation upon a horizontal surface, Btu/sq ft-hr
A_f ..... Fin cross-section, sq ft
C ..... Specific heat of circulating fluid, Btu/pound-°F
d (d_0) .. External (internal) tube diameter, ft
F ..... Fin efficiency factor, dimensionless
F' ..... Collector plate efficiency factor, dimensionless
F_R ..... Collector plate efficiency factor, dimesionless
G ..... Flow rate of circulating fluid, pounds/hr-sq ft of collector
h_a ..... Convection coefficient, collector plate-to-air, Btu/sq ft-hr-°F
h_c ..... Convection coefficient, tube-to-circulating fluid. Btu/sq ft-hr-°F
h_r ..... Simplified radiation coefficient, Btu/sq-ft-hr-°F
I_n ..... Intensity of direct beam sunshine upon a surface normal to the rays, Btu/sq ft-hr
k ..... Thermal conductivity, Btu/ft-hr-F°
L ..... Fin length, ft
M ..... Fin thickness, ft
Q ..... Heat transfer rate, Btu/hr
q ..... Heat transfer rate per sq ft of collector surface, Btu/sq ft-hr
q_A ... total sunshine absorption rate
q_d ... incident diffuse sunshine upon collector
q_i ... incident total sunshine upon collector
q_L ... total loss rate of collector
q_u ... average useful heat collection rate
$q_{u\text{-}o}$ .. useful heat collection rate at entering section of collector
$q_{u\text{-}x}$ .. useful heat collection rate at point x
R ..... Net radiation from a surface to the sky, the surface being an exposed thermally black horizontal plane at air temperature, Btu/sq ft-hr
$t(T)$ .... Temperature, °F (Rankine)
t_a T_a .. air temperature
t_c ..... plate temperature below bond between plate and tube
t_p T_p .. plate temperature
t_t ..... tube temperature
t_w ..... fluid temperature at a given point
$t_{w\text{-}o}$ .... temperature of fluid entering collector
U_b ..... Over-all heat transfer coefficient for loss through bottom of collector, Btu/sq ft-hr-°F
U_c ..... Over-all heat transfer coefficient for heat transfer through bond between plate and tube, Btu/hr-sq ft of bond-°F
U_L ..... Over-all loss rate coefficient for collector, Btu/sq ft-hr-°F
w ..... Tube spacing, ft
α ..... Average absorptivity of surface for total solar radiation incident upon a surface, dimensionless
ϵ ..... Average emissivity or absorptivity of surface for long-wave radiation, dimensionless
θ ..... Altitude of sun relative to collector plane, degrees
σ ..... Stefan-Boltzmann constant, Btu/sq ft-hr-R^4

INTRODUCTION

In problems involving the design or testing of flat-plate solar heat collectors it is very worthwhile to calculate the ratio between the actual useful heat collection rate of a given design and the useful heat collection rate which would have been attained had the entire collector surface been at the temperature of the circulating fluid. There are two useful forms of this "plate-efficiency factor":

$$F' \equiv \frac{\text{actual useful heat collection rate}}{\text{useful heat collection rate attainable with entire collector surface at average fluid temperature}}$$

$$F_R \equiv \frac{\text{actual useful heat collection rate}}{\text{useful heat collection rate attainable with entire collector surface at temperature of fluid entering collector}}$$

* This paper was supported in part by a grant from the National Science Foundation (NSF-G6293).

These factors F' and F_R are particularly useful because, for many types of solar heat collectors, they are essentially design constants determined by the construction details of the collector, and do *not* depend greatly upon such operating conditions as temperature, sunshine intensity, or wind velocity. Efficiency factors of this sort were first used in problems of solar heat collector design by Hottel and Woertz,[1] later by Whillier,[2] and by Hottel and Whillier.[3] The use of such factors tremendously reduces the empiricism associated with the design of solar heat collectors.

For many types of flat-plate collectors, and in particular for water-heating collectors formed of tubes bonded to a metal sheet, the efficiency factors for a given design can be quickly calculated to a high degree of accuracy. Nevertheless, and despite their obvious advantages in collector design, these factors are not utilized as much as they should be.

These notes present a full derivation of several of these "plate-efficiency factors," with the thought that such a full presentation will be helpful in furthering the understanding and use of these basic concepts and heat-transfer equations. Our end results will be found to be in agreement with those which have been stated by Hottel and Whillier.[3] In general we should note that the calculation methods used by the Solar Energy Laboratory in attacking problems of collector design are closely similar and strongly indebted to those of the Massachusetts Institute of Technology group. The chief difference between our "collector equations" and theirs is that we make a small but (we think) worthwhile improvement in allowing for the effects of atmospheric radiation.

These notes are divided into four main sections:

(1) Basic concepts in equation form.

(2) The temperature distribution and over-all heat transfer efficiency of a uniform rectangular fin.

(3) Collection efficiency factors for collectors having uniform flow beneath a flat plate.

(4) Collection efficiency factors for collectors having uniform flow in tubes bonded to a flat plate.

BASIC CONCEPTS IN EQUATION FORM

The fundamental steady-state equation of any solar heat collector amounts to the simple statement that the rate of useful heat collection is equal to the rate at which sunshine is being absorbed less the total loss rate:

$$q_u = q_A - q_L \qquad [1]$$

A good place to start in analyzing the performance of a solar heat collector is to consider the heat transfer from the upper surface of an exposed horizontal plate which is imagined to be held at constant temperature. We can, if we like, look upon this problem as that of setting up the performance equations for a hypothetical collector having the following characteristics:

(a) The collector plate is horizontal, exposed, and at constant temperature over its entire surface.

(b) There are no thermal gradients between collector plate and circulating fluid.

(c) The bottom of the collector is perfectly insulated.

We then set up the performance equations for this idealized collector, assuming various hypothetical cases of increasing complexity.

Case I: Plate Surface Thermally Black, Plate Temperature Equal to Air Temperature

(a) Operating at night:

$$q_u = -q_L \qquad [2]$$

$$q_L = \sigma T_a^4 - A = R \qquad [3]$$

Note:

$$R \equiv \sigma T_a^4 - A \qquad [4]$$

(b) Operating during the day:

$$q_u = q_A - R \qquad [5]$$

$$q_A = q_i \qquad [6]$$

$$q_i = q_d + I_n \sin\theta \qquad [7]$$

Case II: Real Plate Surface, Plate Temperature Equal to Air Temperature

A real plate surface will have average solar absorptivity coefficients and average emissivity and absorptivity coefficients in the long-wave region (2 to 50 mμ), all of which must be reckoned with. We assume that long-wave emissivity and absorptivity can be considered equal. The resulting equations:

(a) Operating at night:

$$q_u = -\epsilon R \qquad [8]$$

(b) Operating during the day:

$$q_u = \alpha q_i - \epsilon R \qquad [9]$$

Case III. Real Plate Surface, Plate Temperature Differs from Air Temperature

Here we must reckon both with absorptivity-emissivity effects and with convective heat transfer to the surrounding air.

(a) Operating at night:

$$q_u = -\epsilon R - (\epsilon h_r + h_a)(t_p - t_a) \qquad [10]$$

(b) Operating during the day:

$$q_u = \alpha q_i - \epsilon R - (\epsilon h_r + h_a)(t_p - t_a) \qquad [11]$$

In Equations [10] and [11] above, the long-wave radiation loss rate from the plate is seen to be split into two components, a procedure which is convenient

VOL. 3 1959

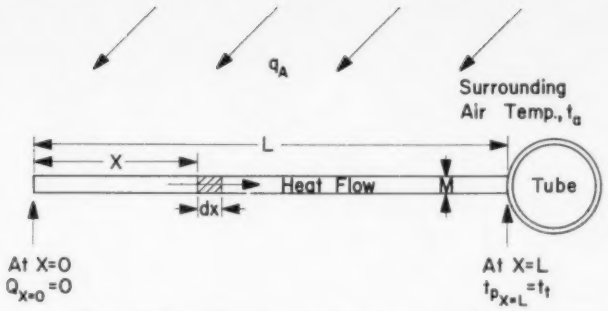

FIG. 1—Heat flow in a uniform rectangular fin.

in later calculations. The equations do yield the correct long-wave radiation loss, which is:

$$q_{L\text{-radiation}} = \epsilon(\sigma T_p^{\,4} - A) = \epsilon(\sigma T_p^{\,4} - \sigma T_a^{\,4} + R) \quad [12a]$$

$$= \epsilon h_r(t_p - t_a) + \epsilon R \quad [12b]$$

We find that the "simplified radiation coefficient" h_r is very convenient for use in calculations. A plot of this coefficient is given in Fig. 4.

THE TEMPERATURE DISTRIBUTION AND OVER-ALL HEAT TRANSFER EFFICIENCY OF A UNIFORM RECTANGULAR FIN

This problem occurs repeatedly in the design of solar heat collectors, as well as in the design of many other types of heat exchangers. The properties of fins are discussed in most of the standard heat transfer texts, but, for reasons of brevity, the pertinent equations are seldom derived in full. Herewith, in "collector nomenclature," a full derivation of the case of a rectangular fin of constant cross-section, with end effects ignored.

Consider a fin of length L as shown in Fig. 1. Sunshine is being absorbed along the entire fin at rate q_A Btu per sq ft-hr. Heat is flowing through the fin as shown, and at the base of the fin the temperature is held constant at t_t. Surrounding temperature is t_a, and the over-all loss rate coefficient is U_L. Assume that the width of the fin (i.e., in the direction perpendicular to the figure) is Δy. Assume also that all heat flow within the fin is essentially parallel to the x-axis.

The cross-section of the fin through which heat is flowing is:

$$A_f = M\Delta y \quad [13]$$

At a point x, the rate of useful heat collection in Btu per sq ft-hr is:

$$q_{u-x} = q_A - \epsilon R - U_L(t_p - t_a) \quad [14]$$

The heat flow through the fin in Btu per hr is:

$$Q = -kA_f\frac{dt_p}{dx} = -kM\Delta y\frac{dt_p}{dx} \quad [15]$$

The heat gain, in Btu per hr, to the fin through the area $\Delta y\,dx$ on top of the fin is:

$$\frac{dQ}{dx}dx = -kM\Delta y\frac{d^2t_p}{dx^2}dx \quad [16]$$

But this same heat gain in Btu per hr is:

$$\frac{dQ}{dx}dx = q_{u-x}\Delta y\cdot dx \quad [17]$$

Substituting between [14], [16], and [17] and letting $b^2 = U_L/kM$:

$$\frac{d^2t_p}{dx^2} = b^2\left(t_p - t_a - \frac{q_A - \epsilon R}{U_L}\right) \quad [18]$$

This has the general solution:

$$t_p = C_1e^{bx} + C_2e^{-bx} + t_a + \frac{q_a - \epsilon R}{U_L} \quad [19]$$

To determine the value of the constants C_1 and C_2 in the preceding equation, we apply the boundary conditions:

$$\frac{dt_p}{dx_{x=0}} = 0 \quad \text{and} \quad t_{p_{x=L}} = t_t \quad [20]$$

Application of these boundary conditions will be found to yield

$$C_1 = C_2 = \frac{(t_t - t_a) - \dfrac{q_a - \epsilon R}{U_L}}{e^{bL} + e^{-bL}} \quad [21]$$

We note that:

$$\cosh bx \equiv \tfrac{1}{2}(e^{bx} + e^{-bx}) \quad [22]$$

Substituting from Equations [21] and [22] into [19] and rearranging, we obtain the solution for the temperature distribution along the fin:

$$t_p = t_t\left(\frac{\cosh bx}{\cosh bL}\right) + \left(t_a + \frac{q_A - \epsilon R}{U_L}\right)\left(1 - \frac{\cosh bx}{\cosh bL}\right) \quad [23]$$

The average useful heat collection rate of the entire fin can be determined conveniently by noting that this average useful collection rate is equal to the total heat flow (Btu per hr) at the base of the fin, divided by the surface area of the fin:

$$q_u = \frac{Q_{x=L}}{L\Delta y} \quad [24]$$

From Equation [15]:

$$\frac{Q_{x=L}}{L\Delta y} = -\frac{kM}{L}\frac{dt_p}{dx_{x=L}} \quad [25]$$

Performing the indicated differentiation, (using the value of t_p found in Equation [23] rearranging, and remembering that $b^2 = U_L/kM$:

$$q_u = \frac{\tanh bL}{bL}[q_A - \epsilon R - U_L(t_t - t_a)] \quad [26]$$

Now we note that the bracketed expression at the right hand side of the above equation gives the useful heat collection rate which would be attainable with the entire fin at the temperature of the base of the fin. Hence the fin efficiency factor of the actual fin is the factor by which the bracketed expression is multiplied:

$$F = \frac{\tanh bL}{bL}$$
$$b = \sqrt{\frac{U_L}{kM}} \qquad [27]$$

It is important to note that the fin efficiency factor is *not* a function of the intensity of absorbed solar radiation or of the temperature level of operation, except insofar as these variables influence U_L.

Two other quantities which are of interest in problems involving fins are the maximum fin temperature and the average fin temperature.

The maximum fin temperature is readily obtained from Equation [23]:

$$t_{p_{max}} = t_{p_{x=0}} = t_t \frac{1}{\cosh bL} + \left(t_a + \frac{q_A - \epsilon R}{U_L}\right)\left(1 - \frac{1}{\cosh bL}\right) \qquad [28]$$

The average fin temperature is also obtained from Equation [23]:

$$t_{p\text{-average}} = \frac{1}{L}\int_0^L t_p\, dx \qquad [29]$$

Performing the indicated integration yields:

$$t_{p\text{-average}} = t_t \frac{\tanh bL}{bL} + \left(t_a + \frac{q_A - \epsilon R}{U_L}\right)\left(1 - \frac{\tanh bL}{bL}\right) \qquad [30]$$

COLLECTION EFFICIENCY FACTORS FOR COLLECTORS HAVING UNIFORM FLOW BENEATH A FLAT PLATE

Consider the situation illustrated in Fig. 2. The temperature of the circulating fluid, as it enters the collector, is t_{w-o}. The fluid flows uniformly under the collector plate and in thermal contact with it. The fluid picks up heat and rises in temperature as it flows along under the plate. At a distance x from the entering edge of the plate, the plate temperature is t_p, and the temperature of the fluid underneath is t_w.

To avoid complications due to tilt, glass covers, etc., all of which are extraneous to the present discussion, we assume the collector plate to be exposed and horizontal.

Then, at the distance x from the entering end of the collector, the local useful heat collection rate may be

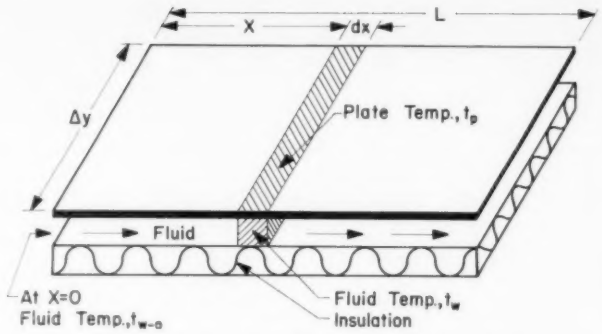

FIG. 2—Circulation of fluid in a flat-plate collector.

expressed, quite closely:

$$q_{u-x} = q_A - \epsilon R - U_L(t_p - t_a) \qquad [31]$$

in which

$$U_L = \epsilon h_r + h_a + U_b \qquad [32]$$

This useful heat collection rate is transferred from the plate to the circulating fluid underneath. Hence:

$$q_{u-x} = h_c(t_p - t_w) \qquad [33]$$

Eliminating t_p between Equations [32] and [33] yields:

$$q_{u-x} = \frac{h_c}{h_c + U_L}[q_A - \epsilon R - U_L(t_w - t_a)] \qquad [34]$$

The average rate of useful heat collection for the entire collector (q_u in our nomenclature) is then:

$$q_u = \frac{1}{L}\int_0^L q_{u-x}\, dx = \frac{h_c}{h_c + U_L}\left[q_A - \epsilon R - U_L\left(\frac{1}{L}\int_0^L t_w\, dx - t_a\right)\right] \qquad [35]$$

But:

$$\frac{1}{L}\int_0^L t_w\, dx = t_{w\text{-average}} \qquad [36]$$

So:

$$q_u = \frac{h_c}{h_c + U_L}[q_A - \epsilon R - U_L(t_{w\text{-average}} - t_a)] \qquad [37]$$

The expression in brackets at the right-hand side of the above equation is the useful heat collection rate attainable with the entire plate at average water temperature. Hence, for this type of collector:

$$F' = \frac{h_c}{h_c + U_L} \qquad [38]$$

We proceed to the determination of F_R. Rewriting Equation [34] as:

$$q_{u-x} = F'[q_A - \epsilon R - U_L(t_w - t_a)] \qquad [39]$$

The differential of the above is

$$dq_{u-x} = -F'U_L\, dt_w \qquad [40]$$

Now the rate, in pounds per hour, at which fluid flows

VOL. 3 1959

under the area $\Delta y\, dx$ is $GL\Delta y$. (Note definition of G in the list of symbols). Hence the useful heat gain (Btu per hr) associated with the area $\Delta y\, dx$ may be equated to the gain to the fluid as it flows under that area:

$$q_{u-x}\Delta y\, dx = G(L\Delta y\, dt_w) \qquad [41]$$

Eliminating dt_w between Equations [40] and [41], and rearranging:

$$\frac{dq_{u-x}}{q_{u-x}} = -\frac{F'U_L}{GCL}\, dx \qquad [42]$$

Integrating Equation [42] and applying boundary condition at $x = 0$ yields:

$$q_{u-x} = q_{u-o}e^{-(F'U_Lx/GCL)} \qquad [43]$$

The average useful heat collection rate is:

$$q_u = \frac{1}{L}\int_0^L q_{u-x}\, dx = q_{u-o}\frac{1}{L}\int_0^L e^{-(F'U_Lx/GCL)}\, dx \qquad [44]$$

Performing the indicated integration yields:

$$q_u = q_{u-o}\frac{GC}{F'U_L}(1 - e^{-(F'U_L/GC)}) \qquad [45]$$

From Equation [39]:

$$q_{u-o} = F'[q_A - \epsilon R - U_L(t_{w-o} - t_a] \qquad [46]$$

Substituting this value into Equation [45]:

$$q_u = F'\frac{GC}{F'U_L}(1 - e^{-(F'U_L/GC)}) \cdot [q_A - \epsilon R - U_L(t_{w-o} - t_a)] \qquad [47]$$

In the above equation the expression in brackets is seen to be the useful heat collection rate attainable with the entire plate at entering water temperature. Hence, the multiplying factor preceding it is, by definition, the over-all efficiency factor F_R.

$$F_R = F'\underbrace{\frac{GC}{F'U_L}(1 - e^{-(F'U_L/GC)})}_{\text{"flow rate factor"}} \qquad [48]$$

The above expression is generally applicable to any type of collector for which Equations [39] and [41] are valid. It may be noted that the expression can be considered as being made up of two factors: F' and a "flow rate factor" (the latter factor being also a function of F').

A plot of Equation [48] is presented in Fig. 5.

COLLECTION EFFICIENCY FACTORS FOR COLLECTORS HAVING UNIFORM FLOW IN TUBES BONDED TO A FLAT PLATE

This case, in one variation or another, occurs frequently in liquid-heating solar heat collectors. The general arrangement is shown in Fig. 3. A series of parallel tubes, of outside diameter d and inside diameter d_o, are spaced w ft on centers along the collector plate by a continuous bond. For the purpose of these calculations the bond width is assumed to be d, the same as the tube diameter, and the over-all thermal conductivity of this bond between plate and tube is taken as U_c Btu per sq ft-hr-°F. The fluid flow in each tube is assumed uniform and in the same direction. Hence, at any given cross-section along the collector,

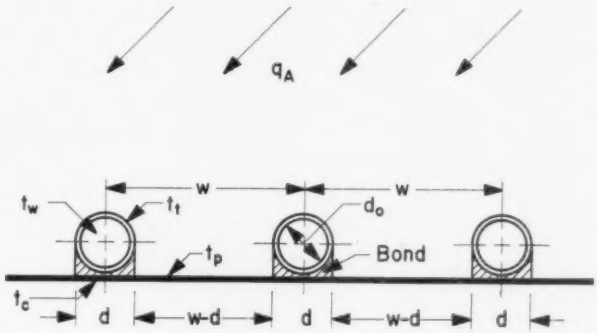

FIG. 3—General arrangement of collector with tubes bonded to a flat plate.

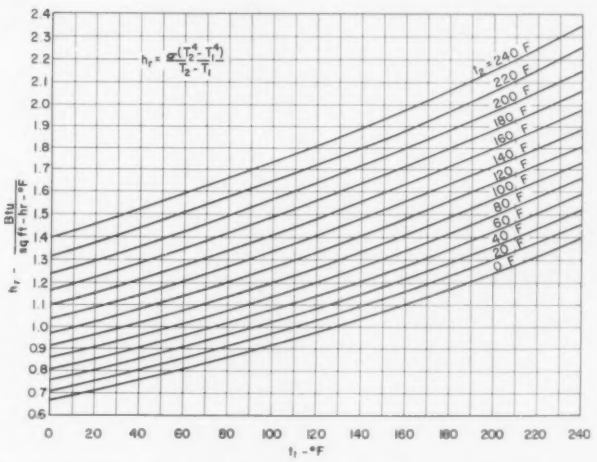

FIG. 4—The "simplified radiation coefficient" h_r. This coefficient is convenient for use in radiative heat transfer equations of the form $q = C_1h_r(t_2 - t_1)$, where C_1 is some constant involving surface emissivities and shape factors.

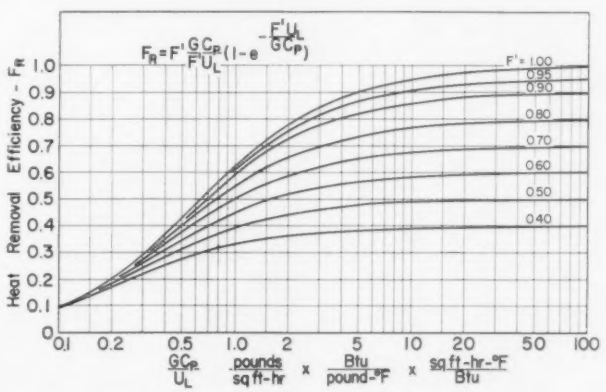

FIG. 5—The over-all efficiency factor F_R.

(such as Fig. 3) the temperatures t_w, t_t, and t_c will be the same at every tube.

We make the following simplifying assumptions:

(1) The thermal resistance around the circumference of a tube is negligible in comparison with all other thermal resistances involved.

(2) The division of incident sunshine between tubes and plate is such that the fraction d/w is absorbed on the tubes and the remaining fraction $1 - d/w$ is absorbed by the plate.

(3) The loss rate factors of the tubes and plate are also proportional to the ratios of their projected areas d/w and $1 - d/w$.

The following five independent equations can then be written, in each case expressing a heat transfer rate on a "per square foot of collector" basis:

(1) The useful heat gain from sunshine striking the tubes:

$$q_{u\text{-tubes}} = \frac{d}{w}[q_A - \epsilon R - U_L(t_t - t_a)] \qquad [49]$$

(2) The useful heat gain from the plate:

$$q_{u\text{-plate}} = \left(1 - \frac{d}{w}\right) F[q_A - \epsilon R - U_L(t_c - t_a)] \qquad [50]$$

A consideration of the above equation, and of Fig. 3, will show that the above F is the fin efficiency factor of a fin of length $(w - d)/2$.

(3) The heat transfer through the bond:

$$q_{u\text{-plate}} = \frac{d}{w} U_c(t_c - t_t) \qquad [51]$$

(4) The heat transfer from tube to fluid:

$$q_u = \frac{\pi d_o h_c}{w}(t_t - t_w) \qquad [52]$$

(5) The total useful heat gain:

$$q_u = q_{u\text{-tubes}} + q_{u\text{-plate}} \qquad [53]$$

The preceding set of five equations contains five "unknowns":

$$q_u\ ,\ q_{u\text{-tubes}}\ ,\ q_{u\text{-plate}}\ ,\ t_c\ ,\ t_t \qquad [54]$$

We should like to eliminate all but the first of these and, furthermore, to determine if the solution for q_u is of the form:

$$q_u = F'[q_A - \epsilon R - U_L(t_w - t_a)] \qquad [55]$$

in which F' is a function of the following variables *only*:

$$\frac{d}{w},\quad \frac{\pi d_0 h_c}{w},\quad F,\quad U_L,\quad \text{and}\quad U_c \qquad [56]$$

The simultaneous solution of Equations [49] through [53] involves fifth-order determinants. The solution is straightforward, but the necessary calculations appeared too voluminous even for inclusion in these notes. However, if the solution is carried through, it will be found that the equation for q_u is indeed of the form given by Equation [55], and that the value for F' is:

$$F' = \frac{C_2(U_c + U_L) + C_1 U_c}{\frac{U_L}{C_3}[C_2(U_c + U_L) + C_1 U_c] + U_c + \frac{C_2 U_L}{C_1}} \qquad [57]$$

in which

$$C_1 = \frac{d}{w}, \qquad C_2 = \left(1 - \frac{d}{w}\right) F, \qquad C_3 = \frac{\pi d_o h_c}{w} \qquad [58]$$

Furthermore, it will be found that Equation [57] can be manipulated into the following continuing fraction:

$$F' = \cfrac{1}{\frac{U_L}{C_3} + \cfrac{1}{C_1 + \cfrac{1}{\frac{U_L}{C_1 U_c} + \frac{1}{C_2}}}} \qquad [59]$$

or substituting values of C_1, C_2, and C_3:

$$F' = \cfrac{1}{\frac{wU_L}{\pi d_o h_c} + \cfrac{1}{\frac{d}{w} + \cfrac{1}{\frac{wU_L}{dU_c} + \cfrac{1}{\left(1 - \frac{d}{w}\right) F}}}} \qquad [60]$$

(general case)

The above equation is the general solution for this type of collector. Several particular cases are of interest.

Case I. $d/w = 1.00$

In this case Equation [60] will be found to reduce to:

$$F' = \frac{1}{\frac{wU_L}{d_o \pi h_c} + 1} \qquad [61]$$

$(d/w = 1.00)$

Note that the above case amounts to assuming that the tubes are side by side, with no space between them. This is essentially the case of the collector with uniform flow under a plate (see Fig. 2) except that the tube area in contact with the fluid is $\pi d_o/w$ sq ft per sq ft of collector. If $\pi d_o/w = 1.00$, Equation [61] reduces to Equation [38], as it should.

Case II. $F = 1.00$

For this case Equation [60] reduces to:

$$F' = \frac{1}{\frac{wU_L}{\pi d_o h_c} + \frac{\frac{w}{d}\left(1 - \frac{d}{w}\right) + \frac{U_c}{U_L}}{\left(1 - \frac{d}{w}\right) + \frac{U_c}{U_L}}} \qquad [62]$$

$(F = 1.00)$

VOL. 3 1959

The above equation may be used to estimate the efficiency factor of collectors having a relatively low thermal conductivity of the "bond" between plate and tubes. An example of such a collector is one formed of a grid of parallel pipes set inside a glass-covered box, with no continuous physical connection between the tubes and the inside of the bottom of the box. In such a case a reasonable estimate of the over-all convective plus radiative coefficient of heat transfer between box bottom and tubes can usually be made, and appropriately substituted for U_c in the equation. In making such a substitution, it should be noted that U_c as used in these equations is the over-all heat transfer coefficient between plate and tubes on a "per square foot of projected area of tube" basis.

Case III. Thermal Resistance of Bond Negligible

In this case $1/U_c = 0$, and Equation [60] becomes:

$$F' = \frac{1}{\dfrac{wU_L}{\pi d_o h_c} + \dfrac{1}{\dfrac{d}{w} + \left(1 - \dfrac{d}{w}\right) F}} \qquad (U_c^{-1} = 0) \qquad [63]$$

As has been mentioned previously, the factor F in the above equation is the fin-efficiency factor of a fin of length $(w - d)/2$. Hence, from Equation [27]:

$$F = \frac{\tanh bL}{bL} \qquad [64]$$

in which

$$b = \sqrt{\frac{U_L}{kM}} \qquad L = \frac{w - d}{2} \qquad [65]$$

Equation [63] represents a case of considerable practical importance, as it is applicable both to collector plates made of tubes soldered to a metal sheet and to plates made of "tube-in-strip" or similar integral-tube type materials. Most water-heating collector plates use one or the other of these constructions.

We have found that one convenient method of using Equation [63] in design calculations is to plot F' against tube spacing for a variety of pertinent conditions. Examples of such graphs are given in Fig. 6 through 11.

Figs. 6, 7, and 8 are plotted for a constant U_L value of 1.2 Btu per sq ft-hr-°F. This value is typical of collector plates insulated on the sunny side with one air-spaced layer of glass or transparent plastic, and well insulated on the back. Such construction is often used in domestic water-heating collectors. The three graphs present F' for copper, aluminum, and steel sheets respectively, and in each case for several sheet thicknesses and for two values of the tube-to-liquid film coefficient h_c. The lower value of h_c (60 Btu/sq ft-hr-°F) is more or less typical of laminar water flow in thermosyphon-type collectors. The higher value of h_c (300 Btu per sq ft-hr) is in the range of turbulent water flow, and may be obtained with pump circulation.

Figs. 9, 10, and 11 present the same data for a U_L value of 2.5 Btu per sq ft-hr-°F which is a value typical of a collector with no cover on the sunny side, moderately insulated on the back, and operating under low wind velocity conditions (3 to 5 mph). This type of construction may be used for solar heat collection at a temperature level not too much above that of the outdoor air, for example in swimming pool heating and in some space-heating applications.

Figs. 6 through 11 are all calculated for $\frac{1}{2}$-in. diameter tubes, and it is assumed that the tube walls are fairly thin, i.e., $d_o \approx d$. Under most conditions no large error will result from using the graphs for any tube diameter between $\frac{3}{8}$ in. and $\frac{3}{4}$ in.

It will be remembered that the various expressions for F' derived in this section are all based on the assumptions that the flow in the parallel tubes is uniform from tube to tube and in the same direction. These assumptions are not realized in collectors in which the flow is unevenly distributed between tubes, nor are they realized when a return bend circuit arrangement gives flow in opposite directions in adjacent tubes. Analytical solutions for these cases are desirable but do not seem to be available. In general, qualitative consideration will show that the F' ratios for collectors with either uneven or opposed direction flow will be somewhat less than the F' ratios covered in this section.

Turning to a consideration of the factor F_R for collectors of the general type discussed in this section, we note that Equations [39] and [41] of the preceding section are applicable. Hence the expression for F_R (Equation [48]) developed in the preceding section is also applicable. The equation is plotted in Fig. 5.

ILLUSTRATIVE EXAMPLES

A few numerical "problems" and their solutions may be helpful in illustrating the practical utility of the efficiency-factor equations.

Example 1

A water-heating collector designed for swimming pool heating uses an integral-tube type of collector plate having $\frac{1}{2}$-in. tubes spaced 4 in. on a 0.025-in. copper plate. The collector plate is uncovered, wind velocity at the level of the collector is in the range of 3 to 5 mph, and the loss rate factor U_L is estimated as 2.5 Btu per sq ft-hr-°F.

(a) If the flow rate through the collector is 3 lb per sq ft-hr, and the flow in the tubes is laminar, what is the efficiency factor F_R?

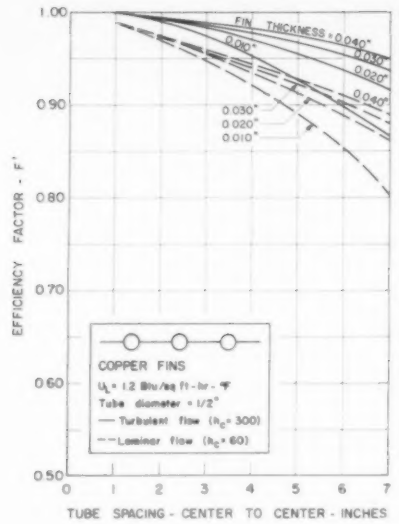
EFFICIENCY FACTOR - F'
TUBE SPACING - CENTER TO CENTER - INCHES
FIN THICKNESS = 0.040"
0.030"
0.020"
0.010"
COPPER FINS
U_L = 1.2 Btu/sq ft - hr - °F
Tube diameter = 1/2"
— Turbulent flow (h_c = 300)
-- Laminar flow (h_c = 60)

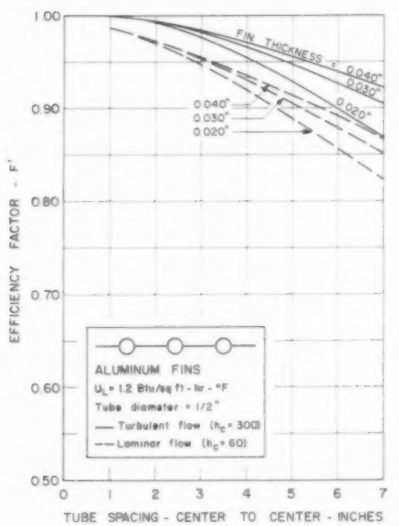
EFFICIENCY FACTOR - F'
TUBE SPACING - CENTER TO CENTER - INCHES
FIN THICKNESS = 0.040"
0.030"
0.020"
ALUMINUM FINS
U_L = 1.2 Btu/sq ft - hr - °F
Tube diameter = 1/2"
— Turbulent flow (h_c = 300)
-- Laminar flow (h_c = 60)

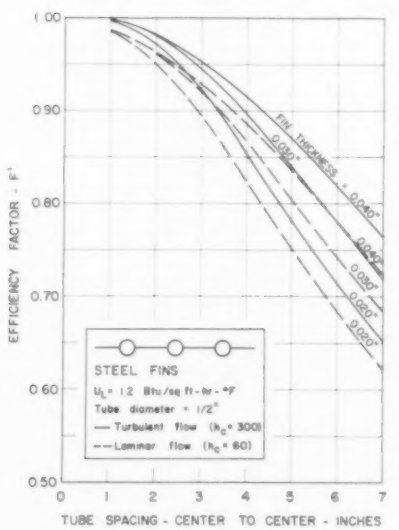
EFFICIENCY FACTOR - F'
TUBE SPACING - CENTER TO CENTER - INCHES
FIN THICKNESS = 0.040"
0.030"
0.020"
STEEL FINS
U_L = 1.2 Btu/sq ft - hr - °F
Tube diameter = 1/2"
— Turbulent flow (h_c = 300)
-- Laminar flow (h_c = 60)

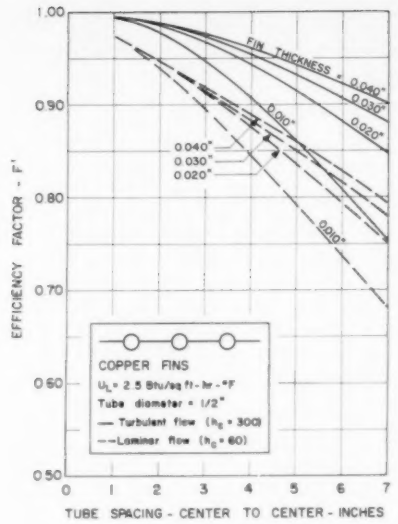
EFFICIENCY FACTOR - F'
TUBE SPACING - CENTER TO CENTER - INCHES
FIN THICKNESS = 0.040"
0.030"
0.020"
0.010"
COPPER FINS
U_L = 2.5 Btu/sq ft - hr - °F
Tube diameter = 1/2"
— Turbulent flow (h_c = 300)
-- Laminar flow (h_c = 60)

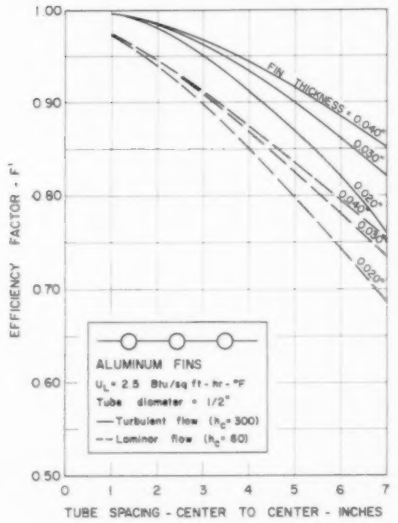
EFFICIENCY FACTOR - F'
TUBE SPACING - CENTER TO CENTER - INCHES
FIN THICKNESS = 0.040"
0.030"
0.020"
ALUMINUM FINS
U_L = 2.5 Btu/sq ft - hr - °F
Tube diameter = 1/2"
— Turbulent flow (h_c = 300)
-- Laminar flow (h_c = 60)

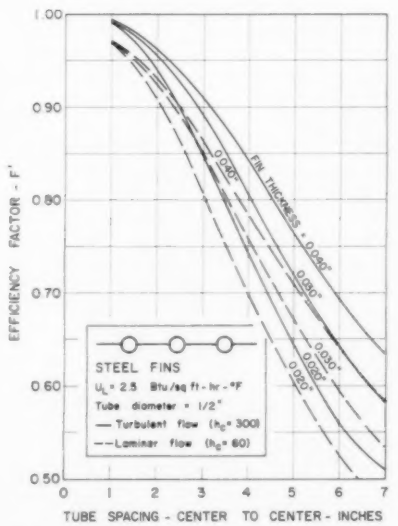
EFFICIENCY FACTOR - F'
TUBE SPACING - CENTER TO CENTER - INCHES
FIN THICKNESS = 0.040"
0.030"
0.020"
STEEL FINS
U_L = 2.5 Btu/sq ft - hr - °F
Tube diameter = 1/2"
— Turbulent flow (h_c = 300)
-- Laminar flow (h_c = 60)

FIG. 6–11—Efficiency factor F' vs. tube spacing for various conditions.

VOL.
3
1959

Solution: From Fig. 9, we find $F' = 0.88$. Entering Fig. 5 with this value of F' and with

$$CG/U_L = (3 \times 1.0)/2.5 = 1.2,$$

we find $F_R = 0.62$.

(b) Assume that the absorptivity of the painted collector plate for solar radiation is 0.95, and that its emissivity and absorptivity in the long-wavelength region is 0.90. Assume further that the collector is operating under the following conditions:

Entering water temperature..... 82°F
Outdoor air temperature..... 65°F
Intensity of sunshine incident upon collector 275 Btu/sq ft-hr
Net outgoing radiation R' from a black surface at air temperature and at collector tilt 20 Btu/sq ft-hr

What will be the useful heat collection rate of the collector in Btu per sq ft-hr?

Solution:

$$\begin{aligned} q_u &= F_R[\alpha q_i - \epsilon R' - U_L(t_{w-o} - t_a)] \\ &= 0.62[0.95 \times 275 - 0.90 \times 20 - 2.5(82 - 65)] \\ &= 125 \end{aligned}$$

(c) If the flow velocity in this collector is such that increasing the flow rate to 7 lb per sq ft-hr would result in turbulent flow, how much will the useful heat collection be increased if the flow rate is increased to this value?

Solution: From Fig. 9 we find $F' = 0.95$ for turbulent flow. Entering Fig. 5 with this new value of F', and with the new value of $GC/U_L = 2.8$, we find the new value of F_R to be 0.80. Under the previous laminar flow conditions we found F_R was 0.62. Hence the change to increased flow rate and turbulent flow will increase useful heat collection by the ratio 0.80/0.62, or about 29 per cent.

Example 2

A manufacturer of glass-covered domestic water-heating collectors produces collector plates by soldering parallel $\frac{1}{2}$-in. diameter tubes to a metal sheet. Several types of sheet metal are available at varying costs, and the tubes can be spaced as desired. The problem is to determine the particular choice of sheet material and tube spacing which will yield the maximum ratio of heat collection per unit of initial cost.

The manufacturer has found that the cost of a complete collector can be broken into three components, as follows:

(a) A fixed cost of $3.00 per sq ft of collector, which covers framing, insulation, glass, supports, painting, etc.

(b) The cost of the sheet metal for the collector plate. There are four available sheets: copper sheet in three thicknesses, 0.010-in., 0.020-in., and 0.030-in. and costing $0.40, $0.80, and $1.20 per sq ft respectively. Steel sheets are available in 0.040-in. thickness costing $0.25 per sq ft.

(c) The total cost of tubes, soldering, and associated headers. This has been found to be proportional to the length of tube used, and amounts to $0.35 per lineal ft of tube.

The flow in the tubes is laminar. The flow rate, for the purpose of simplifying this example, is assumed to be the same regardless of tube spacing.

Solution: The cost of the energy furnished by the collector will be directly proportional to the total cost per square foot of collector, and inversely proportional to the collector efficiency. Hence, if we let the collector cost be S dollars per sq ft, the problem amounts to determining the lowest possible value of the ratio S/F' for the various choices of sheet material and tube spacing.

From the data given, it is readily seen that the total cost S can be expressed:

$$S = 3.00 + B + 4.20/w' \text{ dollars/sq ft}$$

in which B is the cost of the sheet metal used, and w' is the tube spacing in inches.

The elegant method for determining the minimum value of the ratio S/F' is to find the point at which the partial derivatives of S/F' with respect to sheet metal cost and with respect to tube-spacing cost are simultaneously equal to zero. However, this problem, and many similar problems of this type, can be solved

TABLE I—Trial and Error Solution of Example 2

Type of sheet	Tube spacing w' in.	Collector cost S ($/sq ft)	Efficiency factor F'	S/F' $/sq ft—$F'$
0.010″ Copper	7.0	4.00	.802	4.98
0.010″ Copper	6.0	4.10	.851	4.82
0.010″ Copper	5.75	4.13	.862	4.79
0.010″ Copper	5.50	4.16	.871	(4.77)
0.010″ Copper	5.25	4.20	.880	(4.77)
0.010″ Copper	5.0	4.24	.888	4.78
0.010″ Copper	4.0	4.45	.919	4.84
0.010″ Copper	3.0	4.80	.947	5.07
0.020″ Copper	7.0	4.40	.860	5.12
0.020″ Copper	6.0	4.50	.887	(5.07)
0.020″ Copper	5.0	4.64	.910	5.10
0.020″ Copper	4.0	4.85	.933	5.20
0.020″ Copper	3.0	5.20	.954	5.46
0.030″ Copper	7.0	4.80	.878	5.47
0.030″ Copper	6.0	4.90	.901	(5.44)
0.030″ Copper	5.0	5.04	.920	5.47
0.030″ Copper	4.0	5.25	.938	5.60
0.040″ Steel	7.0	3.85	.725	5.31
0.040″ Steel	6.0	3.95	.780	5.07
0.040″ Steel	5.0	4.09	.835	4.90
0.040″ Steel	4.0	4.30	.885	(4.87)
0.040″ Steel	3.0	4.65	.930	5.00

equally quickly by a trial-and-error tabulation. For this problem we use the values of S given by the above equation together with corresponding values of F' determined from Figs. 6 and 8. The resulting tabulation is shown in Table I. The minimum values of the ratio S/F' for the various sheets are those enclosed in parentheses. For the particular set of cost and other conditions specified in this example, the collector plate which "delivers the most Btus for the least money" is seen to be that using 0.010-in. copper sheet with the tubes spaced approximately $5\frac{1}{2}$ in.

CONCLUSION

The efficiency factors derived in these notes are applicable to a wide variety of solar heat collectors. They are also directly applicable to other types of panel heat-exchangers, for example to floor or ceiling panels used for interior temperature control.

The intelligent use of the efficiency factor concept can easily eliminate a large area of guesswork in the design of a solar heat collector. Although, as has been previously mentioned, these efficiency factors are not a new concept in solar heat collector design, they do not seem to have been used as much as they should be. It is hoped that these notes may be helpful in furthering the use of these basic heat-transfer concepts and in reducing unnecessary empiricism in the design of heat exchangers used for collecting solar energy.

REFERENCES

1. H. C. Hottel; B. B. Woertz. "The performance of flat-plate solar-heat collectors". *Trans. Am. Soc. Mech. Engrs.* **64:** 91–104, Feb. 1942.
2. A. Whillier. "Solar energy collection and its utilization for house heating". Sc.D. Thesis, Dept. of Mechanical Engineering, Massachusetts Institute of Technology, May 1953.
3. H. C. Hottel; A. Whillier. "Evaluation of flat-plate solar-collector performance". *Trans. of Conference on the Use of Solar Energy, University of Arizona, 1958.* Vol. II, pp. 74–104.

VOL.
3
1959

A Stationary Solar Energy Concentrator

By Paul B. Archibald

Livermore, California

A parabolic reflector having a short focal length will keep the sun's rays focused within a small area for several hours without the employment of a heliostat mechanism. Its use as a steam generator and as a stove is described.

Among the more frequently proposed applications for solar energy is its employment in cooking. While many clever solar stoves have been built, their widespread use has been restricted mostly to countries poor in natural fuels. Americans do not live in such a country, and it is difficult to see how solar stoves could ever be of much practical importance here. This is not to say that a solar stove has not a certain appeal. The smug feeling of complacency which the solar broiler generates in the backyard chef is to be considered, and one is led to surmise that this feeling might be further enhanced if the cook had made the stove himself.

Some experiments directed toward the development of a solar steam generator indicated a design for a solar stove which would be easy to construct out of material normally available in the home.

The steam generator, from which the solar stove was derived, had as its objective a means of concentrating sunlight which would not involve the use of any moving parts. The parabolic reflector that served as a concentrating device was made in the following manner. A parabola having a focal length of 1 in. and legs of about 16 in. was drawn on a piece of $\frac{1}{2}$-in. plywood, and two parabolas of this size were cut out with a band saw. The area outside the parabolic curve was used to shape and support the reflector. These two pieces were nailed to a board 36 in. apart in such a manner that the open ends of the parabolas both pointed in the same direction. Into these parabolas a piece of 6-mil hardened aluminum sheet was draped and then attached with tape.

The reason for the short focal length of the reflector was to eliminate the need for a heliostat mechanism. The reflector was set level on the ground with its axis in an east-west direction and then tilted into the plane of the sun. This last adjustment was made by observing the shadow of a stick held midway between the two surfaces of the parabola and tilting the reflector until the shadow fell at the bottom or vertex of the parabola.

Once the adjustment was made the reflector was not moved. The focal point of the sun's rays coming in obliquely in the morning and afternoon would be inside the 1-in. maximum which was obtained when the sun was at its zenith. Readjustment to the plane of the sun was necessary only every three or four days.

The boiler tube consisted of a blackened copper tube $\frac{3}{8}$-in. outside diameter within two concentric glass tubes, the outside one being $1\frac{1}{2}$ in. diameter. The boiler tube was placed at the focus of the parabola in such a manner that the upper side of the copper tube was at the 1-in. focal point.

The focal point of the sun's rays, which in the morning and afternoon would strike the reflector obliquely, is equal to $f = f_1 \cos^2 \alpha$, where f_1 is equal to 1 in. and α is the angle of the sun from the zenith. With such an arrangement the $\frac{3}{8}$-in. copper tube is at the focal point for a period of about five hours, and the temperature can be estimated by multiplying the solar constant by the ratio of the projected area of the reflector divided by the area of the copper tube. With the reflector and the boilertube described this ratio was 12, which gives a value of about 24 cal per sq cm per min. The equilibrium temperature for this energy input is, by the Stefan-Boltzmann Law, 463°C. All of the energy is not available at this temperature; however, the quantity and temperature of the steam which can be obtained can be readily calculated.

In the model generator water boiled for seven hours and, when empty, the tube reached a temperature of 350°F during the middle of the day. There were several apparent reasons for this low temperature: the boiler tube was too long—it should be shorter than the reflector, so as to receive the full 24 cal per sq cm per min along its entire length when the sun is not at its zenith; the glass tube outside the copper tube was not evacuated, and water vapor would condense on the inside of the glass. While none of the mechanical problems would appear to be difficult to solve, they would require some effort.

Despite the shortcomings of the first model, its performance was gratifying, and the idea of a non-moving reflector for concentrating solar energy was demonstrated. The improvements that would have to be made plus the cost of instrumentation before worthwhile

data could be collected indicated that as a backyard project further development was not feasible.

However, the use of the reflector as a solar stove seemed to be a possibility which could be investigated. The shape of the food to be cooked should be long and round like the boiler tube. Ears of corn met the requirements, and it was found that corn with the husks removed and wrapped tightly in cellophane and laid at the vertex could be cooked in about forty minutes. The flavor seemed much better than boiled corn, but no effort was spent on trying to get an impartial opinion.

One interesting trick was to set the stove with the corn in it in the shade so that the sunlight would not strike it until about forty minutes before meal time.

While the reflector described was quite adequate as a corn-cooking device, it seemed to be a little too elegant for such a prosaic job, and it appeared that a stove of more common material and simpler construction would be desirable.

For a reflector surface ordinary aluminum foil glued to cardboard was used, and for the parabolic shape stiff wire (from a coathanger) was bent into the desired shape and held in position by a string across the branches of the parabola. The reflector surface was bent around the wire parabola and taped in place. The stove was then placed in a pasteboard box for support.

While the amount of solar energy collected is proportional to the area of the reflector normal to rays of the sun, a shallow—say 8-in. focal length—reflector intercepting the same amount of sunlight did not function as a stove. The reason for this seems to be the heat loss by convecting air currents.

The paper and aluminum stove is a very safe device—even children can operate it—and if of no practical significance it makes a rather nice demonstration of solar energy.

The steam generator can be optimized in various ways. Thus, to increase the diameter of the copper tube from $\frac{3}{8}$ in. to $\frac{1}{2}$ in. will increase the length of time that the tube is at the focus from five to seven hours. However the equilibrium temperature would be lowered. It is not necessary for the boiler tube to be on focus in order for it to intercept a considerable amount of solar energy. This explains why, in the model, boiling was obtained one hour before the focal point moved up to the copper tube. To use a shorter-focal-length reflector would mean that it would have to be much deeper in order to intercept the same amount of sunlight.

While the stationary solar energy concentrator described is probably not as efficient as one with a heliostat mechanism, its simplicity of construction should more than outweigh this disadvantage.

VOL.
3
1959

Calculation of the Concentration of Energy at Points Outside the Focal Spot of a Parabolic Condenser*

By Alfred W. Simon

Scientific and Engineering Staff, Air Force Missile Development Center, Holloman Air Force Base, New Mexico

An analysis of the distribution of intensity and of energy falling outside of the circular projection of the cone of reflected radiation coming from all infinitesimal areas of the surface of a paraboloidal mirror. The results given in a previous paper under the same title are incorrect. The correct theoretical deductions and the correct numerical results are given here. A uniform sun is assumed. The original paper which is corrected here appeared as Chapter 7 of *Solar Furnace Support Studies*, AFMDC-TR-58-7, Holloman Air Force Base, New Mexico, and on pages 22–24 of Volume II, number 2, *Solar Energy*, April 1958.

Under the above title in a previous paper I have calculated the variation in intensity of the energy falling on the focal plane of a parabolic condenser as a function of the distance from the center of the spot. However, I subsequently discovered that the theoretical deductions made in that paper are incorrect and the published results, therefore, wrong. In the present paper I give the correct theoretical deductions and the correct numerical results.

Consider (Fig. 1) the cone of light of angular width α, where α is the angular diameter of the sum, reflected at an angle θ to the axis of the parabola. The base of this cone of light through the focal point F of the parabola makes an angle θ with the focal plane and has a radius R given by the equation:

$$R = \rho\alpha/2 \qquad [1]$$

where ρ is the distance PF. This distance is given in turn by the equation:

$$\rho = 2f/(1 + \cos\theta) \qquad [2]$$

where f is the focal length of the parabola, so that we have R given by the equation:

$$R = f\alpha/(1 + \cos\theta) \qquad [3]$$

The circle constituting the base of this cone of light is projected onto the focal plane, thus forming an ellipse of semiminor axis b given by $b = R$ and semimajor axis a given by $a = b/\cos\theta$. Hence we have:

$$b = f\alpha/(1 + \cos\theta) \qquad [4]$$

$$a = f\alpha/(1 + \cos\theta)\cos\theta \qquad [5]$$

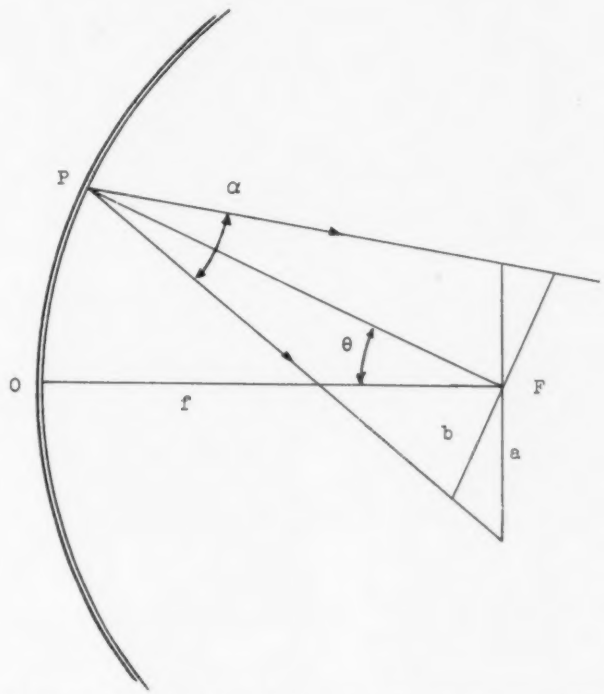

FIG. 1—Geometry of the reflection of a cone of light onto the focal plane of a paraboloid.

For a focal spot of 5 in. in diameter, that is, for $f\alpha = 5$ in., we have the values of a and b corresponding to various values of θ given in Table I.

The corresponding ellipses are plotted in Fig. 2 through 7.

The amount of energy falling into each ellipse is that falling on a ring of radius $\rho \sin\theta$ and thickness $\rho\, d\theta$ on the face of the paraboloid. In particular, if we denote this energy by dE, we have dE given by:

$$dE = 2\pi e\rho^2 \sin\theta\, d\theta \qquad [6]$$

where e is the solar constant.

It will be seen that all the ellipses enclose the focal spot of radius $r_f = 2.5$ in.; hence the fractional portion

---

* Originally issued as AFMDC-TN-59-11, ASTIA Document No. AD 215462. Released by author May 7, 1959.

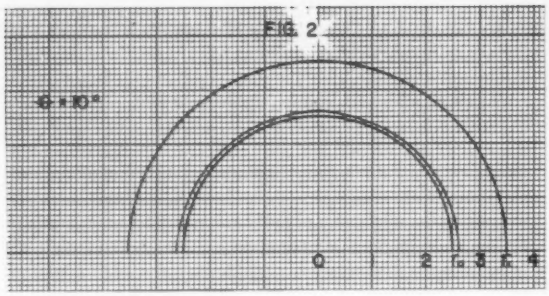

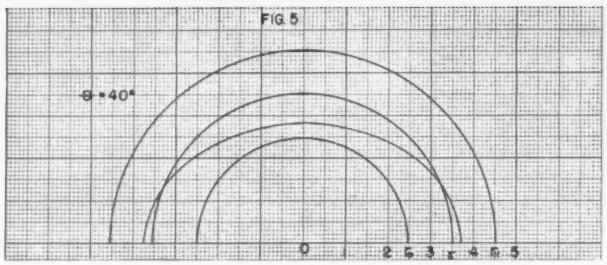

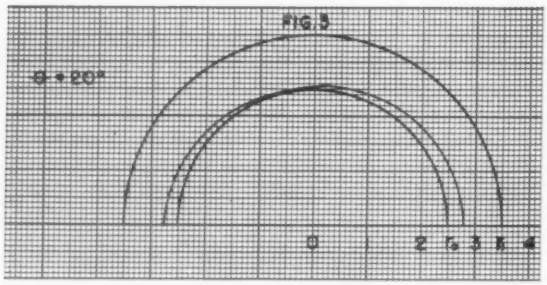

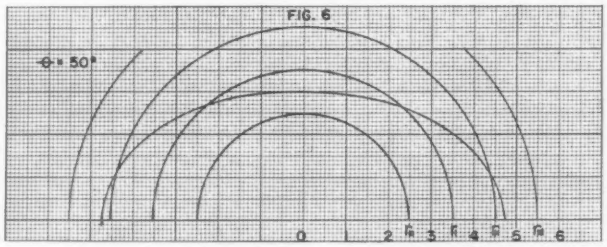

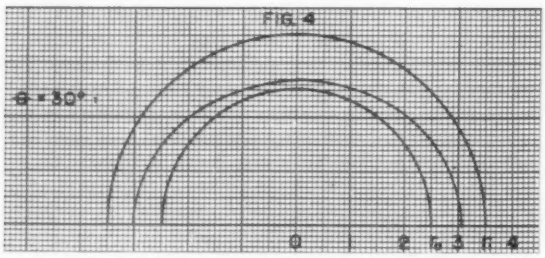

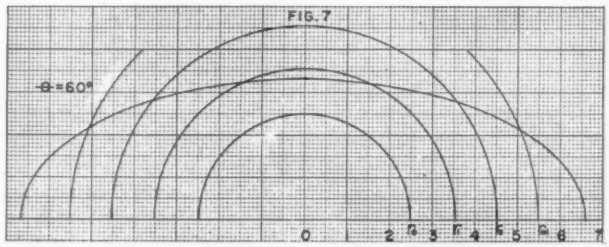

FIGS. 2-7—Ellipsoidal spots produced in the focal plane by cones of light reflected at various angles from the paraboloid.

of the energy collected at an angle θ falling into the focal spot is given by the ratio:

$$\pi r_f^2/\pi ab \qquad [7]$$

and the corresponding intensity dI_f is:

$$dI_f = \frac{\pi r_o^2}{\pi ab}\frac{2\pi e\rho^2 \sin\theta\, d\theta}{\pi r_o^2} = 8e \sin\theta \cos\theta\, d\theta/\alpha^2 \qquad [8]$$

Consequently, I_f is given by:

$$I_f = \frac{8e}{\alpha^2}\int_0^{\theta_1} \sin\theta\cos\theta\, d\theta = \frac{4e}{\alpha^2}\sin^2\theta_1 \qquad [9]$$

where θ_1 is the half angle of opening of the paraboloid.[2]

If now we select a ring of inner radius r_i and outer radius r_o, where $r_o > r_i > r_f$, this ring will intercept a certain area A_θ of the ellipse corresponding to the angle θ.

The energy dE falling into this area will be given by:

$$dE = \frac{A_\theta}{\pi ab} 2\pi e\rho^2 \sin\theta\, d\theta \qquad [10]$$

As the point P moves around the face of the paraboloid the corresponding ellipse rotates, and this energy is scattered over a ring of inner radius r_i and outer radius r_o. Consequently the corresponding *average* intensity dI_a within the ring will be:

$$dI_a = \frac{A_\theta}{\pi ab}\frac{2\pi e\rho^2 \sin\theta\, d\theta}{\pi(r_o^2 - r_i^2)} \qquad [11]$$

and the ratio of this intensity to that in the focal spot will be given by:

$$\frac{dI_a}{I_f} = \frac{A_\theta\, 2e\rho^2\alpha^2 \sin\theta\, d\theta}{\pi ab\,(r_o^2 - r_i^2)\,4e\sin^2\theta_1} = \frac{A_\theta\, 2f^2\alpha^2 \sin\theta\, d\theta}{\pi ab\,(1+\cos\theta)^2(r_o^2 - r_i^2)\sin^2\theta_1} \qquad [12]$$

This equation becomes:

$$\frac{dI}{I_f} = \frac{A_\theta}{\pi ab}\frac{8 \times 5^2 \sin\theta\, d\theta}{3(1+\cos\theta)^2(r_o^2 - r_i^2)} \qquad [13]$$

if we substitute for $f\alpha$ its value of 5 in. and for $\sin^2\theta$ its value $\frac{3}{4}$ corresponding to a diameter of the focal spot of 5 in. and a value of θ_1 equal to 60°, respectively.

VOL. 3 1959

TABLE I

θ	a	b
10°	2.558″	2.519″
20°	2.743″	2.578″
30°	3.094″	2.699″
40°	3.696″	2.831″
50°	4.733″	3.043″
60°	6.666″	3.333″

TABLE II

	x_1	x_2	x_3
40°	3.201″	—	—
50°	2.258″	4.328″	—
60°	1.233″	3.490″	5.305″

TABLE III

r	I_a/I_f	I cal/cm². sec
0–2.5″	1.000	1017
2.5″–3.5″	0.536	545
3.5″–4.5″	.147	149
4.5″–5.5″	.033	46
6.66″	.000	0

Since A_θ is a complicated function of θ, we have to resort to approximate integration, rewriting the above equation in the form:

$$\frac{\Delta I_a}{I_f} = \frac{A_\theta}{\pi ab}\,\frac{2000}{3 \times 57.3}\,\frac{\sin\theta}{(1+\cos\theta)^2\,(r_o^2 - r_i^2)} \qquad [14]$$

where we have taken $\Delta\theta$ equal to 10°.

The various rings of radii 2.5, 3.5, and 4.5 in. have been drawn in Figs. 2 through 7.

In order to calculate the areas A_θ we require the intersections of the various circles with the ellipses.

For these intersections we have, obviously:

$$x_i = \pm a\sqrt{(r_i^2 - b^2)/(a^2 - b^2)} \qquad [15]$$

The values of the abscissas of the points of intersection of the ellipses with the circles of radii $r_1 = 2.5$ in., $r_2 = 3.5$ in., and $r_3 = 4.5$ in., are given in Table II.

As a typical calculation of the areas A_θ let us take the area intercepted between the radii r_1 and r_2 for $\theta = 50°$ (shaded area in Fig. 6).

We have A_{50} given by:

$$A_{50} = 4\int_{x_1}^{x_2} \frac{b}{a}\sqrt{a^2 - x^2}\,dx + 4\int_{x_2}^{r_2} \sqrt{r_2^2 - x^2}\,dx - 4\int_{x_1}^{r_1} \sqrt{r_1^2 - x^2}\,dx \qquad [16]$$

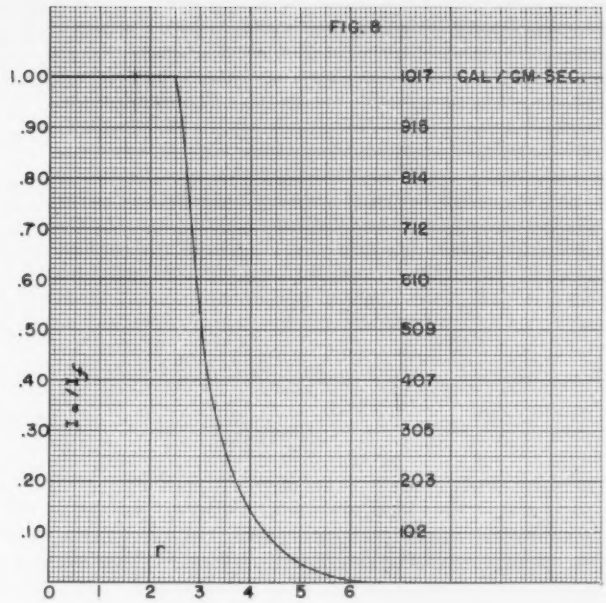

FIG. 8—Variation of average intensities within rings of various diameters in the focal spot plotted against the diameter of the center of the ring.

where $b/a = \cos\theta$. Substituting for x_1, x_2, r_1, r_2, and θ their values and integrating, we find $A_{50} = 9.06$ sq in. If now we note that for $\theta = 50°$, $\pi ab = 45.25$ sq in., $\sin\theta/(1 + \cos\theta)^2 = 0.284$, and that for this case Equation [16] reduces to

$$\frac{\Delta I_a}{I_f} = 1.454\,\frac{A_\theta}{\pi ab}\,\frac{\sin\theta}{(1+\cos\theta)^2} \qquad [17]$$

we obtain $\Delta I_a/I_f = 0.08267$.

If now we calculate the values of $\Delta I_a/I_f$ corresponding to various values of θ for a given set of radii and apply the trapezoidal rule to the results for each ring, we have the *average* intensities within the various rings as given in Table III.

The intensities have been calculated on the basis of 1.76 cal per sq cm per minute received by the paraboloid. In Fig. 8 the calculated values have been plotted against the radius of the *center* of the ring. It should be noted that the intensities are *average* values over the area of the ring, that the results hold only for a uniform sun, and that no losses have been assumed.

REFERENCE

A. W. Simon. "Calculation of the concentration of energy at points outside the focal spot of a parabolic condenser." *Solar Energy* **2**(2): 22–24, Apr. 1958. Also in: *Solar Furnace Support Studies*, AFMDC-TR-58-7, 1958. Ch. 7.

Comments on Papers

Dear Sir:

The paper, "Theory and Design of a Mechanical Blackbody for Solar Radiation" by Winskell and Hsu, which appeared in the April, 1959, issue of *Solar Energy*, contains a number of errors or inconsistencies. Some are important technically; others probably are printing errors.

The first sentence of the Introduction states that "one of the current problems in the field of solar energy utilization is to obtain a durable, high absorptive, low emissive surface to solar radiation." This is technically incorrect, or at least misleading. Besides being durable and of high absorptivity the actual requirement is for a surface of low emissivity not to solar radiation but to the radiation from the collector surface itself which, of course, is at a temperature much lower than that of the sun.

The reader is likely to be confused by the expressions: "angle of incidence," "angle of radiation," and "angle of surface to radiation," which apparently are used interchangeably. The "angle of incidence," of course, refers to the angle between the incident rays and the normal to the surface; but it is not obvious which surface is meant. The other two expressions are ambiguous until it is determined that the former refers to the surface of the sides of the parallelopiped element, while the latter refers to the bottom surface of the parallelopiped element.

With respect to the equations above Fig. 12,

$$D = A - (B + C) \quad \text{and} \quad H = E - (F + G)$$

the author states that "if C is assumed equal to G, D and H are proportional (equal) to $(A - B)$ and $(E - F)$, respectively." This statement is not true except for the trivial case when C and G are both zero. Otherwise all that can correctly be said is that, if C and G were constants and equal to each other, D would vary directly with $(A - B)$ and H would vary directly with $(E - F)$.

In the development of the theory in Phase I the assumption was made that all radiation arrived at the same angle of incidence. Yet in the description of the experimental work in Phase II, the fact that the radiation arrives at widely varying angles of incidence is not mentioned.

Among the smaller errors noted were:

(a) In the equation

$$\text{Absorptivity} = 1 - (1 - \alpha)^n$$

the exponent n is omitted. Or, perhaps, the error was the misplacing of the quantity, $(2b \tan \theta/a)$, which is equal to n, and which should have appeared as the exponent of $(1 - \alpha)$.

(b) In the equation immediately following, the expression $2b \tan \theta/a$ in the right hand member is incorrectly shown as a multiplying factor when it should have been the power to which the term $(1 - \alpha)$ is raised.

(c) The authors mention the results of "the investigations of Daniels and Salem" but give no reference as to where this work may be found. Also they state that "the investigations of Daniels and Salem give values of absorptivity to solar radiation and emissivity at some of the expected operating temperatures of the surface of brass, copper, and copper oxide coatings. This information is given in Fig. 14." The only information given in Figure 14 is for cupric oxide coatings and none of the expected operating temperatures is found.

There are several annoyances which hardly mislead but do detract: in Fig. 12 and 13 it is hard to tell which curve is which since it is difficult to distinguish the O's and X's; the dual ordinate scales, presenting both potentiometer readings and temperatures, are quite unnecessary; also, for no apparent reason, these dual scales are interchanged from one figure to the next; in Fig. 12 the intended reference is to the *Handbook of Chemistry* and degrees Fahrenheit has nothing to do with it; in Phase I the length-width ratio is referred to as b/a while in Phase II the symbols B/A refer to the same quantity; the lower abscissa scale of Fig. 7 is unnecessary since it repeats information contained in Table I on the same page (or vice versa).

E. Lynn Cleveland and Albert Burris
Research Center
New Mexico State University

VOL. 3 1959

Solar Abstracts

AEIC-EEI Heat Pump Committee. "First step of heat storage research program completed: progress report." *Bull. Edison Elec. Inst.* **27**(6): 250–51, June 1959.

Summary of reports by Battelle Memorial Institute and by Comstock and Wescott, Inc., on first phase of a project to determine the status of heat storage development and to analyse the potential applicability of various heat storage materials for use in conjunction with the heat pump and resistance heating. Battelle's report indicates that high-temperature storage, charged with resistance heating properly controlled, offers the most immediate promise as a means of smoothing load curves with either heat pump or other electric heating systems. Second choice is condenser-side storage charged by the heat pump; third choice, evaporator-side storage charged with "free" heat. Comstock and Wescott's report recommends that future research and development work be directed to study of three systems: (1) heat of hydration systems; (2) heat of fusion systems; (3) heat of chemical change systems.

* * *

Battery Research and Development Conference, 12th, Ft. Monmouth, N.J., May 21–22, 1958. *Proceedings.* Power Sources Division, U.S. Army Signal Engineering Laboratories, Ft. Monmouth, N.J. 134 p. Illus.

Includes papers on fuel cells, nickel-cadmium batteries, special purpose batteries (automatically activated zinc-silver oxide batteries), new primary battery designs, low temperature batteries, and other power sources of the future. Papers of particular interest in solar energy utilization are abstracted below.

* * *

Hunrath, George. "Solar energy conversion." (In: Battery Research and Development Conference, 12th, Ft. Monmouth, N.J., 1958 *Proceedings.* p. 111–13. Illus.)

Arctic regions can benefit from solar energy utilization for power requirements of small magnitude because in summer the high latitudes receive 24 hours of sunlight per day, even though it is at low intensity. Three methods for the conversion of solar into electrical energy offer good possibilities: silicon solar cells, thermionic emission (Edison effect), and thermocouples. Concentrators are required for the last two methods, and possibly the first, in northern regions. Conversion efficiencies of 10 per cent have been achieved with the first; 20 per cent with thermionic emission is possible; present conversion efficiencies with thermoelectric generators are fairly low. Silicon solar cells or a cathode and collector in a thermionic emission diode are capable of furnishing power in the Arctic for such applications as navigational aides, and unattended communication or meteorological stations. Energy can be stored in storage batteries for peak power demands or to furnish power during the winter months.

* * *

Kittl, Emil. "Thermal energy conversion." *Ibid.* p. 113–15. Illus.

The thermal energy conversion aspects of solar and nuclear energy are discussed. Additional concentrating equipment is needed for thermoelectric converters utilizing solar energy, and only if considerably higher efficiencies are achieved will this system be comparable to the solid state solar battery. One of the best approaches to meeting military requirements for a portable power source is in the field of solid state thermal energy conversion. The thermionic diode utilizing the Edison effect is discussed in some detail, and a thermionic diode powered by concentrated sun rays and another using nuclear radiation are described. The load characteristics and output voltage vs. output current are compared for the two diodes. A large difference of the emitter and collector work functions is required for large output voltage of the device, and high operating temperature is also necessary to obtain maximum output power. Computed values for the theoretical maximum power output and maximum efficiency of a thermionic diode converter are compared using a group of promising emitter materials. Since the maximum efficiency of the thermionic converter is about three times the theoretical efficiency of the silicon cell, it appears that the thermionic diode offers promise of providing a system having a higher conversion efficiency and higher power output per unit size and weight than any other converter.

* * *

Ziegler, Hans K. "Energy sources for 'space-age' activities." *Ibid.* p. 1000–4. Illus.

Various types of energy sources for artificial satellites and space vehicles are compared, taking into account the basic requirements and unique operating conditions imposed by the outer space environment. Chemical batteries represent the best solution for short time and lower power requirements. They offer up to 80 watt-hr per watt-hr/lb. For long periods of operation in the low, medium, and high-power range, solar conversion systems—with 2600 to 3100 watt-hr/lb for non-storage type and 1200 to 1600 watt-hr/lb for storage type—if one-year life of solar cells is confirmed, or better, if life is longer—appear most favorable. These values apply to space vehicles with no orientation control. Nuclear power devices with presently 500–2000 watt-hr/lb are expected to improve in efficiency and eventually to provide highly reliable sources for medium and high-power and long-life requirements—although competition of solar sources, depending on their long-range behavior and practical reliability, may be quite close. In this area little field experience is yet available.

* * *

Bliss, Raymond W., Jr. "A general description of the solar energy laboratory and its initial research program." Arizona, University, Institute of Atmospheric Physics, May 1, 1959. 45 p. Illus.

The Solar Energy Laboratory at the Institute is designed and built for work in two fields: (1) applied research on the development of moderate-temperature thermal processes for the direct utilization of sunshine; (2) meteorological research on problems involving the measurement of solar, atmospheric, and ground radiation. This report provides a general description of the Laboratory and a preliminary working guide for the laboratory personnel. Construction features of the building are given and components of the solar-heating-cooling system described in detail. A plentiful supply of versatile instrumentation has been installed for the experimental system and for other projects. For its first two years of operation, a major portion of the work will center around the study and analysis of the performance of the heating-cooling system. Other projects will include maintenance of the local pyrheliometer records, atmospheric transmissivity studies, etc. Potential graduate student projects are listed.

Bliss, Raymond W., Jr. "Solar water heating system." *U.S. Patent* 2,838,043, June 10, 1958. 5 p. Illus.

In this simple, relatively inexpensive solar water-heating system the heat collector is placed in its normal elevated position and the storage tank at a low level, and water is circulated during sunshine hours by a small pump. Feed water is supplied by connecting a source of cold water under pressure to the bottom of the tank. An air space is provided, optionally at the top of the tank, above the water outlet, which has a greater volume than the portion of the system above the air space which is to be drained. By providing a bleeder line between the air space and one of the lines providing circulation between the hot water storage tank and the collector, water will automatically flow from the collector to the tank when pump action is discontinued, and air will flow through the bleeder line from the air space into the collector and into the portion of the system above the air space.

* * *

California, University, Institute of Engineering Research, Berkeley. "Sea water conversion program: a technical and economic investigation of certain schemes for producing potable fresh water from sea water. Berkeley progress report for the year ending June 30, 1959." Series No. 75, Issue No. 15, July 24, 1959. 28 p. Illus.

Reports of investigations at the University of California at Berkeley and the Richmond Field Station into various distillation processes, including multiple effect centrifugal evaporators, vacuum flash distillation, solar distillation, reversed osmosis using capillary ultra-filters, ion exchange processes, freezing processes, vapor compression tests, magnetic effects investigation, biological conversion of saline waters, and nuclear reactor studies. The publication includes reports by H. W. McCracken, D. M. Campbell, K. D. Frohman, G. M. Voge and J. W. Weldy on recent work at the University in the construction of various types of solar stills. A small unit made of wood and costing about $60 was the subject of an instruction sheet for distribution in response to inquiries received on small, low-cost stills; its yield varies from 2¾ to ½ gal per day. As the result of detailed discussion by a panel of authorities in the solar distillation field, some generalizations and recommendations for specific projects in the Sea Water Conversion Program are formulated.

* * *

Diamond, P. M. "The central problem of large scale power generation in space waste heat disposal." Institute of Aeronautical Sciences Paper No. 59-96; presented at the IAS meeting, Los Angeles, Calif., June 16–19, 1959. 36 cols. Illus.

A discussion of certain aspects of the characteristics of large power systems designed to operate in a space environment, with special emphasis on the problem of the weight of the unit. The writer concludes that for lower power, very long duration applications, the solar battery appears to offer the greatest potential. The solar turbo-generator systems are among the lightest in weight for large scale power generation. The limitations of the radiant energy collector, however, may ultimately preclude the use of this device for large units.

* * *

Khanna, Mohan Lal; Gardner, A. L.; Davey, T. N.; Suri, S. P. "Plane-glass mirror solar energy concentrators for concentrating sugarcane & palm juices." *J. Sci. Ind. Res.* **18A**(5): 212–16, 1959. Illus.

The design, construction and working details of a plane-glass mirror (9 in. square) solar energy concentrator are described. The results of experiments on the evaporation of water and cane juice, using reflectors with over-all dimensions of 3 by 3 ft and 6 by 3 ft, are presented. The advantages of this type of collector over the conventional concentrators, such as low cost, simplicity of construction, ease of handling, and portability are pointed out, and the probable economy in the sugar cane and palm gur manufacturing industries by the use of this type of reflector, is assessed. (authors' abstract)

* * *

Kiepenheuer, Karl. *The sun.* Ann Arbor, Univ. of Michigan Pr., c1959. 160 p. Illus. (Trans. by A. J. Pomerans from *Die Sonne.* Berlin etc., Springer-Verlag, 1957.)

Nontechnical account of what we know about the sun, including the nature of sunlight, sunspots, northern lights, solar storms, the surface and interior of the sun. Solar energy utilization is mentioned briefly.

* * *

Telkes, Maria. "Apparatus for storing and releasing heat." *U.S. Patent* 2,808,494, Oct. 1, 1957. 5 p. Illus.

Provides a system for storing heat at a relatively high temperature, in the range 300° to 550°F, with a capacity several times that of previous systems. The system makes use of the heat of transition of a dimorphic substance, such as sodium sulfate, alone or admixed with small quantities of other salts as a heat-storing and releasing device.

* * *

Zwick, Eugene B.; Zimmerman, Robert L. "Space vehicle power systems." *J. Am. Rocket Soc.* **29**(8): 553–64, Aug. 1959. Illus.

A review of systems which can be utilized for the generation of secondary and/or propulsion power for advanced space vehicles. Power systems considered include: chemically-fueled power supplies, open and closed cycle; solar power supplies, closed cycle; nuclear power supplies, closed cycle; thermionic and thermoelectric power supplies; solar photovoltaic and solar recycling fuel cell power supplies. Also included in the review are the results of an initial program relating to the optimum temperature ratio, collector and radiator size for general power systems when used with nuclear, chemical, or solar energy sources. Descriptions are presented of a number of typical power systems. An attempt is made to describe the general physical construction as well as to indicate the limitations of the system. Analyses and estimates have been prepared in order to determine the system weight as a function of power level and duration. Comparison of some of the systems studied is presented. Weights and sizes of the significant components are tabulated for 1- and 100-kw systems. Variation of system weight with time and power level is plotted to determine the optimum system from a weight standpoint for various applications. System selection for various missions is summarized, and the role of turbomachinery in space vehicle power systems is noted. (authors' summary)

VOL.
3
1959

OL.
959